University of Alberta

Performance and Productivity of Horizontal, Vertical and Curvilinear
Wellbores and Fractures in Reservoirs with and without
Bottom Water and/or Gas Cap

by

Faramarz Azar-Nejad　　Ⓒ

A thesis submitted to the Faculty of Graduate Studies and Research in partial fulfillment of
the requirement for the degree of Doctor of Philosophy

in

Petroleum Engineering

Department of Mining, Metallurgical and Petroleum Engineering

Edmonton, Alberta

Fall 1996

Canada

University of Alberta
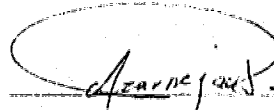
Library Release Form

Name of Author: Faramarz Azar-Nejad

Title of Thesis: Performance and Productivity of Horizontal, Vertical and Curvilinear Wellbores and Fractures in Reservoirs with and without Bottom Water and/or Gas Cap

Degree: Doctor of Philosophy in Petroleum Engineering

Year This Degree Granted: 1996

Permission is hereby granted to the University of Alberta Library to reproduce single copies of this thesis and to lend or sell such copies for private, scholarly, or scientific research purposes only.

The author reserves all other publication and other rights in association with the copyright in the thesis, and except as hereinbefore provided, neither the thesis nor any substantial portion thereof may be printed or otherwise reproduced in any material from whatever without the author's prior written permission.

9011 - 152 St.

Edmonton, Alberta

T5R 1M2
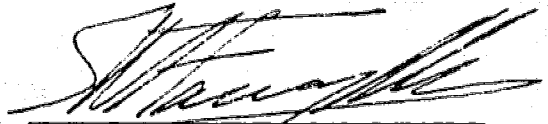
Canada

Dated *August 28th, 1996*
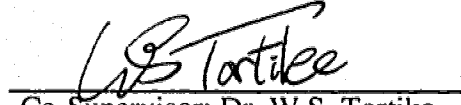
University of Alberta

Faculty of Graduate Studies and Research
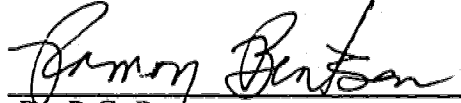
The undersigned certify that they have read, and recommend to the Faculty of Graduate Studies and Research for acceptance, a thesis entitled "Performance and Productivity of Horizontal, Vertical and Curvilinear Wellbores and Fractures in Reservoirs with and without Bottom Water and/or Gas Cap" in partial fulfillment of the requirements for the degree of Doctor of Philosophy in Petroleum Engineering.

Co-Supervisor: Dr. S.M. Farouq Ali

Co-Supervisor: Dr. W.S. Tortike

Dr. R.G. Bentsen

Dr. D. H. Chan

Dr. J. Szymanski

Dr. A. Badakhshan

Dated___Aug 16, 96___

To

my wife, Azita,

and

my world's sun, Arash

ABSTRACT

The mechanism of fluid flow in a reservoir can be determined through knowledge of the potential distribution inside the reservoir. Developing the *Discrete Flux Element Method (DFE)*, this work provides a general analytical solution to the potential distribution due to a producing well with a straight or curvilinear configuration under transient or steady state conditions. The potential distributions of horizontal and vertical partially penetrating wells and fractures are special cases of this solution. The *Discrete Flux Element Method* provides the ability to model any arbitrary outer boundary condition, while maintaining the inner boundary at uniform potential or uniform flux conditions. The *Discrete Flux Element Method* enables predicting the performance as well as the productivity of arbitrary sources such as horizon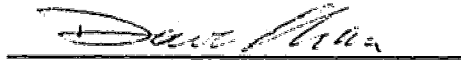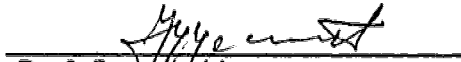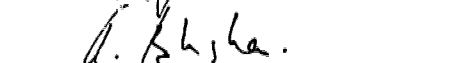tal, vertical partially penetrating line source wells and fractures in an arbitrary reservoir, including infinite, semi-infinite, infinite slab, semi-infinite slab, infinite channel, semi-infinite channel and box shaped reservoirs. The shape of the drainage areas around horizontal and vertical partially penetrating wellbores and line sources with curvilinear configurations and fractures is studied both graphically and mathematically. This study shows that the drainage area around a horizontal well in a rectilinear, isotropic reservoir is first ellipsoidal and then it opens up in the directions perpendicular to the line source until it reaches the no-flow boundaries, and after a transitional period it becomes a vertical cylinder.

One of the common applications of horizontal and vertical partially penetrating wellbores is in reservoirs with bottom water and/or gas a cap. The applicability of the

Discrete Flux Element Method in such reservoirs is examined. For coning studies the interface before breakthrough is treated as a no-flow moving boundary while the initial interface is kept at a constant pressure condition. In the contest of the coning phenomenon in a rectilinear reservoir, this study presents a new dimensionless variable, *Dimensionless Density*, as a function of reservoir geometry, reservoir anisotropy, fluid properties, production rate and the difference in fluid densities. This work reports the existence of a *Critical Dimensionless Density (CDD)* above which the cone is stable. The performance of the wellbore in the presence of a growing cone is also presented.

TABLE OF CONTENTS

LIST OF TABLES

LIST OF FIGURES

$$\alpha = 1 \text{ and } \beta = \sqrt{1/3}.$$

wells with different lengths for different drainage radii.

separated for better demonstration of the model.

that in a reservoir with a solid boundary

NOMENCLATURE

$a = 2h_t$, [L]

B = formation volume factor

B_o = oil formation volume factor

c = dimensionless vertical coordinate of a point source

c_t = fluid compressibility, $[M][L]^{-1}[T]^{-1}$

d = distance between the elements

DD = dimensionless density

DFE = discrete flux element

CDD = critical dimensionless density

F = distance of the horizontal well to a vertical barrier

g = gravity constant, $[L][T]^{-2}$

h_t = reservoir thickness, [L]

h_w = height of the water, [L]

h_{Dw} = dimensionless height of the water cone

h_{Dg} = dimensionless height of the gas cone

h_{wd} = dimensionless height of the cone head

IBC = inner boundary conditions

k = permeability, $[L]^2$

k_h = horizontal permeability, $[L]^2$

k_v = vertical permeability, $[L]^2$

K = diffusivity, $[L]^2[T]^{-1}$

L = length , [L]

L_1 = coordinate of the starting point of the wellbore.

L_2 = coordinate of the ending point of the wellbore.

L_p = dimensionless producing length

L_{pT} = dimensionless producing length in the transformed domain.

p = pressure, $[M][L]^{-1}[T]^{-2}$

Q = production rate, $[L]^3[T]^{-1}$

Q_c critical production rate $[L]^3[T]^{-1}$

q = flux

r_h =dimensionless horizontal distance

SFL sources with finite length

SIL sources with infinite length

t = time in the definition of the dimensionless time, $[T]$

t = reservoir thickness, $[L]$

t_p = dimensionless time

r = radius

r_p = dimensionless radius

w = dimensionless vertical coordinate

WOC water oil contact

x = dimensionless coordinate,

X = coordinate, $[L]$

y = dimensionless coordinate,

Y = coordinate, $[L]$

Z = vertical coordinate, $[L]$

$\Delta\gamma$ = difference of the densities, $[M][L]^{-3}$

$\Delta\gamma_p$ = dimensionless difference of the densities,

γ = density, $[M][L]^{-3}$

ρ = dimensionless horizontal distance

μ = viscosity, $[M][L]^{-1}[T]^{-1}$

ϕ =porosity

φ = potential $[M][L]^{-1}[T]^{-2}$

φ_p = dimensionless potential of a flux element

ψ = mathematical ψ function

ψ' = stream function

Subscript

D = dimensionless

l = line source

e = reservoir boundary

f = fracture

P = point source

i = a counter of the number of the flux elements

T = transformed

W = well

Superscript

l time step

SS Steady State

$Cont.$ = Continuous

$Ins.$ Instantaneous

CHAPTER 1

INTRODUCTION

The potential distribution inside a reservoir is an appropriate tool for studying the flow mechanism and for determining the shape of the drainage area. The potential distribution can be obtained by the application of accurate potential equations. In the literature, these equations have been presented for simple source configurations such as vertical, fully penetrating wellbores with a straight configuration. Moreover, approximate solutions have been provided for partially penetrating line sources in vertical and horizontal wells with a straight configuration. The solutions for horizontal wells have been developed using the uniform flux inner boundary condition assumption [Clonts and Ramey, 1986, Daviau et al., 1988, and Odeh and Babu, 1990]. As these solutions do not satisfy the uniform potential at the inner boundary, the use of an equivalent pressure point is suggested to simulate an infinite conductivity (uniform potential IBC) solution [Clonts and Ramey, 1986, and Daviau et al., 1988]. Gringarten and Ramey [1975], for a vertical partially penetrating wellbore, indicated that an error of 10% or more is associated with the use of an equivalent pressure point. Rosa and Carvalho [1989] modeled a horizontal well by dividing the wellbore length into different segments, each with a uniform flux potential solution which was given by Clonts and Ramey [1986], and showed that the equivalent pressure point was moving at early times.

In the literature, no potential equations are provided for the potential of sources with irregular geometry and arbitrary direction. To apply these solutions [Clonts and Ramey, 1986, Daviau et al., 1988, and Odeh and Babu, 1990] one must assume a straight configuration for the wellbore in the direction of one of the principal permeabilities (principal axis of the medium). This assumption, as will be discussed in more detail in Chapter 6, gives rise to errors in reservoirs with a large directional permeability contrast. The solutions provided by Clonts and Ramey [1986] and by Daviau et al. [1988] are the products of three 1-D solutions (Green's function) each one of which models the flow in the direction of a principal axis of the medium. Thus, the resulting line source equation can model only a straight horizontal well parallel to the principal axis of the medium. However, if the wellbore is not drilled in that direction, this mathematical model provides only an approximate solution.

No steady-state potential equation for partially penetrating fractures and horizontal wells has been presented in literature. Thus the productivity of horizontal wells was modeled by an assumed geometry for the drainage area [Borisove, 1964 and Joshi, 1990].

In this work a general analytical equation is developed to predict the potential of line and plane sources with: i) uniform flux or uniform potential inner boundary condition, ii) arbitrary configuration, iii) arbitrary direction, iv) sealed, constant potential or mixed outer boundaries, and v) steady-state or transient conditions. The new solution is called *Discrete Flux Element (DFE) Method*. Moreover, this solution (DFE Method) is applied to derive new potential derivative equations for transient pressure analysis purposes. Development of the Discrete Flux Element (DFE) Method is presented in Chapter 5.

By using the new solution (DFE Method), the performance and the productivity of line and plane sources with different inner and outer boundary conditions are studied and the results are presented in Chapters 6 and 7, respectively. In Chapter 8 the Discrete Flux Element (DFE) Method is applied to study the shape of the isopotential lines around sources with arbitrary configuration.

In Chapter 9 an alternative solution is developed for calculating the potential of vertical partially penetrating wellbores with straight configuration.

In Chapter 10, the steady-state and transient potential equations developed in this work are used to study the coning and the performance of horizontal and vertical partially penetrating wellbores in reservoirs with bottom water or gas cap.

CHAPTER 2

LITERATURE REVIEW

This is a review of key papers related to the derivation of solutions for similar or related cases. There are other papers that have *applied* these solutions to study special aspects of reservoir engineering. They are not reviewed here.

Although several transient potential equations for horizontal wells and vertical fractures are available, no steady-state potential equations for these sources have been provided yet. However, there are several equations for 1) the productivity index of horizontal wells, and 2) the pseudo-steady state potential of horizontal wells. These are addressed later in this chapter.

2.1   Potential of a Point Source

Kelvin [1884] presented the instantaneous, continuous, and steady-state solution for a point source in an infinite domain.

Madelung [1918] developed an equation for the steady-state potential at any point due to a point source in a rectilinear domain as a function of the horizontal and vertical distances of that point to the point source. As that equation was singular for zero horizontal distance, Muskat [1932] developed an alternative equation which did not have the singularity problem. However, Muskat's equation was valid only for very small values of horizontal distance.

2.2. Potential of Sources with Finite Length

Kelvin [1884] stated that the potential of any source with arbitrary geometry can be constructed by integrating the solution of a point source over the volume of the source:

- The potential solution of a line source is the integral of the potential solution of a point source along the path of the line source.

- The potential solution of a plane source (fracture) is the double integral of the potential of a point source over the surface of the plane or the single integral of the solution of a line source, over the length of the fracture.

Kelvin's statement has been applied widely to derive potential equations for different type of sources with infinite length such as line, plane and cylindrical sources [Carslaw and Jaeger, 1959].

For a source with infinite length(s), both uniform potential and uniform flux Inner Boundary Conditions (IBC) can be satisfied simultaneously, and the method of integration provides the exact solution for such sources. However, for sources with finite length both conditions cannot be met at the same time due to the end effects. The hemispherical flow at the end(s) of the line source and semi-radial flow at the end(s) of the fracture affect the potential distribution inside the reservoir as well as the potential at the source, itself. As the flux distribution for sources with finite length is unknown, the integral over the solution of a point source is possible only when the uniform flux assumption is invoked. Thus the resulting potential equation obtained by the integration method does not satisfy

the uniform potential IBC. However, based on potential theory, the potential on the surface of the source has to be uniform.

Muskat [1932] integrated the steady-state solution of a point source to derive a steady-state potential equation for a vertical, partially penetrating wellbore. This integration was possible only when the uniform flux assumption was invoked. Thus, the resulting equation indicated a potential gradient along the source. To obtain a potential equation satisfying potential theory Muskat applied a superposition method. In this method he used several uniform flux line sources with different lengths and a point source at the bottom of the wellbore to consider the end effects. Equating the potentials at different locations along the wellbore, Muskat determined the flux distribution as well as the wellbore potential with 0.5% accuracy. Muskat discovered that the value of the potential obtained by the superposition method (uniform potential IBC) was approximately the same as that obtained by the uniform flux IBC solution, provided that the latter was calculated at 75% of the wellbore length.

Gringarten and Ramey [1973] applied the Method of Images to develop solutions for an infinite plane in different types of reservoirs, specifically two parallel no-flow boundaries, two parallel constant pressure boundaries and mixed boundaries. By integrating the solution of these infinite planes about a limited interval, they obtained the potential solutions of infinite slab sources with the same type of boundary condition.

Gringarten, Ramey and Raghavan [1974] derived a uniform flux potential equation for a fully-penetrating, vertical fracture in a rectilinear reservoir by integrating the solution of a fully penetrating line source about the horizontal length of the fracture. As was

expected, this solution did not satisfy the uniform potential IBC. The approach taken was similar to Muskat's superposition method for a vertical partially penetrating well. That is, Gringarten et al. divided the length of the fracture into different segments, each with uniform flux, and equated the pressure at the center of the segments to construct the uniform potential IBC solution. This solution is called the infinite conductivity solution. As was the case with Muskat's approximate model, Gringarten et al. suggested that the pressure obtained by the infinite conductivity, superposition method, would be identical to that obtained by a uniform flux solution provided that the latter was calculated at a certain point. This point was named the equivalent pressure point and was proposed to be at $X_{eq} = 0.732X_f$, where X_f was the half length of the fracture.

Clonts and Ramey [1986], using three 1-D solutions given by Gringarten et al. [1973] and Newman's product rule [Clonts and Ramey, 1986], presented an unsteady state, uniform flux equation for horizontal wells in a rectilinear reservoir. By comparing a horizontal well to a fracture, Clonts and Ramey postulated that an equivalent pressure point similar to that of a fracture (i.e. $X_{eq} = 0.732X_f$) could be used to simulate an infinite conductivity solution. Two types of transient pressure behavior, depending on the half length of the wellbore, were detected. If $L_D < 10$ (L_D is dimensionless half length of the horizontal well), flow is characterized by an initial radial flow perpendicular to the wellbore followed by a transition to a pseudo-radial flow period. For $L_D > 10$, flow is characterized by early time linear flow followed by a transition to late time pseudo-radial flow.

Daviau et al. [1988], using an approach similar to that of Clonts and Ramey [1986], applied three 1-D solutions given by Gringarten et al. [1973] and Newman's product rule to construct the potential equation for horizontal wells with uniform flux IBC. Analyzing the pressure (potential) of a horizontal well, they showed that the pressure varies along the wellbore. To simulate the infinite conductivity solution, they used a uniform flux solution at $X_{eq} = 0.7X_f$. As could be expected, the results indicated flow regimes similar to those of Clonts and Ramey [1986].

Kuchuk et al. [1988] used the uniform flux equation presented by Clonts Ramey [1986] for horizontal well pressure analysis. To overcome the non-uniform pressure along the wellbore, they applied an average pressure.

Rosa and Carvalho [1989], using a solution similar to the uniform potential solution for a vertical well given by Muskat [1932] and a solution for a vertical fracture given by Gringarten et al.[1973], constructed an infinite conductivity solution for a horizontal well in a rectilinear reservoir. By dividing the length of the horizontal well into several segments, each with a uniform flux IBC, and by equating the pressure at the center of the segments, they calculated the flux distribution and the wellbore pressure. By comparing the resulting solution with the pressure for a uniform flux solution they showed that the equivalent pressure point at short time is not stationary and that it stabilizes at late time. Furthermore, at late time its position depends on the wellbore length. However, they suggested that at short time one could use a uniform flux solution directly and at late time for short wellbores an equivalent pressure point at $X_{eq} = 0.68X_f$. For a long wellbore the equivalent pressure point has to be obtained for every individual case.

Ozkan et al. [1987], using the uniform flux solution given by Clonts and Ramey [1986], studied the pressure analysis of horizontal wells. Approximate equations were provided for short and long times. An equivalent pressure point was used to simulate the infinite conductivity solution. This solution showed a higher pressure drop at the midpoint of the wellbore length, indicating that flow takes place from both ends toward the middle of the wellbore. They concluded that this model could be used for horizontal wells which were producing from the middle of the wellbore. Comparing the solution of a horizontal well with that of a fracture they showed that the pressure in a horizontal well is greater than that in a fracture and that it approaches the fracture pressure for $L_D > 4$ where L_D is the half length of the horizontal well. Without mentioning the fracture length, they related this to the fact that the fracture pressure was calculated at the centre of the fracture width and that of the horizontal well was calculated at the surface of the source. However, because the pressure drop is highest at the center of the source, it seems that the reason for the higher pressure drop in horizontal wells should be something else. Ozkan et al. stated that: the horizontal well productivity is governed by two parameters: 1) the dimensionless well length and 2) the wellbore radius.

Goode and Thambynayagam [1987], using a Fourier transformation, developed a uniform flux solution for a horizontal well in an semi-infinite reservoir. To approximate an infinite conductivity solution they suggested the use of an equivalent pressure point at $X_{eq} = 0.86 X_f$.

Odeh and Babu [1990] modeled a transient uniform flux pressure (potential) solution for a horizontal well in a box shaped reservoir by integrating the solution of a point source about the length of the source.

2.3 Productivity of Horizontal Wells

Steady-state potential equations for a horizontal well have yet to be presented. However, several workers have developed approximate productivity indices for horizontal wells based on an assumed drainage area shape around a horizontal well and application of Darcy's Law [Borisov, 1964, and Joshi, 1988]. The pseudo-steady state equations for the productivity of horizontal wells in box-shaped reservoirs are presented by Babu and Odeh [1989] and Goode and Kuchuk [1991].

Borisov [1964] presented an equation for the productivity of a horizontal well. The original work was published first in Russian, then translated into French and then to English (1980). Unfortunately the paper is not supported by a detailed derivation and illustrative figures. The method used by Borisov is a general method, involves dividing the drainage area into two vertical tiers. The total resistance to flow is obtained as the sum of the resistances of the outer and inner tiers. The inner resistance is estimated by modeling a horizontal well as a tier.

Joshi [1988] assumed an ellipsoidal drainage area around a horizontal well. He simplified the mathematical model by dividing the 3-D problem into two 2-D problems. Therefore the resulting flow model consisted of 1) a horizontal flow component, and 2) a

vertical flow component into the wellbore in the plane perpendicular to the well axis. In the horizontal section, the isopotential lines are elliptical while the streamlines are hyperbolic. This system of confocal ellipses and hyperbolas is modeled as a complex variable as was suggested by Slichter [Joshi ,1988], from which the production rate for the horizontal flow into the wellbore is derived. The vertical flow is modeled as a sink in a parallel-plate channel. The potential and stream functions are represented as complex variables through the Schwarz-Christoffel mapping function [Joshi. 1988]. From the production rates the resistivities in the horizontal and vertical planes are calculated. The total resistivity is then obtained by linear summation of the two resistivities from which the productivity of the wellbore is obtained. This model shows smaller productivity index than does the model presented by Borisov [1964].

Borisov's equation has been used by Giger et al. [1984] to study some aspects of horizontal wells.

Babu and Odeh [1989], by integrating the solution of a point source in a box-shaped reservoir, derived a uniform flux, transient, potential equation for a horizontal well in a box shaped reservoir. The late time solution for the potential inside the reservoir is obtained as time approaches infinity. The average pressure of the reservoir is obtained by integrating the late time solution over the volume of the reservoir. The pseudo-steady state wellbore pressure is found by subtracting the average reservoir pressure from the late time wellbore pressure. Several aspects of this work are open to discussion.

Babu and Odeh assumed a circular wellbore in an anisotropic reservoir. This implies that the flow into the wellbore is radial. Brigham [1990] and Peaceman [1990 a, c]

stated that, as the perimeter of the wellbore in the transformed domain is elliptical, an average wellbore radius should be used instead of the actual wellbore radius. The shape function in the productivity equation that had been derived by Babu and Odeh was also verified by Peaceman [1990 b] who used different approach. Dietrich [1995] numerically simulated a horizontal well with a uniform potential inner boundary condition. Comparing the simulation and the analytical solution, Dietrich concluded that the two methods showed less than 3% difference at low to moderate well penetrations and isotropic permeability conditions.

Goode and Kuchuk [1991] developed equations for the inflow performance of horizontal wells under pseudo-steady state and steady-state conditions. Pseudo-steady state is defined as the late time transient solution in a reservoir with sealed boundaries. However, the steady-state condition was assumed to be reached only if one of the boundaries of the reservoir was of the constant pressure type. This case corresponded to reservoirs with bottom water or a gas cap. Therefore, two different equations one for pseudo-steady state and one for steady-state, were developed. By assuming the horizontal well to be a fracture, the 3-D partial differential equation was reduced to a 2-D diffusion equation. Therefore the problem was turned into finding the potential solution of a fully penetrating fracture. By assuming a uniform flux into the fracture, and by applying a finite fourier cosine transform and a Laplace transform, the partial differential equation was reduced to an ordinary differential equation. By solving the resulting equation for a uniform flux IBC, two solutions were obtained for the pressure in a horizontal well, one for pseudo-steady state and one for steady-state flow. For the case of a box-shaped

reservoir, the average reservoir pressure was obtained by integrating the pressure over the volume of the reservoir. Subtracting this value from the wellbore pressure the pseudo-steady-state wellbore pressure was obtained.

2-4 Horizontal and Vertical Partially Penetrating Wellbores in Reservoirs with Bottom Water or Gas Cap

When producing from a reservoir with bottom water or a gas cap, one needs to have knowledge about:

1. The critical production rate (Coning) - this is the rate above which the interface is not stable and the water and/or gas will breakthrough.

2. The time to breakthrough of the undesired liquid into the producer.

3. The well production performance - due to the existence of a moving boundary before breakthrough well testing of such reservoirs is different from that of regular reservoirs with fixed boundary.

These three topics are discussed below.

2.4.1. Critical Production Rate

Muskat and Wykoff [1935] presented the fundamentals of coning. By using the concept of static equilibrium, they developed the critical production rate as a function of cone height and potential distribution inside the reservoir. As the cone height and potential

distribution are interrelated. and as both depend on the production rate, the equation could not be solved without further assumptions. They then assumed that the initial interface was a no-flow boundary and calculated the potential at the cone head. It was postulated that, if the actual interface were used as the real no-flow boundary, the critical production rate would have been lower. This implies that Muskat and Wykoff's solution for the critical rate had to be the upper limit on the exact solution. This solution was presented graphically for vertical partially penetrating wells with a dimensionless radius of 0.001 and several drainage areas.

Arthur [1944] modified the Muskat and Wykoff solution for any type of wellbore and drainage radius. He presented a set of graphs for vertical partially-penetrating wells from which one can calculate the critical production rate for any arbitrary wellbore and drainage radius and penetration depth.

Meyer and Garder [1954], by using the potential definition given by Hubbert [1940], modeled a vertical partially penetrating well under steady-state conditions. They assumed that the shape of the cone in a vertical section is a triangle with one corner at the bottom of the wellbore and two others at the outer boundary. Assuming that the water reaches the bottom of the wellbore at breakthrough they presented an equation for the critical production rate. The critical production rate obtained by Meyer and Garder is the lower limit to the solutions. This might be due to the triangular geometry of the cone which results in a smaller area for oil flow as compared to that for a curved interface.

Chaney and Noble [1956], by applying both mathematical and potentiometric methods, determined the critical production rate for both water and gas coning. The

results are in the graphical form for a single oil viscosity (1 cp), permeability (1000 md) and fluid density difference (for an oil water system 0.3 g / cc and for a gas oil system 0.6 g / cc) for a 1000 ft drainage radius and a dimensionless wellbore radius equal to 0.001 for several reservoir thicknesses. From the results of this study it was concluded that the wellbore radius did not affect the critical production rate. For a given reservoir geometry and fluid properties, the critical production rate obtained from the curves has to be corrected to the actual reservoir conditions. This method provides an approximate solution to the coning problem without considering the geometry of the cone. Moreover, it enables one to find the best location and perforation interval inside a rectilinear reservoir for both water and gas coning.

Henly et al. [1961] who performed experimental work on a physical model under bottom water drive, found that the capillary forces have negligible influence on coning phenomena.

Chierici, et al. [1964] presented a graphical solution to the coning problem based on potentiometric experiments and the theoretical model of Muskat and Wykoff [1935]. This solution can be used to determine 1) the critical production rate and 2) the optimal location and length of the perforation interval in a gas-oil-water system. In this solution the effect of water-oil contact (WOC) geometry has not been considered. The main advantage of this method as compared to Muskat and Wykoff's method is its ability to consider arbitrary perforation intervals and locations within the reservoir.

Bournazel and Jeanson [1971] modeled a water coning problem in the laboratory. They introduced approximate empirical equations for the time to breakthrough, water-oil

ratio and critical production rates. The results of their studies showed that 1) increasing the production rate reduces the breakthrough time, 2) increasing the penetration depth reduces the critical production rate, 3) the water-zone thickness has no effect on the critical production rate and time to breakthrough, but it does increase the water-oil ratio (WOR), 4) the well radius has no significant effect on the critical production rate and the breakthrough time, 5) the external boundary radius has little effect on the WOR, 6) increasing the oil viscosity decreases the time to breakthrough and 7) the breakthrough time is proportional to the anisotropy ratio k_x k_y.

Schols [1972] constructed an empirical equation for the critical production rate which was based on extensive experimental work.

Kuo and DesBrisay [1983] presented an empirical equation for water cut performance prediction. For calculation of the critical production rate they suggested the use of the equations given by any of 1) Meyer and Garder [1954], 2) Chaney et al [1956] and 3) Schols [1972]. However, the critical production rates obtained by these methods are different.

Wheatly [1985] developed an equation for the critical production rate by assuming that the water oil contact is a no-flow boundary and by taking into account the cone geometry. To model a uniform-potential vertical, partially, penetrating well under steady-state conditions, Wheatly superimposed different wellbores with different lengths. He also derived the equation for the streamline passing through the points located on the outer boundary and at the bottom of the wellbore. The potential distribution inside the reservoir was found from the potential equations of different line sources and a streamline equation.

The critical production rate obtained from this solution is smaller than that prtedicted by Muskat and Wykoff [1935].

Chaperon [1986] used the dynamic equilibrium condition for the stability of a cone and modeled a vertical well as a point source. The stability condition is found when the vertical potential gradient at the WOC is smaller than the gravitational gradient. The case of coning due to production from a horizontal well is also studied by considering a horizontal well without end effects; that is one of infinite length. Because a 3-D problem was approximated by a 2-D problem, the coning was studied only in the plane perpendicular to the wellbore axis.

Høyland et al. [1989] used a numerical, finite-difference simulator to model the coning in a vertical well under steady-state conditions. Based on numerous runs, they developed an empirical correlation for the critical production rate. Although the result of the simulator itself is in complete agreement with Wheatly's model, the range of applicability of the correlation is limited.

2.5   Active Bottom Water Drive

Muskat [1947] presented a model for fully developed reservoirs with bottom-water drive. This model provides the breakthrough time as well as the water-cut performance of reservoirs with closed lateral and upper boundaries. A steady-state potential equation, based on a vertical, partially penetrating wellbore with a constant potential boundary at the initial WOC, is derived to calculate the potential distribution. The vertical velocity is calculated using the derivative of the steady-state potential equation. The time to breakthrough is obtained by calculating the time that a point located

initially on the WOC reaches the bottom of the wellbore. The assumptions made to obtain these solutions are:

1. The difference in fluid densities is negligible (zero).

2. The reservoir pressure remains above the bubble point pressure during production. (This is a necessary assumption for calculating the displacement efficiency through a material balance; Muskat assumes that the depleted zone is to be filled by water).

3. The mobilities in both the oil and the water invaded zones are the same.

4. The system is operating under steady-state conditions. It was explained by Muskat that this assumption guarantees a constant potential at the boundary.

5. There is no oil stripping in the flooded zone.

In his original paper, Muskat [1947] assumed a constant potential boundary at the initial interface location, but through Elkins' discussion and Muskat's reply [Muskat, 1947] it is clear that a constant potential at the initial WOC is not a necessary condition for modeling an active water drive. The active water drive concept was used for material balance purposes. In the absence of any other drive mechanism, for example gas drive or a edge-water drive, the total oil production must be equal to the volume of water encroached. Applying this material balance Muskat presented the displacement efficiency as the ratio of the total oil production to the total pore volume at the time of breakthrough.

Ozkan and Raghavan [1990-b] applied Muskat's model [1947]. assuming the initial WOC as a constant potential boundary, to construct an approximate solution for the time to water breakthrough for a horizontal well.

2.6 Performance of Partially Penetrating Wellbores in Reservoirs with Active Bottom Water or Gas Cap

Kuchuk et al. [1988] developed a transient potential solution for a horizontal well in an infinite slab reservoir with bottom water or a gas cap. Neglecting gravity they modeled the effect of the bottom water by assuming a constant potential boundary at the initial WOC. Kuchuk et al. used the average pressure of the wellbore to simulate an infinite conductivity solution. By analogy they postulated that their model could be applied to the reservoirs with a gas cap.

Ozkan and Raghavan [1990-a]. again neglecting gravity, presented a transient uniform-flux potential equation for a horizontal well in a laterally-closed reservoir with bottom water or a gas cap. Similar to the work of Kuchuk et al. [1988], the effect of bottom water or a gas cap was accounted for assuming a constant potential at the initial WOC. To simulate the infinite conductivity solution the use of an equivalent pressure point, as proposed by Clonts and Ramey [1986], was suggested. Even though the outer boundary conditions of the two models are totally different, no justification is provided for using the same location of the equivalent pressure point.

CHAPTER 3

STATEMENT OF THE PROBLEM

It was shown in the preceding chapters that the available potential solutions for horizontal wells [Clonts and Ramey, 1986 and Daviau et al., 1988, and Kuchuk et al., 1988, and Odeh and Babu, 1990] had been developed with certain assumptions. These include:

1) a straight line configuration,

2) the wellbore is in the direction of one of the principal axis of the medium,

3) uniform flux Inner Boundary Conditions, IBC.

Due to drilling technologies and geological conditions the configuration of most horizontal wells is curvilinear rather than straight. When applying the above solutions to potential equations, one must assume a straight line configuration for the source in the direction of one of the principal axes of the medium. Therefore by stretching a 3-D curvilinear line and transforming it into a straight and horizontal line, one neglects certain flow mechanism inside the reservoir. A 3-D curvilinear line has two curvilinear projections in the vertical and horizontal planes. In an anisotropic reservoir with significant contrast in horizontal and vertical permeabilities, the impact of each directional flow component on the reservoir performance and depletion is different. By omitting the vertical flow component and increasing the horizontal length instead, one changes the depletion pattern

of the reservoir. The effect of wellbore configuration on the performance of the wellbore is studied in Chapter 6. Increasing the wellbore length in the horizontal direction causes the ends of the well to approach or pass through any vertical barrier present in the reservoir. The effect of the distance of a horizontal wellbore to a vertical barrier on performance of the wellbore is studied in Chapter 6.

Horizontal wells are usually not drilled in the direction of one of the principal permeabilities. The solutions for horizontal wells based on Green's function [Clonts and Ramey, 1986, Daviau et al., 1988] and integral over the potential of a point source [Odeh and Babu, 1990] are based on the assumption that the wellbore is in the direction of one of the coordinate axes. If the principal axes and the coordinate axes are not the same then a permeability tensor with 9 elements must be used. Assuming the same direction for the coordinate axis and the principal axis of the medium is another approximation that affects directly the performance of the wellbore.

The uniform flux solution does not satisfy the uniform potential inner boundary conditions. To simulate a uniform potential solution, the use of a uniform flux at an equivalent pressure point [Clonts and Ramey, 1986, and Daviau et al., 1988] or an average wellbore pressure [Kuchuk et al., 1988], were suggested. One might accept an approximate solution for the wellbore potential but the applicability of this solution is inappropriate for cases where the potential distribution inside the reservoir is important as in interference testing and coning.

The pressure derivative with respect to time is another variable, besides pressure itself, that is used in well testing. A pressure derivative shows the sensitivity of the

wellbore pressure with respect to time. This information, applied both qualitatively and quantitatively, helps demonstrate the flow regimes, the closeness to no-flow barriers or boundaries, water table movement, and so forth. As the potential equations discussed above are not true solutions, but incorporate several assumptions and approximations, the quality and the accuracy of the pressure derivative is compromised. The same is true for vertical, partially, penetrating wells and fractures.

At this time, no steady-state potential equation has been provided for partially penetrating horizontal wells and fractures.

Consequently, the principal objective of this work is to use potential theory for line and plane sources with finite length and arbitrary configuration in a reservoir with arbitrary outer boundary conditions to derive the solutions for the following cases:

1. transient potential;

2. potential derivative;

3. steady state potential;

4. productivity index.

A study of the flow regimes and drainage areas described by this solutions is also undertaken.

One common application of vertical or horizontal, partially-penetrating wellbores is in reservoirs with bottom water and/or a gas cap. To examine the application of the new potential solutions to these conditions, one needs to know the type of outer boundary

condition which pertains. Different types of outer boundary conditions are defined in the literature for modeling bottom water or a gas cap.

The final objective of this work is to consider coning and the performance of a vertical or a horizontal well in bottom-water and gas-cap reservoirs. Specifically it is planned to:

1) Investigate the boundary conditions;

2) Develop the cone height equation, find the critical production rate and breakthrough time;

3) Study the wellbore performance in the presence of a growing cone.

A schematic representation of the different problems studied in this thesis is given in Figure 3.1.

Horizontal wells   Vertical partially-penetrating wells   Fractures

| Uniform Flux IBC solution | Uniform Potential IBC solution | Uniform flux IBC solution | Uniform potential IBC solution |

Steady State   Unsteady State   Steady state   **Productivity index**

Productivity index   static boundary   Bottom water or a gas cap   Unsteady State   **Pressure response P_D vs t_D**

Drainage area   **Pressure response of the wellbore (P_D vs t_D)**   **Time of breakthrough**

Pressure derivative with respect to time and flow regimes

Water and/or gas coning

Critical production rate

Optimal well perforation interval size and location

Figure 3.1:   Flow diagram showing statement of the problem. The objectives are shown in highlighted boxes.

CHAPTER 4

TYPES OF SOURCES

To simplify the discussion in the following chapters, the sources are clasified in this chapter. Also, here, the transient potential solutions for point sources in a rectilinear reservoir (infinite slab) and semi-infinite slab reservoir are presented. The potential solution for other sources from the literature are presented in Appendices A, B and C. These are used in subsequent chapter to develop the discrete flux element (DFE) method.

4.1 Classification of Sources

As the potential equation of a line source with infinite length is not affected by end effects, the flow into the wellbore at any section perpendicular to the wellbore is radial. This implies that the both potential and the flux into the wellbore are uniform along the wellbore. The potential equation for such wellbores can be obtained by integrating the solution of a point source over the length of the source i.e. from $-\infty$ to $+\infty$ [Kelvin, 1884, and Carslaw and Jaeger, 1959]. However, also, due to the radial nature of the flow into the wellbore, the potential can be found directly by solving the diffusivity equation in the radial form (Equation 4.1.1).

$$\frac{1}{r}\frac{\partial}{\partial r}\left(r\frac{\partial p}{\partial r}\right) = \frac{1}{K}\frac{\partial p}{\partial t} \qquad \qquad \dots\dots\dots\dots\dots\dots(4.1.1)$$

Both methods leads to the *Exponential Integral* or E_i solution.

For cases where the wellbore is not fully penetrating, the flow into the wellbore at the end(s) is spherical. The effect of this on the well performance is called "end effect". These are classified in this work as sources with finite length. Muskat [1932] showed that the flux into the wellbore is non-uniform due to the existence of the end effects. Therefore the Laplace or diffusivity equation in radial form cannot be applied as the governing differential equation in reservoirs being produced by such wellbores. Instead, the true potential equation will have to be a 3-D partial differential equation.

The potential equation for a fracture with infinite dimensions can also be derived by the double integral of a point source over the lengths of the fracture; that is X and Y from $-\infty$ to $+\infty$. This solution can be obtained also by solving the Laplace or diffusivity equations in 1-dimensional form (Equation 4.1.2).

$$\frac{\partial^2 p}{\partial X^2} = \frac{1}{K}\frac{\partial p}{\partial t} \quad\quad\quad\quad\quad\quad\quad\quad\quad\quad\quad\quad\quad\quad\quad\quad\quad\quad\quad ....(4.1.2)$$

Similar to the case of line sources, the potential equation of the fractures with infinite length satisfies both uniform flux as well as uniform potential Inner Boundary Conditions (IBC), simultaneously. However, for fractures with finite length(s), due to the end effects, the flow into the fracture is non-uniform.

For simplicity of discussion through this work, in Section 4.1.1 the sources are classified based on the governing differential equations (dimensions of the source). However, in Section 4.1.2 line sources are classified based on their geometry with respect to reservoir boundaries.

4.1.1. Classification Based on the Dimensions of the Source

4.1.1.1   Sources with Infinite Length(s)

Line source. This type of source is characterized by radial flow into the line source. The most common type of these sources is fully penetrating wells in rectilinear reservoirs. The potential equation of these sources can be derived directly by solving the diffusivity equation in radial form which leads to the *exponential integral* or E_i (Theis) solution. Carslaw and Jaeger [1959] showed that the same solution can be obtained also by integrating the solution of a point source from $-\infty$ to $+\infty$.

Plane source (Fracture). This type of source is characterized by linear flow into a plane. A good example of this type of flow is channel flow. The potential equation can be derived by solving the 1-D governing differential equation directly (Equation 4.1.2). However, taking a double integral of the solution of a point source over the length and height of the fracture leads to the same potential equation [Carslaw and Jaeger, 1959].

4.1.1.2.   Sources with Finite Length

Line source. This type of source is characterized by semi-spherical flow at the end(s) of the wellbore. The flow into the wellbore is not radial due to the end effects. Therefore, the governing differential equation is the diffusivity or Laplace's equation in 3-dimensional form. The most common example of this type of problem is the partially penetrating wellbore in vertical or horizontal wells.

Plane source (Fracture). The flow characteristics of this type of source are: i) semi-radial flow at the end(s), and ii) linear flow at the center of the fracture. Depending on the

fracture dimension, linear or radial flow may be dominant. The governing differential equation for production from such sources is 3-D.

A direct solution of the 3-D governing partial differential equations for line or plane sources is impractical and has not been presented yet. Moreover, integrating the solution of a point source is possible only by making use of the uniform flux assumption, and this leads to unrealistic flow characteristics.

4.1.2 Classification of Line Sources

At first glance, a horizontal and a vertical line source look different. But, the governing differential equations have to be solved for the potential (hydraulic, electrical or thermal). Consequently, from a derivation point of view, there is no difference between horizontal and vertical sources. The main factor that could be used for classification of line sources is the type of outer boundary and its position with respect to the source.

4.1.2.1 Line Sources in Rectilinear Reservoir (Infinite Slab)

Fully penetrating wells. This type of source is perpendicular to the no-flow boundaries (see Figure 4.1.2.1.1). The potential solution for this type of source is derived exactly as the exponential integral. As petroleum reservoirs are mostly horizontal, a fully penetrating well in such a reservoir is vertical. However, for an infinite solid slab, with a thermal or electrical source, regardless of the position of the slab, the governing potential equation is always exponential integral.

The flow characteristic of this type of source is radial flow into the wellbore. The source can be either horizontal or vertical. Indeed this group is of the type of sources with infinite length.
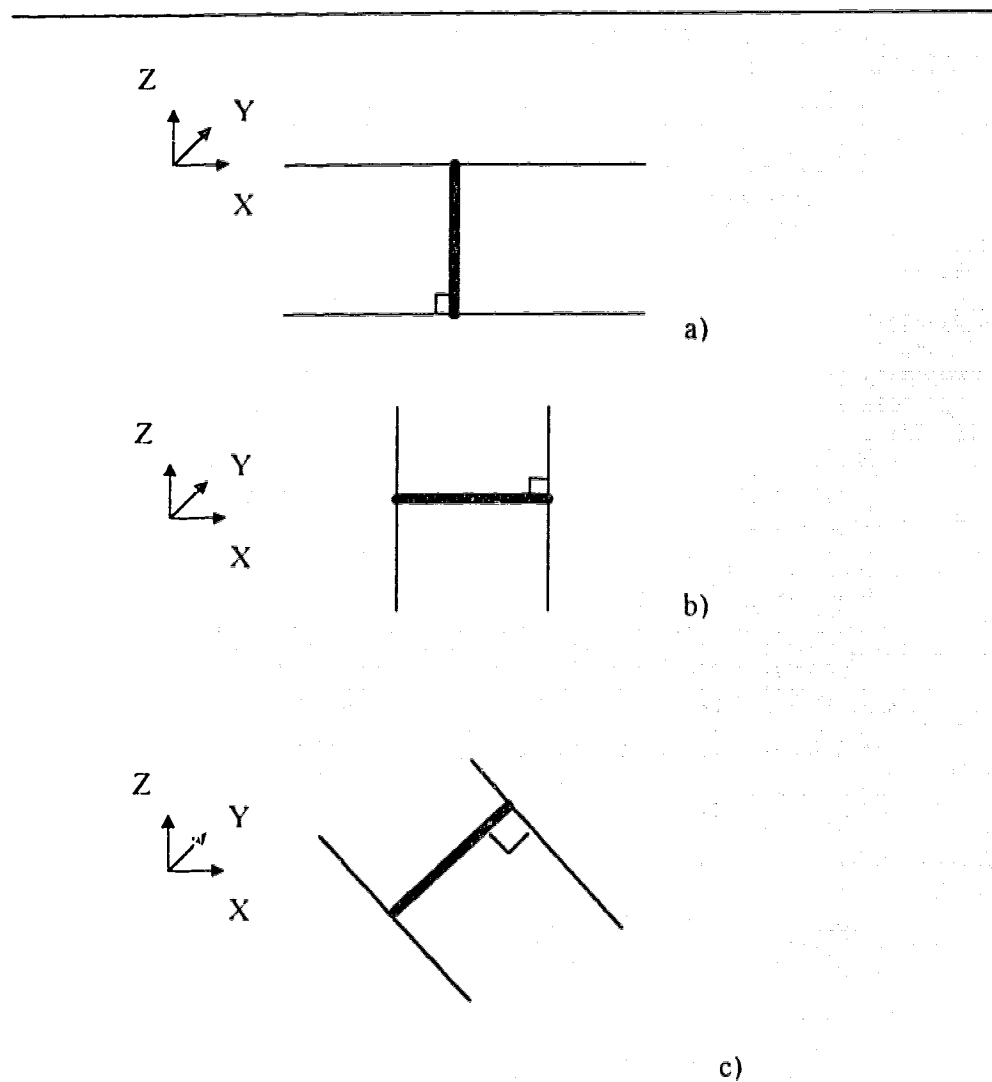
Figure 4.1.2.1.1:   Possible configurations of a vertical source;

a) in a horizontal slab, b) in a vertical slab and

c) in an inclined slab

Vertical partially penetrating wells. Here the wellbore direction is perpendicular to no-flow boundaries in a rectilinear reservoir (see Figure 4.1.2.1.2). However, the end(s) of the wellbore is not connected to these boundaries. This type of source is characterized by hemispherical flow at the end(s) of the wellbore and is of the type of the sources with finite length.
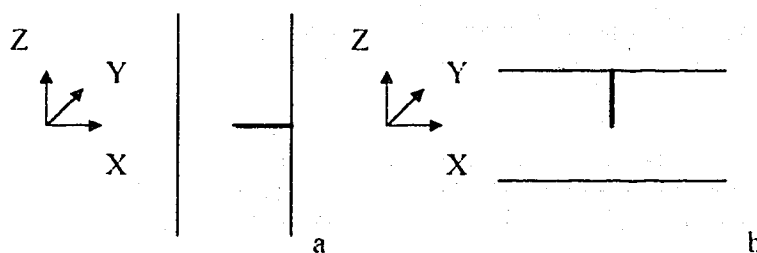
Figure 4.1.2.1.2:   Possible configurations of a vertical partially penetrating source in a) a vertical slab and b) a horizontal slab

Horizontal partially penetrating wells. Here the wellbore direction is parallel to the no-flow boundaries in a rectilinear reservoir (see Figure 4.1.2.1.3). This group is of the type of sources with finite length.
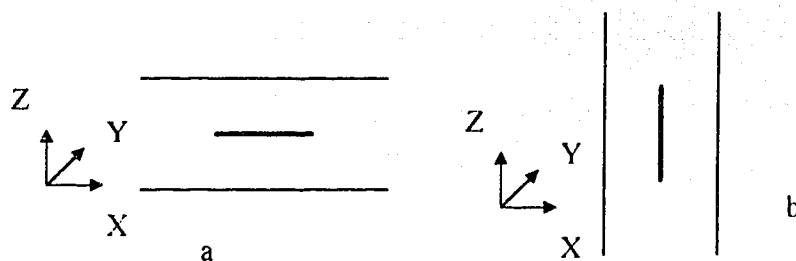
Figure 4.1.2.1.3:   Possible configurations of a horizontal partially penetrating source in a) a horizontal slab and b) a vertical slab

Inclined wells. The angle between the wellbore direction and the normal to the plane of the no-flow boundaries is between $0''$ and $90''$. As the flow into the wellbore is not radial this type of source belongs to the group of sources with finite length.

Line Sources With Irregular Geometry. Due to technical restrictions or to the geological structure of the reservoir, often happens that the well cannot be drilled in a straight direction. The best examples of this group are long horizontal wells. This type of source is also of the type of sources with finite length. The potential equation for this type of source, for the first time, is presented in this work (Chapter 5).

Line Sources in Semi-Infinite and Box-Shape Reservoirs. Any type of partial line sources in box-shaped or semi-infinite reservoirs are of the type of sources with finite length.

4.2   Point Source Potential Equation

The instantaneous and transient potential solution to a point source in an infinite, isotropic domain and steady-state solution to a point source in a rectilinear isotropic domain are presented in Appendix A. In this section 1) the definition for the flux term and the diffusivity coefficient for fluid flow problem, and 2) the transient potential to a point source in anisotropic, infinite and rectilinear domains are developed. It is necessary to introduce the dimensionless variables first.

Dimensionless Variables. To put the potential equations into dimensionless form, an arbitrary reference length, a, is used. The appropriate reference length in a reservoir with constant thickness is

$$a = 2h_t$$ ....(4.2.1)

where, h_t is the reservoir thickness.

The remaining dimensionless variables can be defined using a.

Thus the potential of a continuous point source (Equation A.2.1) in dimensionless form can be written as:

$$\varphi_D = \frac{1}{2r_D} \operatorname{erfc} \frac{r_D}{\sqrt{4t_D}}$$ ....(4.2.2)

where

$$\varphi_D = \frac{2\pi k a}{Q\mu} \Delta\varphi$$ ....(4.2.3)

and where

$$\varphi = p - \gamma g z,$$ ....(4.2.4)

$$t_D = \frac{kt}{\mu\phi c_t a^2},$$ ....(4.2.5)

$$r_D = \frac{r}{a},$$ ....(4.2.6)

$$r_D = \left(x^2 + y^2 + z^2\right)^{1/2},$$ ....(4.2.7)

$$x = \frac{X}{a},$$ ....(4.2.8)

$$y = \frac{Y}{a},$$ ....(4.2.9)

and

$$z = \frac{Z}{a} .$$ ....(4.1.10)

4.2.1 Flux Term and Diffusion Coefficient for Fluid Flow Problems

For a fluid flow problem, the diffusivity coefficient is defined as [Earlougher, 1977]:

$$K = \frac{k}{\mu \phi c_t}$$ ....(4.2.1.1)

where k, μ, ϕ and c_t are the permeability, viscosity, porosity and total compressibility, respectively.

The definition of the flux, q, for a thermal problem was obtained by Carslaw and Jaeger [1959]. By analogy, the definition of the flux, q, for fluid flow problems is derived as follows.

For a point source with a total flux Q in an isotropic infinite domain one can write:

$$Q = \int_{-\infty}^{+\infty} \int_{-\infty}^{+\infty} \int_{-\infty}^{+\infty} \phi c_t \varphi dX dY dZ$$ ....(4.2.1.2)

where φ is the instantaneous potential given by Equation A.1.2 as:

$$\varphi(X,Y,Z,t) = \frac{q}{8(\pi K t)^{3/2}} e^{-\left[(X-X')^2+(Y-Y')^2+(Z-Z')^2\right]/4Kt}$$ ....(A.1.2)

Substituting φ from Equation A.1.2 into Equation 4.2.1.2:

$$Q = \frac{q\phi c_t}{8(\pi K_t)^{3/2}} \int_{-\infty}^{+\infty} e^{-(X-X')^2/4K_t} dX \cdot \int_{-\infty}^{+\infty} e^{-(Y-Y')^2/4K_t} dY \cdot \int_{-\infty}^{+\infty} e^{-(Z-Z')^2/4K_t} dZ$$

.................................(4.2.1.3)

Using the substitution [Gradshteyn and Ryzhik, 1980]:

$$\int_{-\infty}^{+\infty} e^{-X^2 p^2} dX = \frac{\sqrt{\pi}}{p}$$

.................................(4.2.1.4)

one obtains:

$$Q = q\phi c_t$$

.................................(4.2.1.5)

or

$$q = \frac{Q}{\phi c_t}$$

.................................(4.2.1.6)

4.2.2   Continuous Point Source in an Infinite Anistropic Domain

The instantaneous point source solution in an anisotropic domain is given in Appendix A:

$$\varphi(X,Y,Z,t) = \frac{q}{8(\pi t)^{3/2}(K_X K_Y K_Z)^{1/2}} e^{-\left[(X-X')^2 K_X + (Y-Y')^2 K_Y + (Z-Z')^2 K_Z\right]/4t}$$ ....(A.1.3)

where K_X, K_Y and K_Z are the diffusivity coefficients in each of the X-, Y- and Z-directions. A simple form of Equation A.1.3 can be found.

From Equations 4.2.1.1 and 4.2.1.6 the diffusivity coefficients and flux term can be written as:

$$K_X = \frac{k_x}{\mu\phi c_t},$$ ....(4.2.2.1)

$$K_Y = \frac{k_y}{\mu\phi c_t},$$ ....(4.2.2.2)

$$K_Z = \frac{k_z}{\mu\phi c_t}$$ ....(4.2.2.3)

and

$$q = \frac{Q}{\phi c_t}$$ ....(4.2.2.4)

Applying Equations 4.2.2.1 to 4.2.2.4 Equation A.1.3 reduces to:

$$\varphi = \frac{Q(\mu\phi c_t)^{3/2}}{8\left(\pi^3 t^3 K_X K_Y K_Z\right)^{1/2}} \exp\left\{-\frac{\mu\phi c_t}{4t}\left[\frac{(X-X')^2}{k_X} + \frac{(Y-Y')^2}{k_Y} + \frac{(Z-Z')^2}{k_Z}\right]\right\}$$

.................................(4.2.2.5)

Defining:

$$\alpha = \sqrt{\frac{k_Y}{k_X}}$$ ....(4.2.2.6)

and

$$\beta = \sqrt{\frac{k_Z}{k_X}}$$ ....(4.2.2.7)

Equation 4.2.2.5 reduces to:

$$\varphi = \frac{1}{\alpha\beta} \frac{Q(\mu\phi c_t)^{3/2}}{8\left(\pi^3 t^3 K_x^3\right)^{1/2}} \exp\left\{-\frac{\mu\phi c_t}{4tk_x}\left[\frac{(X-X')^2}{1} + \frac{(Y-Y')^2}{\alpha^2} + \frac{(Z-Z')^2}{\beta^2}\right]\right\}$$

$$\dots\dots\dots\dots\dots\dots\dots(4.2.2.8)$$

Defining

$$r^2 = (X-X')^2 + \left(\frac{Y-Y'}{\alpha}\right)^2 + \left(\frac{Z-Z'}{\beta}\right)^2 \qquad \dots\dots\dots\dots\dots\dots\dots(4.2.2.9)$$

Equation 4.2.2.8 reduces to:

$$\varphi = \frac{1}{\alpha\beta} \frac{Q}{8(\pi tK)^{3/2}} \exp\left[-\frac{r^2}{4Kt}\right] \qquad \dots\dots\dots\dots\dots\dots\dots(4.2.2.10)$$

where

$$K = \frac{k_x}{\mu\phi c_t} \qquad \dots\dots\dots\dots\dots\dots\dots(4.2.2.11)$$

Equation 4.2.2.10 defines the potential of an instantaneous point source in an anisotropic reservoir with anisotropic coefficients, α and β, given by Equations 4.2.2.6 and 4.2.2.7.

Integrating with respect to time from 0 to t, in Equation 4.2.2.10, and substituting K from Equation 4.2.2.11, one can find the continuous potential solution as:

$$\varphi = \frac{1}{\alpha\beta} \frac{Q\mu}{4\pi k_x r} \mathrm{erfc}\left(\frac{r}{\sqrt{4\frac{k_x}{\mu\phi c_t}t}}\right) \qquad \dots\dots\dots\dots\dots\dots\dots(4.2.2.12)$$

Equation 4.2.2.12 in dimensionless form can be written as:

$$\varphi_{D} = \frac{1}{\alpha\beta}\frac{1}{2r_{D}}\operatorname{erfc}\frac{r_{D}}{\sqrt{4t_{D}}} \qquad \dots\dots\dots\dots(4.2.2.13)$$

where the dimensionless parameters are now defined with respect to K_x:

$$\varphi_{D} = \frac{2\pi k_x a}{Q\mu}\Delta\varphi \qquad \dots\dots\dots\dots(4.2.2.14)$$

$$t_{D} = \frac{k_x t}{\mu\phi c_t a^2} \qquad \dots\dots\dots\dots(4.2.2.15)$$

and

$$r_{D} = \frac{r}{a} \qquad \dots\dots\dots\dots(4.2.2.16)$$

Assuming both α and β equal to 1, Equation 4.2.2.13 reduces to Equation 4.2.2 which provides the solution for a point source in an isotropic reservoir.

4.2.3 Continuous Point Source in a Rectilinear (Infinite Slab) Anisotropic Reservoir

The term rectilinear is used here to describe an infinite slab reservoir.

The performance of a source depends on the boundary conditions. Typically, no-flow or constant potential BCs are found in reservoir engineering.

Solving partial differential equations for different combinations of outer boundary conditions is difficult and sometimes impossible without further simplifying assumptions. However, the Method of Images can be used to introduce a no-flow or a constant potential boundary into an existing solution. The Method of Images and mirrors originated

with the discovery of crystal structure and crystallography science, and was used by Madelung [Muskat, 1932] in electrical science to model a steady state point source in a rectilinear solid. Muskat [1932] modified that point source solution for fluid flow problems.

In this section the transient solution of a point source in a rectilinear reservoir, by application of the Method of Images to Equation 4.2.2.13 (Figure 4.2.3.1), is derived as;

$$\varphi_D(R,w) = \frac{1}{\alpha\beta}\left(\sum_{N=0}^{\infty}\frac{1}{2R_1}\text{erfc}\frac{R_1}{\sqrt{4t_D}} + \sum_{N=0}^{\infty}\frac{1}{2R_2}\text{erfc}\frac{R_2}{\sqrt{4t_D}} + \right.$$

$$\left.\sum_{N=1}^{\infty}\frac{1}{2R_3}\text{erfc}\frac{R_3}{\sqrt{4t_D}} + \sum_{N=1}^{\infty}\frac{1}{2R_4}\text{erfc}\frac{R_4}{\sqrt{4t_D}}\right)$$

.............................(4.2.3.1)

where

$$R_1 = \left[R^2 + (N+w+c)^2/\beta^2\right]^{1/2}.$$ ....(4.2.3.2)

$$R_2 = \left[R^2 + (N+w-c)^2/\beta^2\right]^{1/2}$$ ....(4.2.3.3)

$$R_3 = \left[R^2 + (N-w+c)^2/\beta^2\right]^{1/2}$$ ....(4.2.3.4)

$$R_4 = \left[R^2 + (N-w-c)^2/\beta^2\right]^{1/2}$$ ....(4.2.3.5)

and where

$$R = \left[(x-x')^2 + (y-y')^2/\alpha^2\right]^{1/2}$$ ....(4.2.3.6)

where w is the dimensionless vertical coordinate (z) of an arbitrary point.
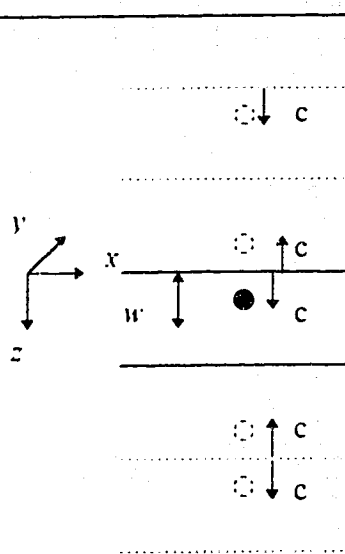
Figure 4.2.3.1: Schematic drawing of Method of Images.

4.2.4. Transient Point Source in a Semi-Infinite Slab

Applying the Method of Images one can introduce a no-flow boundary (see Figure 4.2.4.1) perpendicular to the no-flow upper and lower boundaries. The resulting mathematical solution models the performance of a source in front of a vertical barrier.
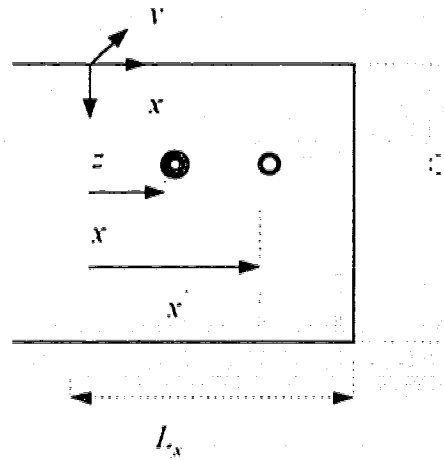
Figure 4.2.4.1: Modeling a no-flow barrier by the Method of Images.

$$\varphi_D(R,w) = \frac{1}{\alpha\beta} \{ \sum_{N=0}^{\infty} \frac{1}{2R_1} \mathrm{erfc} \frac{R_1}{\sqrt{4t_D}} + \sum_{N=0}^{\infty} \frac{1}{2R_2} \mathrm{erfc} \frac{R_2}{\sqrt{4t_D}} +$$

$$\sum_{N=1}^{\infty} \frac{1}{2R_3} \mathrm{erfc} \frac{R_3}{\sqrt{4t_D}} + \sum_{N=1}^{\infty} \frac{1}{2R_4} \mathrm{erfc} \frac{R_4}{\sqrt{4t_D}} +$$

$$\sum_{N=0}^{\infty} \frac{1}{2R_1'} \mathrm{erfc} \frac{R_1'}{\sqrt{4t_D}} + \sum_{N=0}^{\infty} \frac{1}{2R_2'} \mathrm{erfc} \frac{R_2'}{\sqrt{4t_D}} +$$

$$\sum_{N=1}^{\infty} \frac{1}{2R_3'} \mathrm{erfc} \frac{R_3'}{\sqrt{4t_D}} + \sum_{N=1}^{\infty} \frac{1}{2R_4'} \mathrm{erfc} \frac{R_4'}{\sqrt{4t_D}} \}$$

..............................(4.2.4.1)

where

$$R_1 = \left[R^2 + (N + w + c)^2 / \beta^2 \right]^{1/2} .$$ ....(4.2.4.2)

$$R_2 = \left[R^2 + (N + w - c)^2 / \beta^2 \right]^{1/2} \qquad \text{.............................(4.2.4.3)}$$

$$R_3 = \left[R^2 + (N - w + c)^2 / \beta^2 \right]^{1/2} \qquad \text{.............................(4.2.4.4)}$$

$$R_4 = \left[R^2 + (N - w - c)^2 / \beta^2 \right]^{1/2} \qquad \text{.............................(4.2.4.5)}$$

$$R = \left[(x - x')^2 + (y - y')^2 / \alpha^2 \right]^{1/2} \qquad \text{.............................(4.2.4.6)}$$

$$R_1' = \left[R'^2 + (N + w + c)^2 / \beta^2 \right]^{1/2} . \qquad \text{.............................(4.2.4.7)}$$

$$R_2' = \left[R'^2 + (N + w - c)^2 / \beta^2 \right]^{1/2} \qquad \text{.............................(4.2.4.8)}$$

$$R_3' = \left[R'^2 + (N - w + c)^2 / \beta^2 \right]^{1/2} \qquad \text{.............................(4.2.4.9)}$$

$$R_4' = \left[R'^2 + (N - w - c)^2 / \beta^2 \right]^{1/2} \qquad \text{.............................(4.2.4.10)}$$

and where

$$R' = \left[(x + x' - 2 I_x)^2 + (y - y')^2 / \alpha^2 \right]^{1/2} \qquad \text{.............................(4.2.4.11)}$$

where w is the dimensionless vertical coordinate (z) of an arbitrary point.

CHAPTER 5

DEVELOPMENT OF DISCRETE FLUX ELEMENT (DFE) METHOD

As discussed earlier several approximate solutions for the pressure and pressure derivatives of horizontal wells with uniform flux and straight configuration assumptions [Clonts and Ramey, 1986, Daviau et al., 1988, Kuchuk et al., 1988] have been presented in the literature. Rosa and Carvalho [1989] presented an infinite conductivity pressure solution for horizontal wells with straight configuration. It may be of concern that the pressure derivatives evaluated by these approximations vary in value, and that this could affect interpretation in pressure transient analysis and productivity calculations. Specific limitations of these solutions include:

i)   *Geometry of the source:* Horizontal wells are assumed to be a straight line source in the direction of one of the principal axes, but most wellbores, particularly horizontal ones, are curvilinear. If the wellbore were not in the direction of one of the principal axes of the medium the K-matrix would be a tensor with 9 elements. Thus, by assuming a straight line source in the direction of one of the principal axes one neglects the 6 flow components which directly affect the potential of the source as will be shown below.

Darcy's law in an anisotropic domain in the simplest form can be written as [Collins, 1961]:

$$v_i = -\frac{\rho}{\mu}\left(K_{i1}\frac{\partial\varphi}{\partial x_1} + K_{i2}\frac{\partial\varphi}{\partial x_2} + K_{i3}\frac{\partial\varphi}{\partial x_3}\right) \qquad i = 1,2,3 \qquad \text{............(5.1)}$$

where, in this notation, 1,2 and 3 represent the x, y and z directions and V_i is the volumetric flux, ρ and μ are the fluid density and viscosity, respectively, and φ is the potential. Equation 5.1, in a general form, can be written as:

$$v_i = \frac{\rho}{\mu}Kij\frac{\partial\varphi}{\partial x_j} \qquad (i=1,2,3 \text{ and } j=1,2,3)$$

$$\text{............(5.2)}$$

where K_{ij} is a tensor with nine elements:

$$K = \begin{pmatrix} K_{11} & K_{12} & K_{13} \\ K_{21} & K_{22} & K_{23} \\ K_{31} & K_{32} & K_{33} \end{pmatrix} \qquad \text{............(5.3)}$$

Assuming that the K-matrix is symmetric, one can rotate it to a particular coordinate system (principal axes of the medium) to produce a diagonal matrix called the K'-matrix:

$$K' = \begin{pmatrix} K_1 & 0 & 0 \\ 0 & K_2 & 0 \\ 0 & 0 & K_3 \end{pmatrix} \qquad \text{............(5.4)}$$

Thus, it can be inferred that the coordinate system, of any potential solution with three orthogonal principal permeability components, is parallel to the principal axes of the porous medium. Therefore, when using the product of three 1-D solutions (Green's function) in the x, y and z directions [Clonts and Ramey, 1986, and Daviau et al., 1988], one implicitly assumes that the wellbore is in the direction of a principal axis of the

medium. However, the configuration of most horizontal wells is irregular and independent of the principal axes.

Assuming a straight configuration along a principal axis, one neglects six flow components (Equation 5.1):

$$v_1 = -\frac{\rho}{\mu}\left(K_{12}\frac{\partial\varphi}{\partial x_2} + K_{13}\frac{\partial\varphi}{\partial x_3}\right) \quad\quad\quad ....(5.5)$$

$$v_2 = -\frac{\rho}{\mu}\left(K_{21}\frac{\partial\varphi}{\partial x_1} + K_{23}\frac{\partial\varphi}{\partial x_3}\right) \quad\quad\quad ....(5.6)$$

$$v_3 = -\frac{\rho}{\mu}\left(K_{31}\frac{\partial\varphi}{\partial x_1} + K_{32}\frac{\partial\varphi}{\partial x_2}\right) \quad\quad\quad ....(5.7)$$

ii) ***Potential distribution inside the reservoir***: Even if one uses an equivalent pressure point to get an approximate value for the potential on the surface of a wellbore or a fracture, how can one calculate the potential distribution inside the reservoir? The potential distribution inside the reservoir is required for

      a)   Interference well testing;

      b)   Coning;

      c)   Flow mechanisms:

      d)   Drainage area calculation.

In addition no steady-state solution has been presented in the literature for, partially penetrating, horizontal wells and fractures.

In this chapter, a new general solution for the potential of sources with finite length and arbitrary geometry is presented. Applying this method one can determine the potential and potential derivative for both uniform flux and uniform potential IBCs for any type of outer boundary conditions for any source type such as:

1. Horizontal or inclined wells with straight or curvilinear configuration.

2. Vertical, fully or partially penetrating wells.

3. Arbitrary geometry fractures.

This general solution can be used for both transient and steady state conditions. In the next chapters the application of this method will be shown by solving several problems in petroleum reservoir engineering. However, the dimensionless potential is provided, it can be used generally in other applications of potential theory with the appropriate coefficient of diffusivity.

5.1   Potential Equation

The potential due to a source is the solution of the diffusivity equation in the form of:

$$K_x \frac{\partial^2 \varphi}{\partial X^2} + K_y \frac{\partial^2 \varphi}{\partial Y^2} + K_z \frac{\partial^2 \varphi}{\partial Z^2} = \frac{\partial \varphi}{\partial t} \qquad \ldots\ldots\ldots\ldots\ldots\ldots\ldots\ldots(A.1.3)$$

A direct solution to this equation for an arbitrary source with respect to potential theory is impractical. However, it has been solved for an instantaneous point source [Kelvin, 1884]:

$$\varphi(X,Y,Z,t) = \frac{q}{8(\pi t)^{3/2}(K_X K_Y K_Z)^{1/2}} \, e^{-\left[(X-X')^2 K_X + (Y-Y')^2 K_Y + (Z-Z')^2 K_Z\right]4t} \quad \dots\dots(A.1.4)$$

The potential due to an arbitrary source can be obtained by integrating the point source solution over the volume of that source [Kelvin, 1884]. For sources with infinite dimensions in the direction of the principal axis of the medium, this method provides an exact solution based on potential theory. However, the application of this method for sources with finite length is associated with certain assumptions that were discussed earlier in this chapter.

The solution due to a line source can be obtained by integration of a point source over the length of the source (Figure 5.1.1):

$$\varphi_L(x,y,z,t) = \int_a^h \int_0^t q(x',y',z',\tau)\varphi_p^{ms}(x-x',y-y',z-z',\tau)dldt \quad \dots\dots(5.1.1)$$
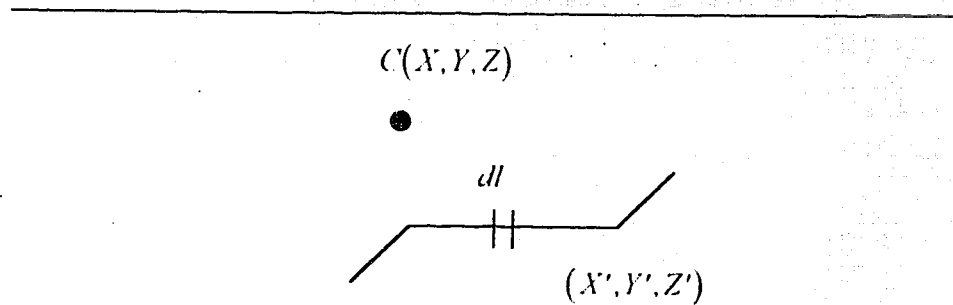
Figure 5.1.1: A line source with arbitrary geometry in an infinite domain

where $\varphi_L(x,y,z,t)$ is the potential due to a line source at point $c(x,y,z)$ at time t, $\varphi_p^{ins.}$ is the potential due to an instantaneous point source located on the line source with strength q, $a(x_a,y_a,z_a)$ and $h(x_h,y_h,z_h)$ are the two ends of the integration path and

$$(dl)^2 = (dx)^2 + (dy)^2 + (dz)^2.$$ ....(5.1.2)

It was shown in Chapter 2 for sources with infinite length and straight configuration that the uniform flux IBC is a valid assumption. However, for sources with finite length, q is a function of time and position in space (x',y',z').

By applying superposition in time one can remove q from under the first integral:

$$\varphi_L(x,y,z,t) = \int_a^h q(x',y',z',t) \int_0^t \varphi_p^{ins.}(x-x',y-y',z-z',\tau)\,dl\,d\tau$$ ....(5.1.3)

The integral of an instantaneous point source over time is actually the solution for a continuous point source:

$$\varphi_L(x,y,z,t) = \int_a^h q(x',y',z',t)\varphi_p^{cont.}(x-x',y-y',z-z',t)\,dl$$ ....(5.1.4)

This integration can be completed by applying various assumptions such as:

1. uniform flux IBC,

2. straight line configuration,

3. the direction of the wellbore is in the direction of one of the principal permeabilities.

The final form of Equation 5.1.4 has to be integrated numerically.

Eliminating the above restrictions this study presents a new solution called the *"Discrete Flux Element (DFE) Method"*.

Changing the integral sign into a series one can write:

$$\varphi_L(x,y,z,t) = \sum_{i=1}^{n} q_i(x_i,y_i,z_i,t) \varphi_{p_i}^{cont.}(x-x_i,y-y_i,z-z_i,t)$$

$$\dots\dots\dots\dots\dots\dots\dots\dots(5.1.5)$$

where n is the number of flux elements, q_i is the strength of the ith flux element and $\varphi_{p_i}^{cont.}$ is the potential of the ith flux element at point (x,y,z).

A schematic of this model, is shown in Figure 5.1.2.
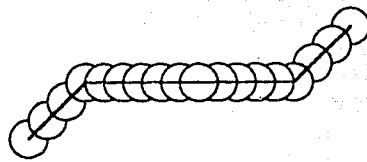
Figure 5.1.2.: Schematic drawing of the line source with irregular geometry modeled by DFE Method

The series in Equation 5.1.5 will converge once the distance between two flux elements becomes equal to the well radius (Section 5.3). Writing the potential in the form of Equation 5.1.5. has certain advantages.

i) The geometry of the source can be taken into account without losing accuracy. It can be used for modeling the potential of vertical, horizontal, inclined and curvilinear line sources.

ii) All the point source (flux elements) solutions are in a coordinate system parallel to the principal axes of the medium. Thus a line source with arbitrary direction can be modeled without rotation of the coordinate system.

iii) Any type of outer boundary condition (sealed, constant potential or mixed) can be modeled using the method of images.

iv) A uniform flux or uniform potential inner boundary condition is possible.

For a horizontal well extending from (x_1, y_w, z_w) to (x_2, y_w, z_w) Equation 5.1.5. can be written as:

$$\varphi_L(x,y,z,t) = \sum_{i=1}^{n} q_i(x_i, y_w, z_w, t) \varphi_{p_i}^{cont.}(x - x_i, y - y_w, z - z_w, t)$$

.................................(5.1.6)

where

$$x_i = x_1 + i \times \delta x$$

.............................(5.1.7)

and

$$\delta x = r_w$$

...............................(5.1.8)

where

$$n = \frac{x_2 - x_1}{\delta x} + 1 \qquad \qquad \dots\dots\dots\dots\dots\dots(5.1.9)$$

Line source with uniform flux IBC

For a uniform flux IBC (using normalized total flux = 1):

$$q_i = \frac{1}{n} \qquad \qquad \dots\dots\dots\dots\dots\dots(5.1.10)$$

Therefore, Equation 5.1.5 reduces simply to:

$$\varphi_L(x, y, z, t) = \frac{1}{n} \sum_{i=1}^{n} \varphi_p^{cont.}(x - x_i, y - y_i, z - z_i, t) \qquad \dots\dots\dots\dots\dots(5.1.11)$$

Line Source With Uniform Potential IBC

For a uniform potential IBC, one must find the flux distribution along the source. Therefore one needs $n + 1$ equations to solve for the flux strengths of n flux elements and the source potential.

Of the total, n equations are found by writing the solutions for potential at the surface of n flux elements. Using the dimensionless form these are:

$$\varphi_{Lsw} = q_1 \varphi_{D11} + q_2 \varphi_{D12} + \dots + q_n \varphi_{D1n}$$

$$\varphi_{Lsw} = q_1 \varphi_{D21} + q_2 \varphi_{D22} + \dots + q_n \varphi_{D2n}$$

$$\varphi_{Lsw} = q_1 \varphi_{D31} + q_2 \varphi_{D32} + \dots + q_n \varphi_{D3n}$$

$$\varphi_{Lsw} = q_1 \varphi_{Dn1} + q_2 \varphi_{Dn2} + \dots + q_n \varphi_{Dnn}$$

$$\dots\dots\dots\dots\dots\dots(5.1.12)$$

The $(n - 1)$st equation is the total flux strength constraint equation:

$$\sum_{i=1}^{n} q_i = 1$$ ....(5.1.13)

The complete system of equations can be written in matrix form as:

$$
\begin{bmatrix}
\varphi_{D11} & \varphi_{D12} & \cdots \varphi_{D1n} & -1 \\
\varphi_{D21} & \varphi_{D22} & \cdots \varphi_{D2n} & -1 \\
\cdots & & & \\
\varphi_{Dm1} & \varphi_{Dm2} & \cdots \varphi_{Dmn} & -1 \\
1 & 1 & 1 & 0
\end{bmatrix}
\begin{bmatrix}
q_1 \\
q_2 \\
\cdot \\
q_n \\
\varphi_{Dw}
\end{bmatrix}
=
\begin{bmatrix}
0 \\
0 \\
\cdot \\
0 \\
1
\end{bmatrix}
$$ ....(5.1.14)

Fracture

The potential due to flow to a fracture can be obtained by integration of the potential solution for an instantaneous line source with respect to time and the length of the fracture. Following the same approach used for a line source one can obtain an equation similar to Equation 5.1.5 for a fracture. For a vertical, fully penetrating fracture extending from x_1 to x_2 the potential can be written as:

$$\varphi_{fD}(x,y,t_D) = \sum_{i=1}^{n} q_i(x_i,y_w,t_D)\varphi_{LDi}^{cont.}(x - x_i, y - y_w, t_D).$$

..................(5.1.15)

where, φ_{fD} is the dimensionless potential due the fracture and φ_{LDi} is the dimensionless potential due to the ith flux element, with flux q_i.

Outer Boundary Conditions

Any type of outer boundary condition can be introduced into the point source solution in Equation 5.1.5 by using the method of images. This method was explained in Chapter 4. Specific cases are illustrated in later chapters where the DFE method is applied to various real problems.

5.2 Potential Derivative

The potential derivative with respect to $\ln(t_D)$ is used to study flow regimes. The potential derivative with respect to $\ln(t_D)$ can be obtained using:

$$\frac{d\varphi_{DW}}{d\left(\ln(t_D)\right)} = t_D \frac{d\varphi_{DW}}{dt_D} \qquad \qquad \dots\dots\dots\dots\dots\dots\dots\dots\dots\dots\dots(5.2.1)$$

The potential equation in a general form can be written (using Equation 5.1.5):

$$\varphi_{DW} = \sum_{i=1}^{n} q_i \varphi_{PDi} , \qquad \qquad \dots\dots\dots\dots\dots\dots\dots\dots\dots\dots\dots(5.2.2)$$

where φ_{DW} is the potential due to the source, and φ_{PDi} is the potential of the ith flux element with flux q_i. Substituting Equation 5.2.2 into Equation 5.2.1, one can write:

$$\frac{d\varphi_{DW}}{d\left(\ln(t_D)\right)} = t_D \left(\sum_{i=1}^{n} \left(\varphi_{PDi} \frac{dq_i}{dt_D} + q_i \frac{d\varphi_{PDi}}{dt_D} \right) \right) \qquad \dots\dots\dots\dots\dots\dots\dots(5.2.3)$$

The derivative of the potential of a single point source is found from Equation 4.2.3.1 through 4.2.3.6:

$$\frac{d\varphi_{PD}}{dt_D} = \frac{1}{\alpha\beta} \frac{1}{4\pi\sqrt{t_D^3}} (\sum_{n=0}^{\infty} e^{\frac{-R_1^2}{4t_D}} + \sum_{n=0}^{\infty} e^{\frac{-R_2^2}{4t_D}} + \sum_{n=1}^{\infty} e^{\frac{-R_3^2}{4t_D}} + \sum_{n=1}^{\infty} e^{\frac{-R_4^2}{4t_D}}) \quad\text{..............(5.2.4)}$$

where

$$R_1 = \left[R^2 + (N + w + c)^2 / \beta^2 \right]^{1/2} . \qquad\qquad\text{..................(5.2.5)}$$

$$R_2 = \left[R^2 + (N + w - c)^2 / \beta^2 \right]^{1/2} \qquad\qquad\text{..................(5.2.6)}$$

$$R_3 = \left[R^2 + (N - w + c)^2 / \beta^2 \right]^{1/2} \qquad\qquad\text{..................(5.2.7)}$$

and

$$R_4 = \left[R^2 + (N - w - c)^2 / \beta^2 \right]^{1/2} \qquad\qquad\text{..................(5.2.8)}$$

where

$$R = \left[(x - x')^2 + (y - y')^2 / \alpha^2 \right]^{1/2} \qquad\qquad\text{..................(5.2.9)}$$

Equation 5.2.3. can be used for both uniform flux and uniform potential IBC.

5.2.1 Uniform Flux IBC

For a uniform flux IBC and a constant production rate, the first term in Equation 5.2.3 is zero. Therefore Equation 5.2.3 reduces to:

$$\frac{d\varphi_{DW}}{d(\ln(t_D))} = \frac{t_D}{n} \sum_{i=1}^{n} \frac{d\varphi_{PD_i}}{dt_D} . \qquad\qquad\text{..................(5.2.1.1)}$$

5.2.2 Uniform Potential IBC

As was shown previously, a uniform potential IBC implies that the flux, q, be a function of time and coordinates. However, at late times, once the flow stabilizes, q is independent of time, yet it is a function of the coordinates. Therefore, the potential derivative at late and short times can be written as discussed below.

Late time potential derivative. At late times, after flow stabilization, the first term of Equation 5.2.3 becomes zero and thus

$$\frac{d\varphi_D}{d\left(\ln(t_D)\right)} = t_D \sum_{i=1}^{n} q_i \frac{d\varphi_{P_i}}{dt_D} .$$ ....(5.2.2.1)

Potential derivative before flow stabilization. As the function of q is unknown, the first term in Equation 5.2.3 can not be evaluated. In this study, numerical differentiation is used to evaluate the pressure derivative as follows:

$$\frac{d\varphi_{Dw}}{d\left(\ln(t_D)\right)} = t_D \left(\lim_{t_D' \to t_D} \frac{\varphi_{Dw}\left(t_D'\right) - \varphi_{Dw}\left(t_D\right)}{t_D' - t_D} \right) .$$ ....(5.2.2.2)

5.3   Convergence

To check the convergence of the series given by Equation 5.1.5, a horizontal well with $L_D = h_t$ and $r_{DW} = 0.001$ was modeled with different numbers of point sources. The resultant potential and its derivative with respect to $\ln(t_D)$ for different values of the distance between point sources are given in Figures 5.3.1 and 5.3.2, respectively. The potential value converges as the dimensionless distance between two flux elements

becomes equal to 0.002- 0.001 $\left(2r_{Dif} - r_{Dif}\right)$. However, the potential derivative. for all cases, converges at $t_D > 10^{-4}$. This indicates that beyond a certain time one can use large distances between the flux elements for calculating the pressure derivative.

The minimum in the pressure derivative curve (Figure 5.3.2) is the effect of the no-flow boundaries. Further explanation about this curve can be found in Section 6.1.
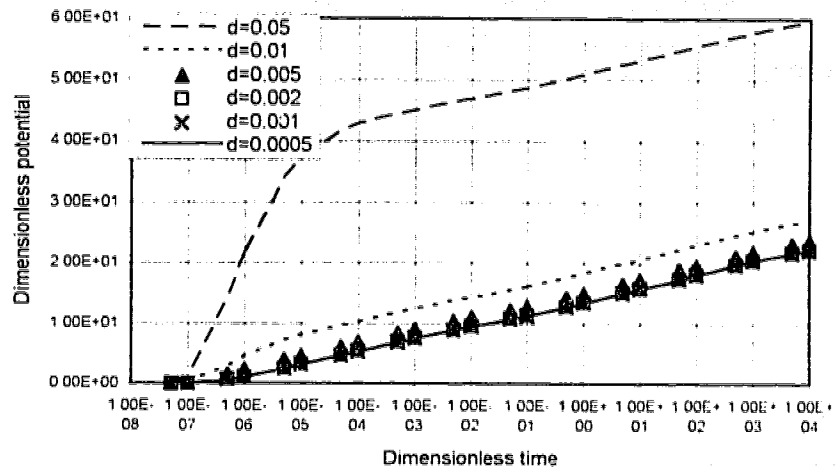
Figure 5.3.1: Potential of a horizontal well in a rectilinear reservoir with different distances d between the flux elements.
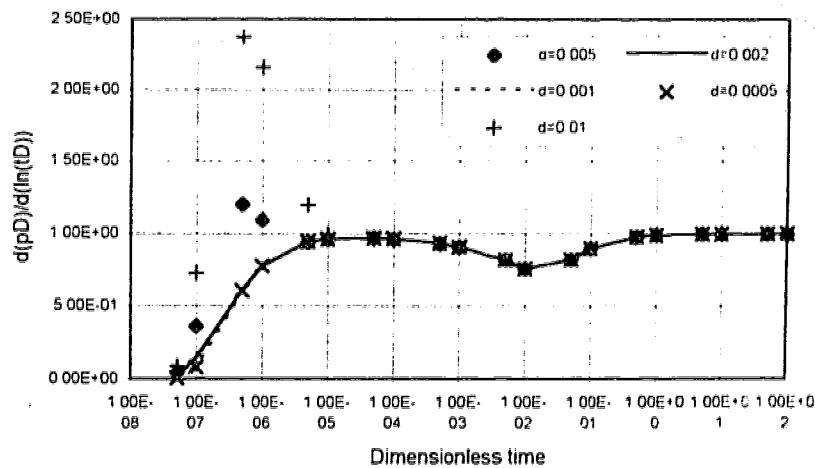
Figure 5.3.2: Potential derivative of a horizontal well in a rectilinear reservoir with different distances d between the flux elements.

5.4 Validity of the Discrete Flux Element Method

To check the validity of Equations 5.1.5 and 5.1.15, a vertical, fully penetrating line source and a vertical uniform flux solution fracture were modeled using the DFE method.

Vertical, Fully Penetrating Line Source

The exact solution for a vertical line source is known as the E_i or exponential integral solution:

$$\varphi_D = -E_i\left(-\frac{r_D^2}{4t_D}\right). \qquad\qquad\qquad\qquad (5.4.1)$$

A wellbore with $r_{DW} = 0.001$ is modeled using DFE method. Figure 5.4.1 shows that the potentials calculated from both the DFE method and the exponential integral solution are identical. Table 5.4.1 indicates that the potential values obtained using DFE Method are larger than those obtained using exponential integral in the range of 0.095% - 0.017% corresponding to short and late times.
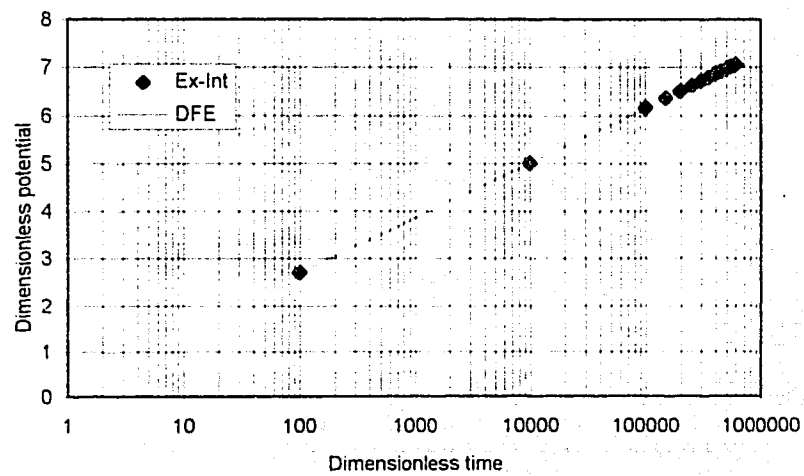
Figure 5.4.1: Comparison of the potential of a vertical fully penetrating wellbore modeled using the DFE method and exponential integral.

Table 5.4.1: Comparison of the pressures of a vertical fully penetrating wellbore with $R_{\eta\eta\tau} = 0.001$ in an isotropic reservoir obtained using the DFE Method and the exponential integral.

Dimensionless time	Dimensionless pressure		Error (%)
t_D	DFE Method (p_{DFE})	Ex. integral (p_{EX})	$100 \times \dfrac{(p_{EX} - p_{DFE})}{p_{EX}}$
2×10^{-5}	3.8209	3.8183	-0.095
6×10^{-5}	4.9113	4.9076	-0.075
1×10^{-4}	5.4204	5.4167	-0.068
4×10^{-4}	6.8048	6.8012	-0.053
8×10^{-4}	7.4977	7.494	-0.049
2×10^{-3}	8.4138	8.4101	-0.044
6×10^{-3}	9.5123	9.508	-0.039
1×10^{-2}	10.023	10.019	-0.035
4×10^{-2}	11.409	11.406	-0.029
8×10^{-2}	12.103	12.099	-0.034
2×10^{-1}	13.019	13.015	-0.029

Dimensi- onless time	Dimensionless pressure		Error (%)
6×10^{-1}	14.117	14.114	-0.022
1	14.628	14.625	-0.024
4	16.015	16.011	-0.026
8	16.708	16.704	-0.024
60	18.723	18.719	-0.022
100	19.233	19.230	-0.017

Vertical Fracture with Uniform Flux IBC.

A vertical fracture, extending from x_1 to x_2, is modeled by both continuous integration of a line source and the *DFE* Method.

Continuous integration. The potential due to a vertical, fully penetrating line source is given by Equation B.2.2, or by the log approximation [Earlougher, 1977], which, using the dimensionless variables applied in this work, can be written as:

$$\varphi_{LD} = \ln\left(\frac{t_D}{r_D^2}\right) + 0.80907 \qquad \text{.............................(5.4.2)}$$

where

$$r_D^2 = (x - x')^2 + (y - y')^2 \qquad \text{.............................(5.4.3)}$$

The potential response due to a vertical fracture can be written as:

$$\varphi_{Df} = \int_{x1}^{x2}\left[\ln\frac{t_{Df}}{r_{Df}^2} + 0.80907\right]dx' \qquad\qquad\dots\dots\dots(5.4.4)$$

or

$$\varphi_{Df} = (x_2' - x_1')\left[\ln(t_{Df}) - 1.19093\right] + (x - x_2')\ln\left[(x - x_2')^2 + y'^2\right]$$

$$-(x - x_1')\ln\left[(x - x_1')^2 + y'^2\right] - 2y\left[a\tan\frac{x - x_2'}{y'} - a\tan\frac{x - x_1'}{y'}\right]$$

$$\dots\dots\dots(5.4.5)$$

The potential at the center of a fracture with dimensionless thickness equal to 0.001 and uniform flux IBC obtained from Equation 5.4.5 and the DFE Method are compared in Figure 5.4.2. As can be seen, there is almost complete agreement. Table 5.4.2 indicates that the potentials obtained using DFE Method (dimensionless distance between the elements equal 0.001) are smaller than those obtained by continuous integration in the range of 1% - 0.19% corresponding to short and late times, respectively.
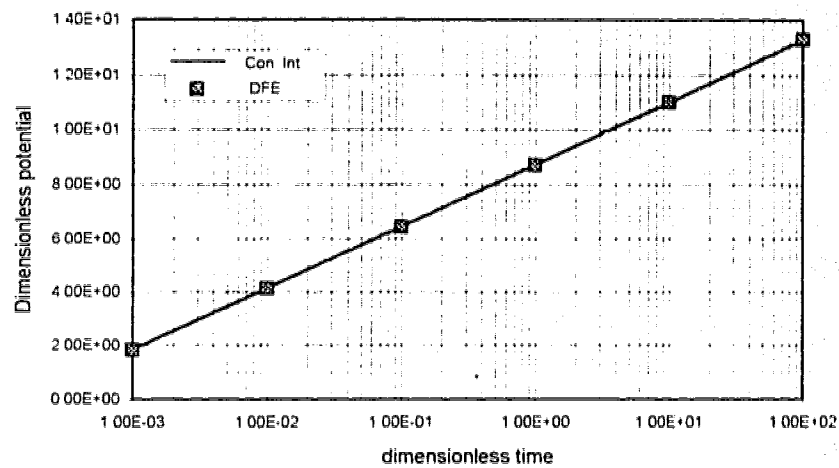
Figure 5.4.2:   Potential at the center of a vertical fracture with dimensionless length equal to 0.1 modeled using the DFE method and analytical integration of a vertical line source.

Table 5.4.2: Comparison of the pressures at the center of a vertical fully penetrating fracture with $L_{f} = 0.2h_{f}$ and thickness equal to 0.001 obtained using the DFE Method and continuous integration (both with a uniform flux IBC).

Dimensionless time t_D	Dimensionless pressure of a vertical fracture		Error (%) $100 \times \dfrac{\left(p_{Cont} - p_{DFE}\right)}{p_{Cont}}$
	DFE Method $\left(p_{DFE}\right)$	Continuous integral $\left(p_{Cont.}\right)$	
0.001	1.8307	1.8111	-1.09
0.01	4.1333	4.1137	-0.48
0.1	6.4359	6.4163	-0.31
1.0	8.7385	8.7188	-0.22
10.0	11.0411	11.0214	-0.17
100.0	13.3433	13.3240	-0.19

5.5 Comparison of the Discrete Flux Element and Infinite Conductivity Methods

The examples given by Ozkan et al. [1987] were solved using DFE method. To compare the results of the two methods the dimensionless variables used by Ozkan et al. have been used. These are;

$$p_D = \frac{2\pi k h}{QB\mu} \Delta p \qquad \qquad \qquad (5.5.1)$$

$$t_D = \frac{kt}{\mu\varphi c_t (L/2)^2} \qquad \qquad \qquad (5.5.2)$$

$$r_{wD} = \frac{r_w}{(L/2)} \qquad \qquad \qquad (5.5.3)$$

where L is the wellbore length.

Ozkan et al. [1987] simulated the infinite conductivity solutions for horizontal wellbores by calculating a uniform flux solution at an equivalent pressure point that is $X_{eq} = 0.732 X_f$, where

$$X_f = L/2 \qquad \qquad \qquad (5.5.4)$$

Thus to compare these solutions, the DFE Method is applied to obtain the uniform flux solutions for three different horizontal wells at the equivalent pressure point ($X_{eq} = 0.732 X_f$). All the wellbores with dimensionless radii equal to 0.0001 and with dimensionless lengths 0.25, 1 and 25 are located at the mid-height of the infinite slab reservoir.

The comparison of the dimensionless pressures obtained using DFE Method and the infinite conductivity solutions are shown in Figure 5.5.1.
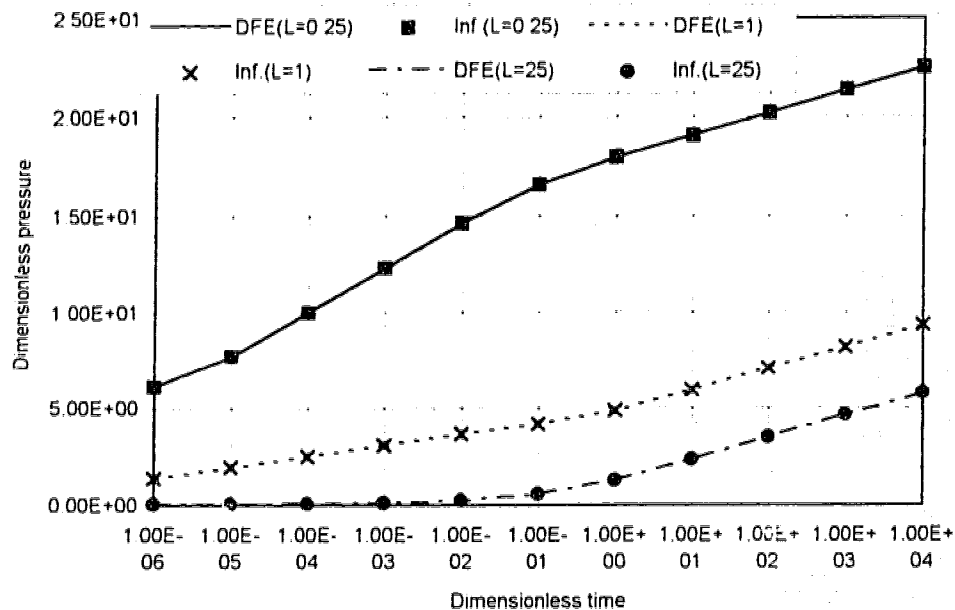
Figure 5.5.1: Comparison of the potentials for a horizontal well modeled by the DFE method and the infinite conductivity solution.

5.6 Equivalent Pressure Point

5.6.1 Horizontal Well in an Infinite Slab Reservoir

Using the uniform potential IBC, the potential and potential derivative with respect to $\ln(t_D)$ were calculated for two horizontal wells. $L_p = h_t$ and $L_p = 2h_t$. The results are shown in Columns 1 and 4 of Tables 5.6.1.1 and 5.6.1.2. Also, using uniform flux IBC, the same values were calculated for the whole length of the wellbore. The coordinates of

the points where the potential and its derivative are identical to the uniform potential IBC solution are reported in Columns 2 and 5. These coordinates are calculated as a percentage of the wellbore half length and are shown in Columns 3 and 6. Inspecting Column 3 one can see that 1) the equivalent pressure (potential) point is moving in time and stabilizes at late times once the semi-log pressure derivative approaches 1 (radial flow), 2) even at late times (radial flow period) these values are not identical for different well lengths, and 3) the equivalent points for the potential and its derivative are not identical. Moreover, for the case of $l_p = 2h_t$, no point on the wellbore (at $t_D = 10^{-3}$) with uniform flux IBC, can simulate the uniform potential IBC.

Table 5.6.1.1: Equivalent pressure point (EPP) and equivalent derivative point EDP, for a horizontal well with $l_p = h_t$

t_D	$PUPIBC$ 1)	XD, EPP 2)	% 3)	$DUPIBC$ 4)	XD, EDP 5)	% 6)
2×10^{-4}	6.01228	0.228	90.2%	-	-	-
10^{-3}	7.51719	0.213	85.2%	0.9094	0.19	76%
10^{-2}	9.46127	0.189	75.6%	0.75504	0.15	60%
0.1	11.2676	0.18	72%	0.899	0.156	62.4%
1	13.47379	0.179	71%	0.9886	0.158	63.2%

Table 5.6.1.2: Equivalent pressure point (EPP) and equivalent derivative point EDP for a horizontal well with $L_p = 2h_t$.

t_D	PUPIBC 1)	XD, EPP 2)	% 3)	DUPIBC 4)	XD, EDP 5)	% 6)
10^{-5}	1.5642	0.492	98.4%	0.1174	*	*
10^{-4}	2.69	0.479	95.8%	0.3391	0.493	98.6%
10^{-3}	3.808	0.452	90.4%	0.454	0.441	88.2%
10^{-2}	4.8672	0.404	80.8%	0.4342	0.344	68.8%
0.1	6.0781	0.355	71%	0.7098	0.304	60.8%
1	8.0624	0.344	68.8%	0.9563	0.316	63.2%
10	10.325	0.343	68.6%	0.9954	0.318	63.6%
100	12.623	0.343	68.6%	0.99977	0.092	63.6%

1) PUPIBC = potential due to uniform potential inner boundary condition.

2) XD, EPP = location of equivalent pressure point.

3) % of the half length of the horizontal well.

4) DUPIBC = log derivative due to uniform potential inner boundary condition.

5) XD, EDP = location of equivalent derivative point.

6) % of the half length of the horizontal well.

*) there is no point on the wellbore to indicate the pressure derivative.

It can be seen, from Columns 4, 5 and 6 of the Tables 5.6.1.1 and 5.6.1.2, that the equivalent pressure derivative point does not follow a regular pattern.

5.6.2 Horizontal Well in a Semi-Infinite Slab Reservoir

In this section the location of the equivalent pressure point for a horizontal well in a semi-infinite reservoir is investigated. The wellbore with $r_{wD} = 0.001$ and $L_p = h_t$ is located at the mid-height of a semi-infinite slab (Figure 5.6.2.1). The vertical barrier is perpendicular to the wellbore axis. The distance of the wellbore end to this barrier is 0.

No-flow boundary

Vertical barrier

No-flow boundary
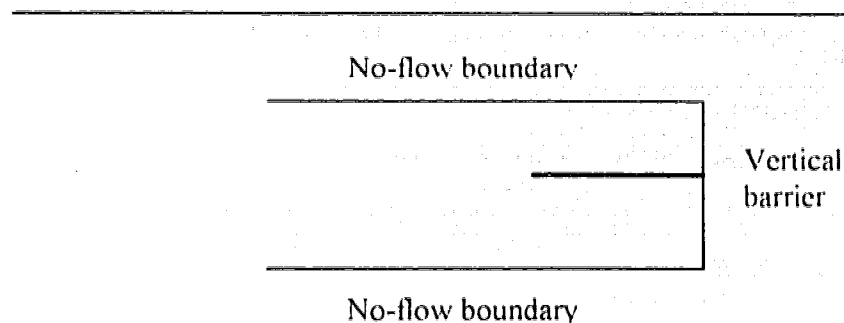
Figure 5.6.2.1: Schematic drawing of a horizontal well located at the mid-height of a semi-infinite slab.

Applying the DFE method, both uniform flux and uniform potential IBCs are modeled. The locations on the wellbore at which the uniform flux potential solution is identical to the uniform potential solution for different times are calculated and are shown in Table 5.6.2.1. Column 2 of Table 5.6.2.1 shows the dimensionless potential obtained by a uniform potential IBC. Columns 3 and 4 indicate the location of the equivalent pressure point (EPP) as a percentage of the total and half lengths of the wellbore length.

Table 5.6.2.1: Equivalent pressure point for a horizontal well with $L_p = h_t$ and
$r_{itp} = 0.001$ located at the mid-height of a semi-infinite slab reservoir.
(EPP = equivalent pressure point).

1) t_p	2) φ_p (Uniform pot. IBC)	3) EPP Based on the wellbore length	4) EPP Based on the wellbore half length
$2 \cdot 10^{-6}$	1.62	99%	98%
$2 \cdot 10^{-5}$	3.80	97%	95.2%
$2 \cdot 10^{-4}$	6.06	95.8%	91.6%
$2 \cdot 10^{-3}$	8.27	87.6%	75.2%
$2 \cdot 10^{-2}$	10.34	77.2%	54.4%
$2 \cdot 10^{-1}$	13.22	69.4%	38.8%
2	17.47	68.4%	36.8%
20	22.03	68.4%	36.8%

As can be seen from Table 5.6.2.1, the equivalent pressure point is moving in time and stabilizes at late times and is located at 68.4 % of the wellbore length (measured from the vertical barrier) or 36.8% of the half length of the wellbore. However, for the same horizontal well in an infinite slab, the equivalent pressure point at late times was located at 71% of the half length of the wellbore (Section 5.6.1).

5.6.3 Concluding Remarks

From Sections 5.6.1 and 5.6.2 it can be concluded that:

1. The equivalent pressure point is moving in time; however, it stabilizes at late times (radial flow period).

2. The equivalent pressure point location at late times depends on the wellbore length.

3. The equivalent pressure point location depends on the reservoir geometry and no-flow barriers.

4. The equivalent points for pressure and pressure derivative are not the same.

CHAPTER 6

PERFORMANCE OF SOURCES WITH FINITE LENGTH

6.1   Performance of Horizontal Wells

The potential and semi-log potential derivative of a horizontal well with $L_p = h_t$ and uniform potential inner boundary condition have been considered for three different cases:

1. wellbore in an isotropic infinite reservoir (that is a reservoir with no boundary) using Equations 5.1.5 and 4.2.2.13;

2. wellbore at the mid-height ($z_w = 0.25$) of an isotropic rectilinear reservoir (infinite slab) using Equations 5.1.5 and 4.2.3.1;

3. wellbore at a point close to the upper boundary ($z_w = 0.15$) in an isotropic rectilinear reservoir (infinite slab) using Equations 5.1.5 and 4.2.3.1.

The results are shown in Figures 6.1.1 and 6.1.2 for the potential and the potential derivative respectively. Both figures show that in an infinite reservoir the response of the wellbore potential levels off and approaches steady-state at early times. The response of the two other cases follows the same pattern as that of an infinite reservoir for a certain period of time. Once the transient drainage area reaches the no-flow boundaries the response at the wellbore in a rectilinear reservoir deviates from that in an infinite reservoir.

Figure 6.1.1 and 6.1.2 indicate that this deviation happens quicker when the well is closer to the no-flow boundary. Thus the deviation point of the potential and its derivative from the response of a similar wellbore in an infinite reservoir can be used to determine the distance of the wellbore from the no-flow boundaries.

Figure 6.1.1 indicates that the potential due to the wellbore closer to the no-flow boundary is higher than that for the wellbore located at the mid-height of the reservoir. However, at late times the semi-log potential derivatives for both are equal to 1, which is an indication of radial flow (the semi-log potential derivative equal to 1 is identical to 1/2 using the traditional definition of dimensionless variables).

Figures 6.1.3 and 6.1.4 show the potential and its semi-log derivative for two horizontal well lengths $L_p = h_t$ and $L_p = 2h_t$ located at the mid-height of a rectilinear reservoir. The potential drop due to the shorter wellbore is higher than that for the longer one. However, both indicate radial flow with slope 1 at late times.
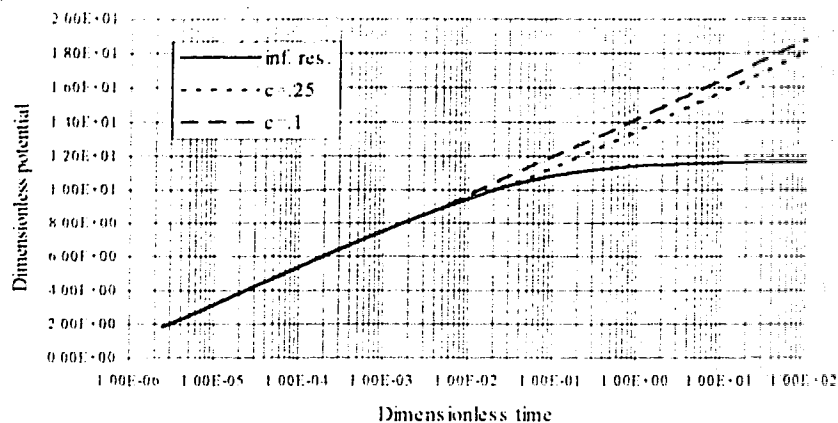
Figure 6.1.1: Potential of a horizontal well with $L_p = h_t$ located in a rectilinear reservoir at different heights and an infinite reservoir.
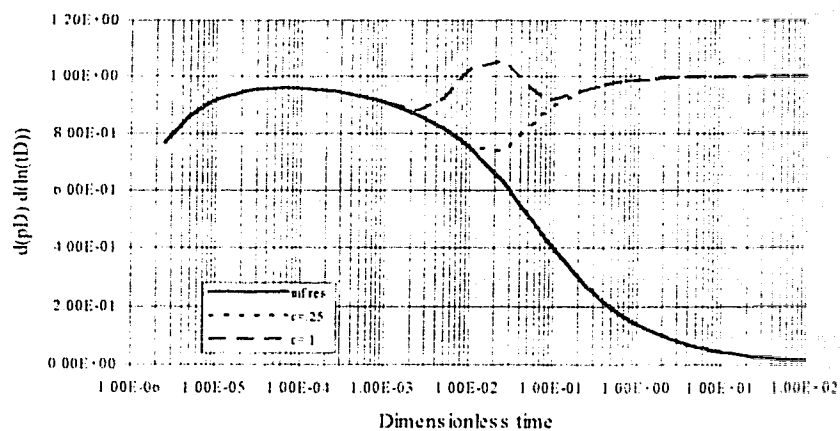
Figure 6.1.2: Potential derivative with respect to $\ln(t_D)$ for a horizontal well with $L_p = h_t$ in a rectilinear reservoir located at different heights and an infinite reservoir.
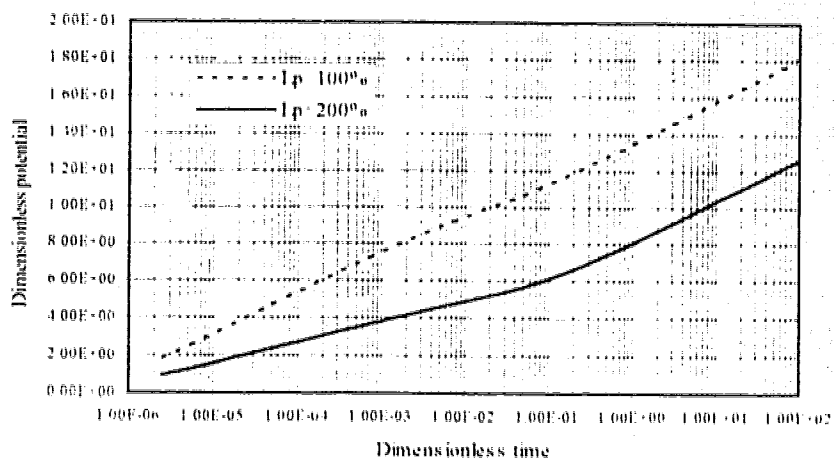
Figure 6.1.3: Comparison of potentials of two horizontal wells with $I_p = h_t$ and $I_p = 2h_t$ located at the mid-height of a rectilinear reservoir.
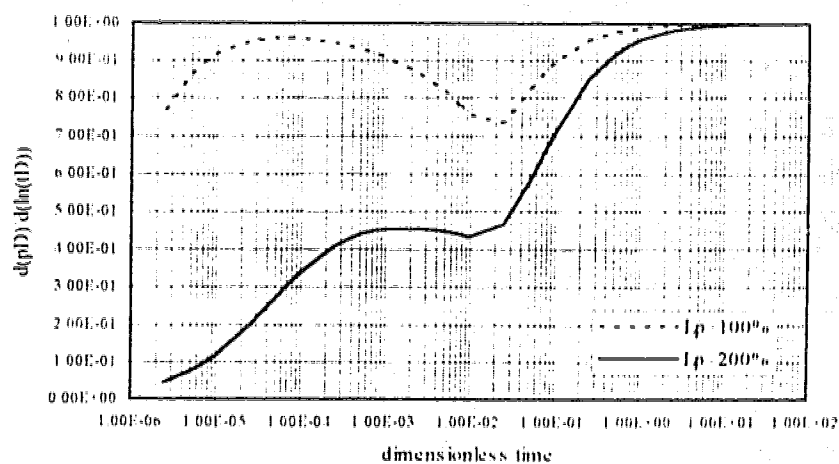
Figure 6.1.4: Comparison of potential derivative of two horizontal wells with $I_p = h_t$ and $I_p = 2h_t$ located at the mid-height of a rectilinear reservoir.

6.2   Vertical Partially Penetrating Wells

The potential and potential derivative with respect to $\ln(t_D)$, for different penetration depths are shown in Figures 6.2.1 and 6.2.2. At late times all cases indicate radial flow with slope 1. In Figure 6.2.1, the intercept of the late times part of the curve with time axis is an indication of well penetration depth. Figure 6.2.2 indicates that the value of the potential derivative with respect to $\ln(t_D)$ at early time could also be used as an indicator of effective well penetration depth or reservoir thickness.
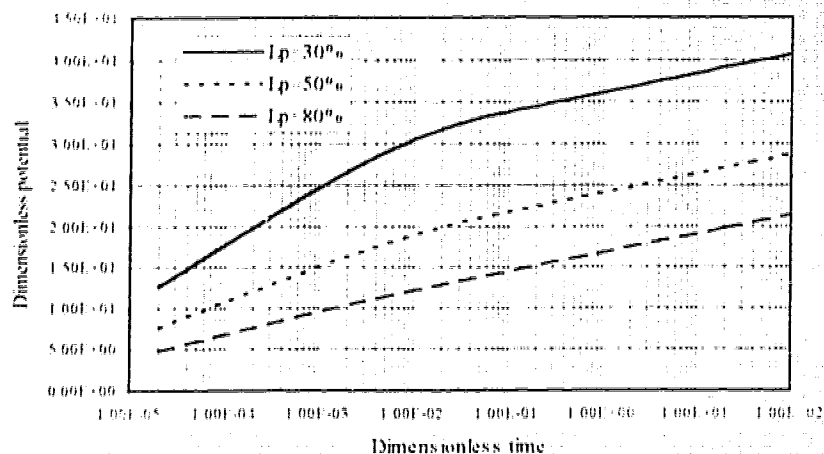
Figure 6.2.1: The potential response of vertical partially penetrating wellbores with different lengths in a rectilinear reservoir.
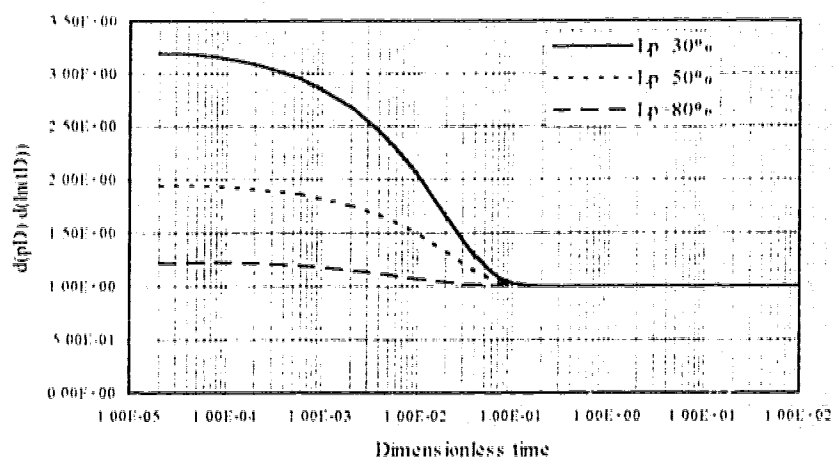
Figure 6.2.2: The potential derivative of vertical partially penetrating wellbores with different lengths in a rectilinear reservoir.

6.3   Vertical Fractures

The potential response of a fully penetrating vertical fracture with dimensionless thickness 0.001 and different lengths has been calculated using Equation 5.1.5 with uniform potential IBC. Equation 5.1.5 for a fracture can be written as:

$$\varphi_f = \sum_{i=1}^{n} q_i \varphi_{L,i} \qquad\qquad\qquad ....(6.3.1)$$

where φ_f is the potential due to a fracture and $\varphi_{L,i}$ is the potential due to a line source element with flux strength q_i. For the potential of a vertical line source, the log approximation has been used.

$$\varphi_L = \ln\left(\frac{t_D}{r_D^2}\right) + 0.80907 \qquad\qquad ....(6.3.2)$$

The results are shown in Figure 6.3.1. The intercept with the time axis is an indication of fracture length.
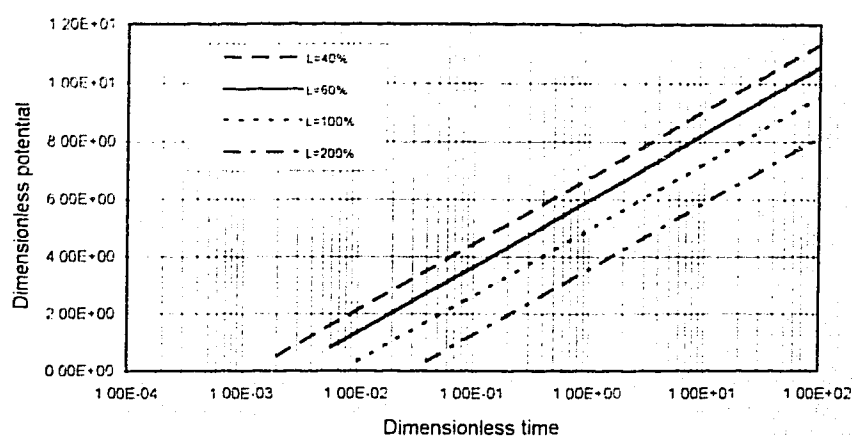
Figure 6.3.1: Dimensionless potential of vertical fully penetrating fractures with different length and dimensionlesss thickness 0.001.

6.4 Performance of Line Sources with Irregular Geometry

The configuration of most horizontal wells is curvilinear rather than a straight line. Applying the approximate potential solutions, for horizontal wells, provided by Clonts and Ramey [1986], Daviau et al. [1988], Kuchuk et al. [1988] and Odeh and Babu [1990], one has to assume a straight line geometry for the wellbore in the direction of one of the principal permeabilities.

In this section the effect of the wellbore configuration has been studied using a simple example. A one-quarter circle with radius $R=0.2$ is modeled in three different rectilinear (infinite slab) reservoirs. In each case the performance of the curvilinear line source is compared to that of a straight horizontal well with the same producing length. The wellbore model is located in the plane $y=0$. In isotropic reservoirs the value of one of

the isopotentials parallel to the wellbore has been taken as the wellbore potential. However, in anisotropic reservoirs the ispotential lines are elliptical. In this section the cross section of the wellbore is assumed to be elliptical. This assumption does not have any effect on the quality of the results. The wellbore pressures are calculated at $y = 0.001$.
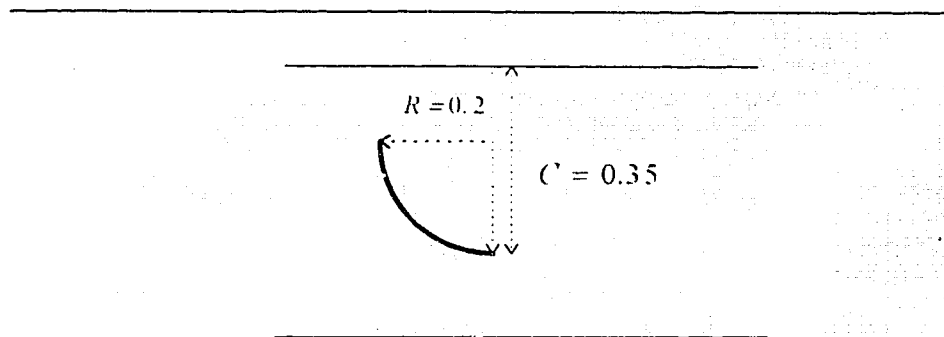
Fig. 6.4.1:   Schematic drawing of a curvilinear source (1/4 of a circle with radius 0.2) in a rectilinear reservoir.

Case I. The vertical permeability is considered to be greater than the horizontal permeability:

$$\alpha = \sqrt{\frac{k_y}{k_x}} = 1 \qquad \qquad \text{..................(6.4.1)}$$

and

$$\beta = \sqrt{\frac{k_z}{k_x}} = \sqrt{3} \qquad \qquad \text{..................(6.4.2)}$$

Comparison of the potential and its semi-log potential derivative are shown in Figures 6.4.2 and 6.4.3. Figure 6.4.2 shows that the dimensionless potential (pressure) of the curvilinear source is higher than that of the straight horizontal well. In other words, the productivity of a curvilinear line source is smaller than that of a straight horizontal wellbore with the same producing length. Figure 6.4.3 shows that the semi-log potential derivative of the curvilinear source is higher than that of the straight horizontal line source. However, at late times, the responses of both configurations indicates radial flow.
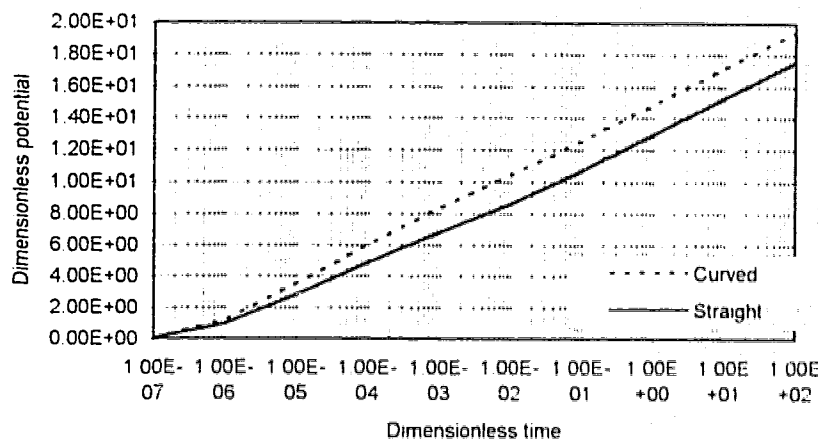
Figure 6.4.2: Comparison of dimensionless potentials of a 1/4 circle and a straight horizontal well with the same producing length in a rectilinear, anisotropic reservoir with $\alpha = 1$ and $\beta = \sqrt{3}$.
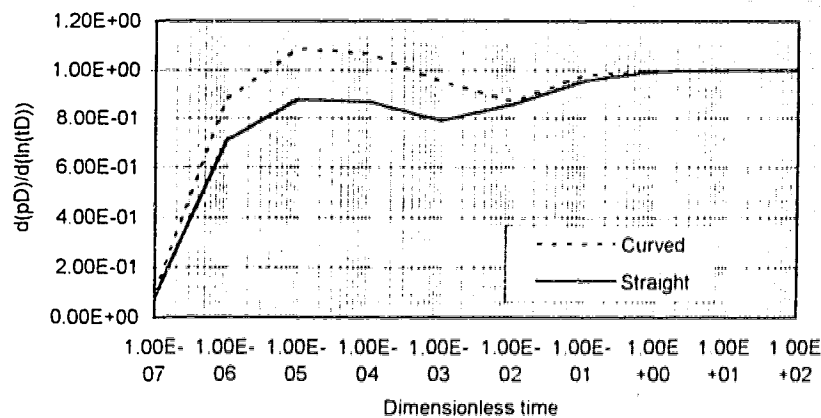
Figure 6.4.3: Comparison of dimensionless semi-log potential derivatives of a 1/4 circle and a straight horizontal well with the same producing length in a rectilinear, anisotropic reservoir with $\alpha = 1$ and $\beta = \sqrt{3}$.

Case II. Horizontal permeability is higher than the vertical permeability as follows.

$$a = \sqrt{\frac{k_y}{k_x}} = 1 \quad , \quad \dots\dots\dots\dots\dots\dots(6.4.3)$$

and,

$$b = \sqrt{\frac{k_z}{k_x}} = \sqrt{\frac{1}{3}} \quad \dots\dots\dots\dots\dots\dots(6.4.4)$$

Figures 6.4.4 and 6.4.5 show that the potential and semi-log potential derivative of a curvilinear line source are smaller than those of a straight horizontal wellbore. However, the semi-log potential derivatives of both cases at late time approach 1, which is an indication of radial flow. Figure 6.4.5 shows that the radial flow response of the curvilinear wellbore starts sooner than that of the straight horizontal wellbore.
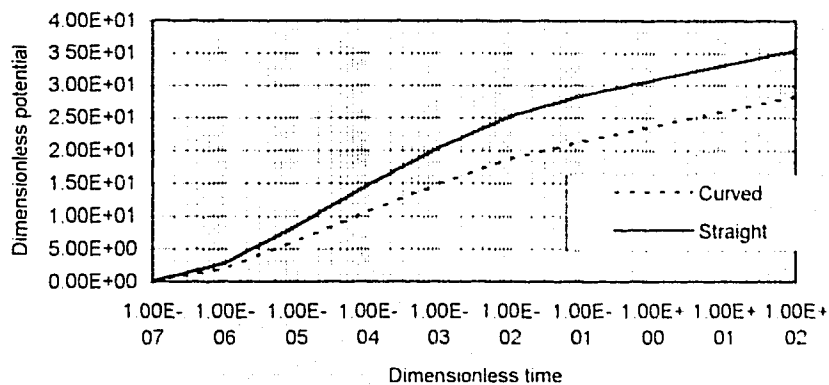
Figure 6.4.4: Comparison of dimensionless potentials of a 1/4 circle and a straight horizontal well with the same producing length in a rectilinear, anisotropic reservoir with $\alpha = 1$ and $\beta = \sqrt{1\ 3}$.
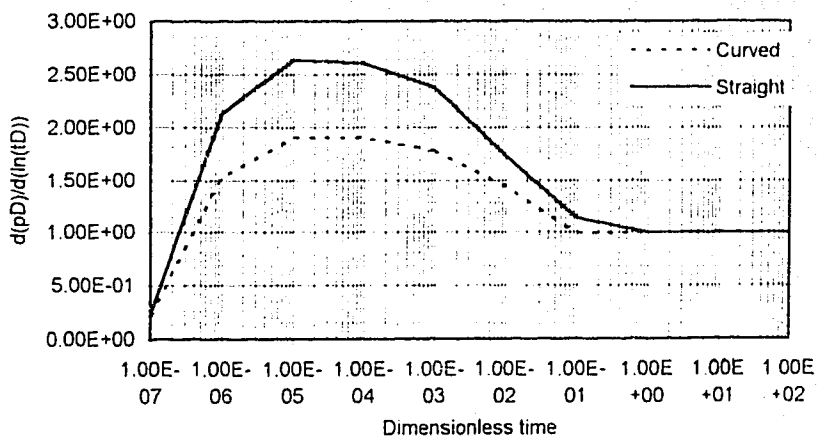
Figure 6.4.5: Comparison of dimensionless semi-log potential derivatives of a 1/4 circle and a straight horizontal well with the same producing length in a rectilinear, anisotropic reservoir with $\alpha = 1$ and $\beta = \sqrt{1\ 3}$.

Case III. For this case the model reservoir is assumed to be isotropic with

$$\alpha = \beta = 1, \qquad\qquad\qquad\qquad \text{...........................(6.4.5)}$$

Figures 6.4.6 and 6.4.7 show that the potential and semi-log potential derivative of both curvilinear and straight horizontal wells are almost identical. Figure 6.4.7 shows that the radial flow response of the curvilinear line source starts sooner than that of the straight horizontal line source.
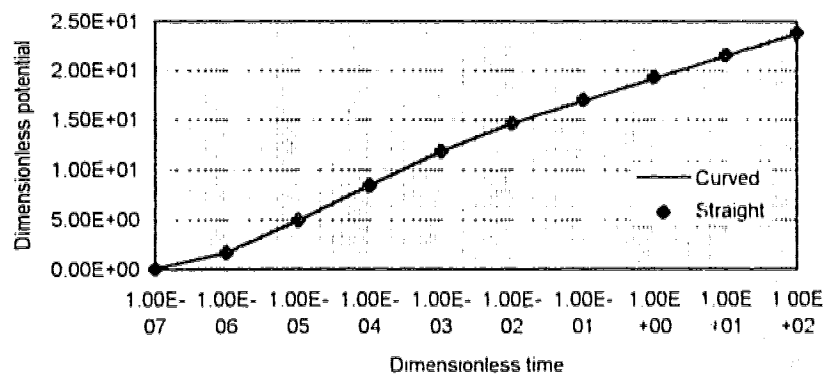
Figure 6.4.6:   Comparison of dimensionless potentials of a 1/4 circle
and a straight horizontal well with the same producing
length in a rectilinear, isotropic reservoir with
$\alpha = 1$ and $\beta = 1$.
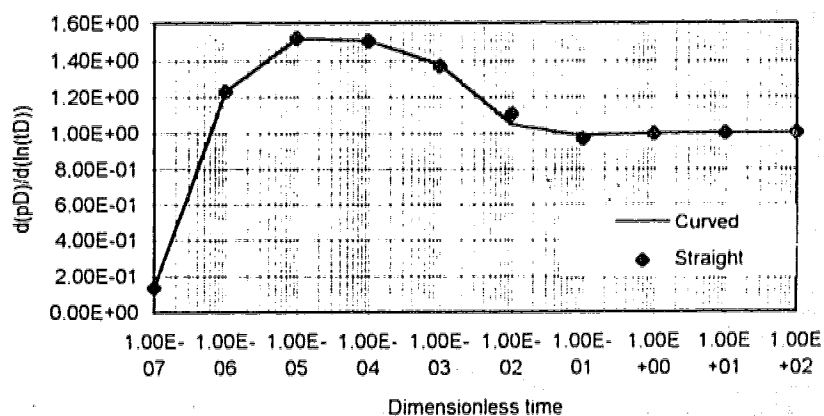
Figure 6.4.7:   Comparison of dimensionless semi-log potential derivatives
of a 1/4 circle and a straight horizontal well with the same
producing length in a rectilinear, isotropic reservoir with
$\alpha = 1$ and $\beta = 1$.

6.4.1 Discussion

A wellbore with curvilinear geometry has a horizontal and a vertical component. In reservoirs with a significant difference in horizontal and vertical permeabilities, the role of each component in the reservoir depletion is different. In reservoirs with higher vertical permeability, the productivity of the horizontal component is higher than that of the vertical component. Thus, if one models a curvilinear line source with a straight horizontal well, one underestimates the dimensionless potential drop (Case I). In reservoirs with higher horizontal permeability, the productivity of the vertical component is higher than that of a horizontal well with the same producing length. Thus, if one models a curvilinear wellbore by a straight horizontal wellbore, one overestimates the dimensionless potential (Case II). Moreover, the potential derivatives of a curvilinear and a straight horizontal well are different.

In isotropic reservoirs a curvilinear line source can be modeled by a straight horizontal well (Case III). However, the potential derivatives show different values for the time to the start of the radial flow response.

6.4.2 Concluding Remarks

Based on the results of this study it was found that modeling a curvilinear line source with a straight horizontal line source creates errors in the calculated pressure and pressure derivative response. This error increases with an increase in the anisotropic coefficient.

6.5 Performance of a Horizontal Well in a Semi-Infinite Slab Reservoir

A reservoir with two parallel no-flow boundaries and a vertical barrier can be considered as a semi-infinite slab. The potential equation for a horizontal well in a semi-infinite slab is modeled by the method of images as explained in Chapter 5. A schematic drawing of a horizontal well with $L_{p} = h$, at the mid-height of such a reservoir is shown in Figure 6.5.1. The reservoir is assumed to be isotropic. The potential and its derivative with respect to $\ln(t_{D})$ with uniform flux IBC for such a wellbore for different distances from the vertical barrier are shown in Figures 6.5.2 and 6.5.3, respectively. Two cases with the distance (F) to the barrier equal to 0 and 0.5 are studied. The potential drop for the wellbore closer to the vertical barrier is highest. The potential derivative at late times is 2. As the potential derivative for the case of horizontal and vertical wells in a rectilinear reservoir at late times is 1, which indicates a cylindrical drainage area, it can be concluded that for the case of a semi-infinite reservoir a potential derivative equal to 2 (double slope) is an indication of a semi-cylindrical drainage area.

No-flow boundary

Vertical
barrier

F

No-flow boundary
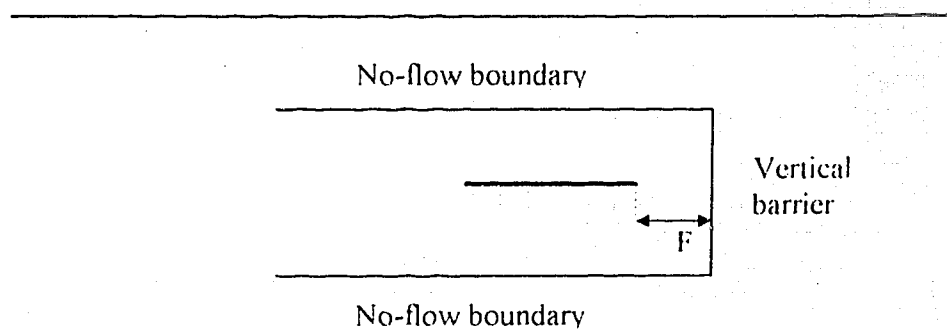
Figure 6.5.1: Schematic drawing of a horizontal well in an semi-infinite slab reservoir.
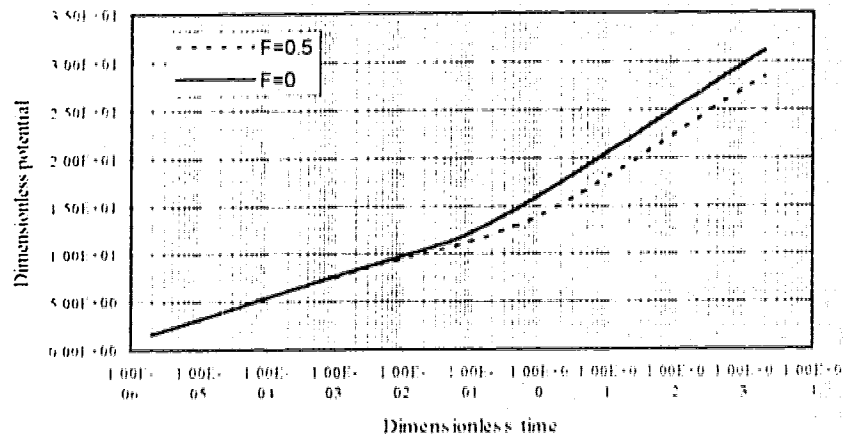
Figure 6.5.2: Dimensionless potential for a horizontal well in a semi-infinite slab reservoir (F is the dimensionless distance of the wellbore end to the vertical barrier).
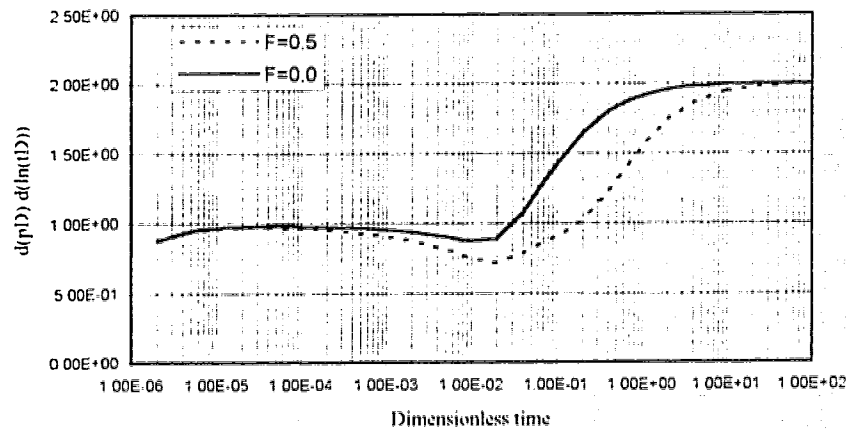
Figure 6.5.3: Potential derivative for a horizontal well in an semi-infinite slab reservoir (F is the dimensionless distance of the wellbore end to the vertical barrier).

6.6   Flux Distribution Along the Source

The flux distribution for a horizontal well in a rectilinear reservoir is shown in Figure 6.6.1. Due to symmetry, only the wellbore half length is used. As can be seen at short time ($t_D = 2 \times 10^{-7}$) the flux distribution is almost uniform. However, at a longer time ($t_D = 1$) the flux at the ends is significantly larger.

The flux distribution along a horizontal well, with $L_D = 2h_t$, $r_{wD} = 0.001$ and $F = 0$, located at the mid-height of a semi-infinite slab isotropic reservoir with zero distance to the vertical boundary is shown in Figure 6.6.2. Due to the existence of the vertical barrier the flux distribution is asymmetric in contrast to the symmetric distribution in the rectilinear case.

The concept in the literature [Clonts and Ramey, 1986, and Daviau et al., 1988] of using an equivalent pressure point was based on a symmetric flux distribution along the wellbore. This is clearly not the case for the semi-infinite slab reservoir, and probably not for other geometries involving vertical barriers to flow.
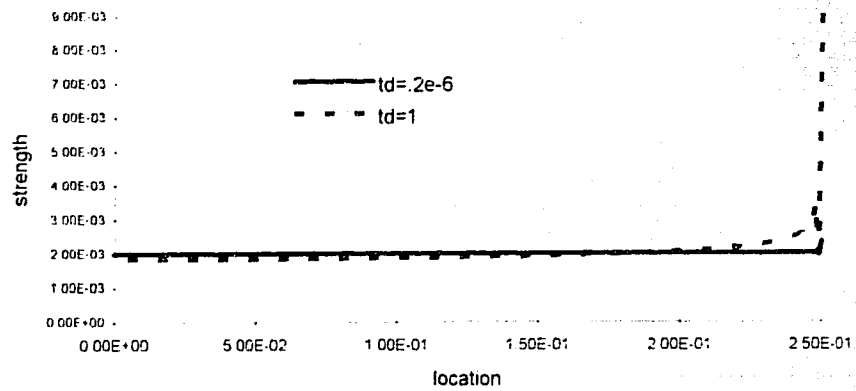
Figure 6.6.1: Flux distribution along a horizontal well in a rectilinear reservoir
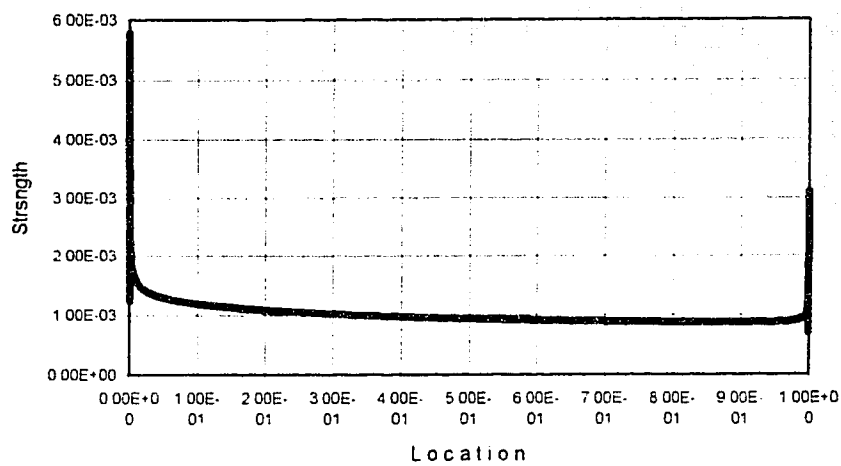
Figure 6.6.2: Flux distribution along a horizontal well in a semi infinite slab

CHAPTER 7

PRODUCTIVITY OF SOURCES WITH FINITE LENGTH

The steady-state potential equations for horizontal wells and fractures have not been presented before. In this chapter, by applying the DFE method, the steady-state potential equations and productivity indices for these sources are developed.

Equation 5.1.5 is a general equation that can be used for both transient and steady-state conditions.

$$\varphi_{DSFL}^{SS} = \sum_{i=1}^{n} q_i \varphi_{Dfei}^{SS} \qquad \dots\dots\dots\dots\dots\dots\dots(7.1)$$

where φ_{DSFL}^{SS} is the dimensionless potential of a source with finite length and φ_{Dfei}^{SS} is the dimensionless potential of a flux element with flux, q_i. Equation 7.1 can be used for a uniform potential IBC by calculating the flux distribution along the source as was discussed in Chapter 5. If Equation 7.1 is used for a uniform flux solution, it reduces to:

$$\varphi_{DSFL}^{SS} = \frac{1}{n} \sum_{i=1}^{n} \varphi_{Dfei}^{SS} \qquad \dots\dots\dots\dots\dots\dots\dots\dots(7.2)$$

In this chapter all the calculations are made for uniform potential IBC, isotropic, rectilinear reservoirs.

To apply the DFE method under steady-state conditions (Equation 7.1), one needs the potential solutions for point and line sources to model a line or a plane source, respectively.

7.1 Steady-State Potential of Flux Elements

7.1.1 Point Source

Madelung developed a steady-state potential equation for a point source in a rectilinear (infinite slab) domain [Muskat, 1932]:

$$\varphi_p(w,\rho,w_p) = 4q\left[2\sum_{n=1}^{\infty}\left(K_0(2\pi n\rho)\cos(2\pi n w)\cos(2\pi n w_p)\right) + \ln(2/\rho)\right]$$

..................................(A.4.1)

Muskat [1932] defined the flux term, q, for fluid flow problems as (Equation A.4.2):

$$q = \frac{Q\mu}{4\pi k a}$$

..................(A.4.2)

where

$$a = 2h_t$$

..................................(A.4.3)

where h_t is the reservoir height

$$\varphi = p - \gamma g z$$

..................................(7.1.1.1)

In this study the dimensionless potential for a steady-state condition is defined as;

$$\varphi_D^{ss} = \frac{2\pi k a}{Q\mu}\varphi$$

..................................(7.1.1.2)

Thus equation A.4.1 in dimensionless form can be written as:

$$\varphi_{Dp}(w,\rho,w_p) = 2\left[2\sum_{n=1}^{\infty}\left(K_0(2\pi n\rho)\cos(2\pi n w)\cos(2\pi n w_p)\right) + \ln(2/\rho)\right]$$ ....(7.1.1.3)

7.1.2 Line Source

The steady-state solutions for line sources are given in Appendix C. To model a vertical, fully penetrating fracture, one can use a vertical line source solution (Equation C.3.1):

$$\varphi = 2q \ln(2/\rho) \qquad\qquad\qquad\qquad (C.3.1)$$

where

$$\rho = \left((x - x_L)^2 + (y - y_L)^2 \right)^{1/2} \qquad\qquad\qquad (C.1.2)$$

and

$$q = \frac{Q\mu}{4\pi k a x} \qquad\qquad\qquad\qquad (C.1.7)$$

By substitution of

$$x = 0.5 \qquad\qquad\qquad\qquad (7.1.2.1)$$

for a fully penetrating wellbore, equation C.1.7 reduces to:

$$q = \frac{Q\mu}{2\pi k a} \qquad\qquad\qquad\qquad (7.1.2.2)$$

Thus Equation C.3.1 in dimensionless form can be written as:

$$\varphi_{DL} = 2\ln(2/\rho) \qquad\qquad\qquad\qquad (7.2.1.3)$$

where the potential φ and the dimensionless potential φ_{DL} have the same definitions as does the point source (Equations 7.1.1.1 and 7.1.1.2, respectively).

7.2 Productivity Index

The productivity index is the ratio of the production to the pressure drop at the wellbore.

The potential drop between the producer and reservoir boundary (Figure 7.2.1), for a production rate Q, can be written as:

$$\Delta\varphi = \varphi_e^{ss} - \varphi_{w}^{ss} = \left(p_e - \gamma g h_e - p_w + \gamma g h_w \right) \qquad \text{................(7.2.1)}$$
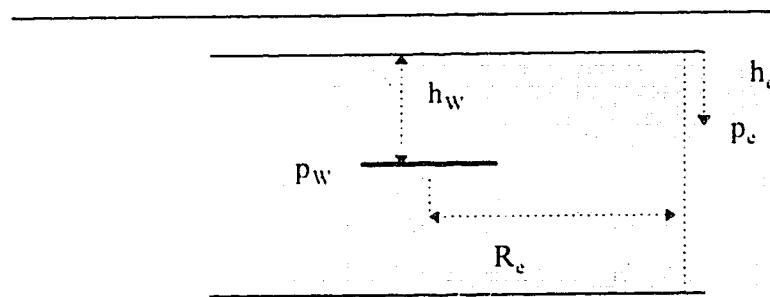
Figure 7.2.1: Schematic drawing of a horizontal well in a rectilinear reservoir.

where φ_e^{ss} is the potential at the outer boundary and φ_{w}^{ss} is the potential on the surface of the source (either line source or fracture), p_e is the pressure at the outer boundary at the height h_e and p_w is the pressure of the source at the height h_w.

Considering the pressure at the outer boundary at the top of the reservoir:

$$\Delta\varphi = \left(p_e - p_w + \gamma g h_w \right). \qquad \text{................(7.2.2)}$$

Using Equation 7.1.1.2 the steady state dimensional potential can be written as:

$$\varphi^{SS} = \frac{Q\mu}{2\pi ka} \varphi^{SS}_{Dfci} . \qquad\qquad\qquad \text{.................(7.2.3)}$$

the potential drop between producer and the outer boundary can then be calculated:

$$\Delta\varphi = \frac{Q\mu}{2\pi ka} \left(\sum_{i=1}^{n} \left(q_i \varphi^{SS}_{Dfci} \right)_{r_e} - \varphi^{SS}_{DW} \right) \qquad\qquad \text{.................(7.2.4)}$$

where the first term within the brackets is the dimensionless, steady-state potential at the

outer boundary and φ^{SS}_{DW} is the steady-state, dimensionless potential on the surface of the

source.

Equating Equations 7.2.2 and 7.2.3, the general equation for the productivity index can be

derived as:

$$PI = \frac{Q}{\left(P_e - P_W + \gamma g h_W \right)} = \frac{2\pi ka}{\mu \left(\left(\sum q_i \varphi^{SS}_D \right)_{r_e} - \varphi^{SS}_{DW} \right)}, \qquad\qquad \text{.................(7.2.5)}$$

Assuming unit values for permeability, viscosity and reservoir height, the Unit Productivity

Index (UPI) is introduced as:

$$UPI = \frac{4\pi}{\left(\sum (q_i \varphi^{SS}_{Dfci})_{r_e} - \varphi^{SS}_{DW} \right)} \qquad\qquad \text{.................(7.2.6)}$$

The UPI for horizontal wells of different lengths at different locations, and for vertical

partially penetrating wells with different penetration depths, is calculated and the results

are shown in Figures 7.2.2 through 7.2.4. The UPI for vertical fractures with different

lengths is calculated and the results are shown in Figure 7.2.5. The UPIs for each of a

horizontal well, a vertical well and a vertical fracture as a function of drainage radius are

shown in Figure 7.2.6.
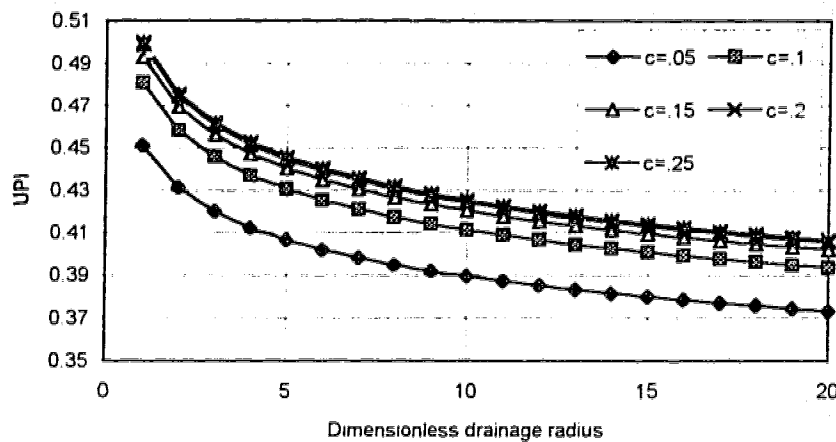
Figure 7.2.2: Unit productivity index of a horizontal well with $L_p = h_t$ located at different heights in a rectilinear reservoir.
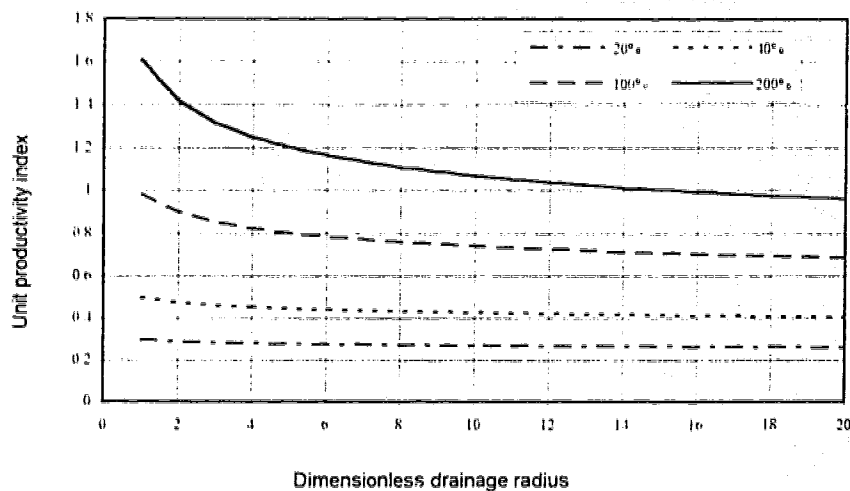
Figure 7.2.3: Unit productivity index for horizontal wells with different lengths and drainage radii located at mid-height in a rectilinear reservoir.
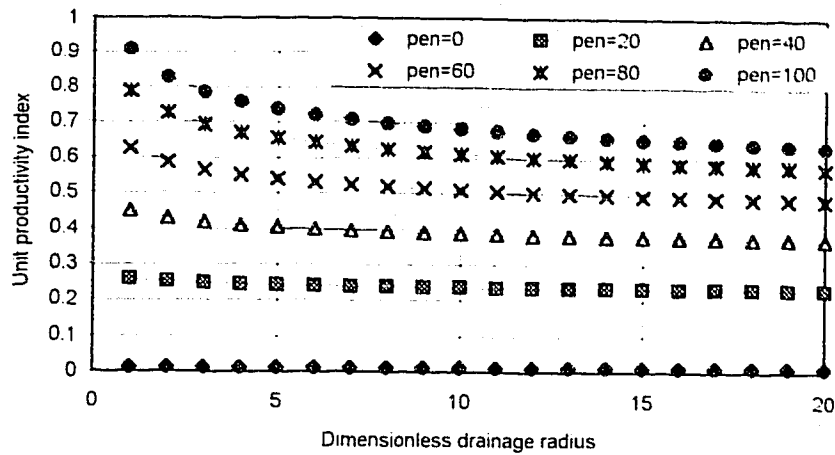
Figure 7.2.4: Unit productivity index of vertical partially penetrating wells with different lengths for different drainage radii.
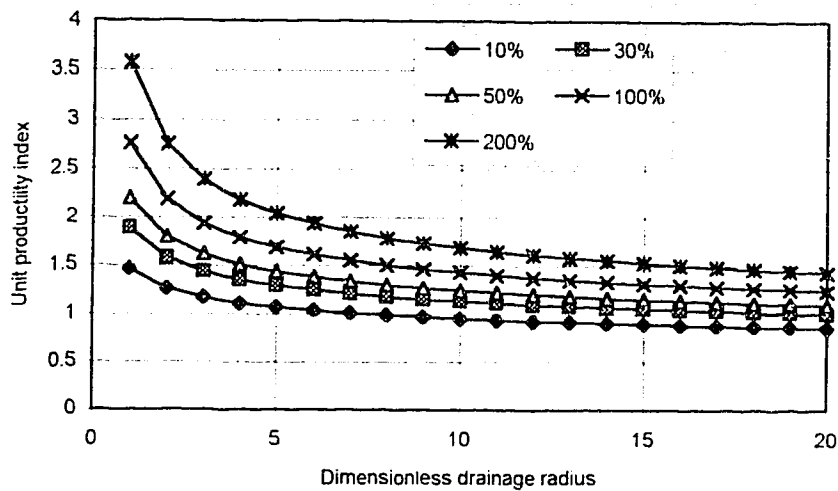
Figure 7.2.5: Unit productivity index of a vertical fracture for different lengths and drainage radii.
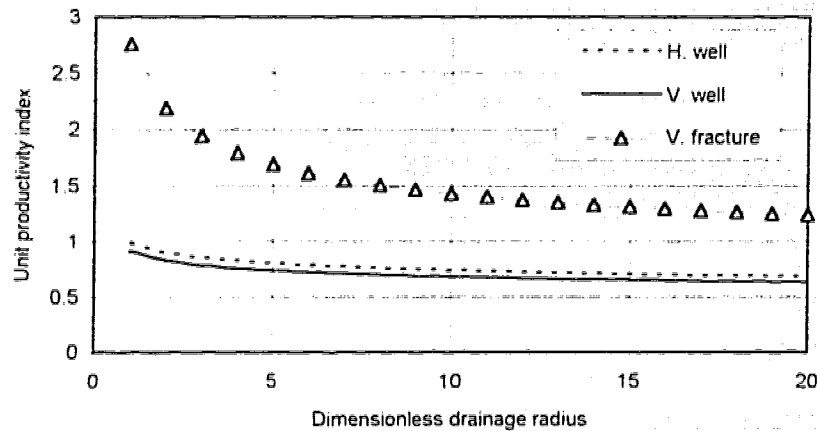
Figure 7.2.6:   A comparison of the unit productivity index for a horizontal well, vertical well and a vertical fracture, each with a producing length equal to the reservoir height.

Inspecting the UPI curves in Figures 7.2.2 through 7.2.6, one can see that:

• The UPI for a horizontal well is higher than that of a vertical well having the same producing length. While the length of a vertical well is limited to the height of the reservoir, the length of a horizontal well has no such limitation (Figure 7.2.6).

• The UPI for a horizontal well as a function of the drainage radius is less than for a vertical fracture, provided that the well radius is identical to the fracture thickness (Figure 7.2.6).

• The UPI for a partially penetrating well increases with increasing length for both horizontal and vertical wells (Figures 7.2.3 and 7.2.4).

- The UPI for a horizontal well decreases as the well location approaches the no-flow boundaries, and is maximum for wells located at the mid-height of the reservoir (Figure 7.2.2).

7.3   Comparison of Different Methods

Assuming a horizontal well with length equal to the reservoir height, that is, $L_p = 0.5$, the Unit Productivity Index has been calculated using three different methods: 1) Borisov [Joshi, 1991] 2) Joshi [1991] and 3) the DFE method. The results are plotted in Figure 7.3.1 and indicate that:

- the UPI obtained by Borisov's method is about 4% less than that obtained by the DFE method presented here.

- the UPI obtained by Joshi's method is 23% less than the DFE solution.
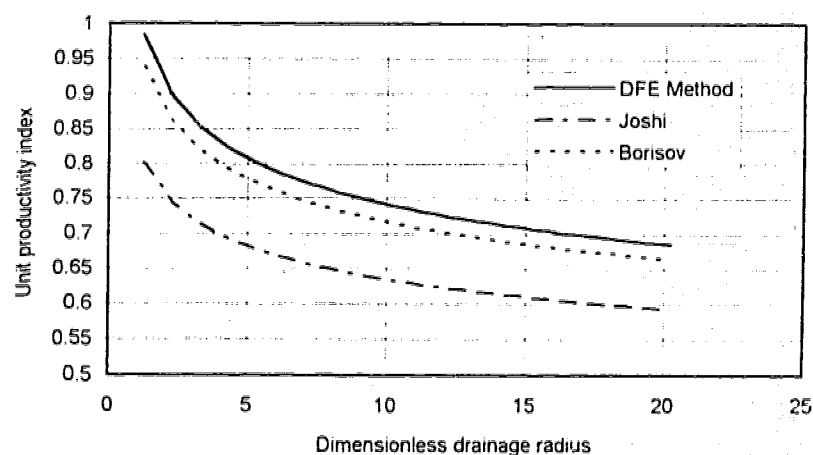
Figure 7.3.1:   A comparison of unit productivity indices obtained by different methods.

7.3.1 Comments

In Chapter 5 the validity of DFE Method in modeling transient potential solutions for horizontal and vertical wellbores is demonstrated. The calculated error for a vertical fully penetrating wellbore, for the distance between the elements equal to the wellbore radius is 0.017% at late times (Chapter 5). However, one can reduce this error to zero, by decreasing the distance between the flux elements. Moreover, in Chapter 9 the validity of DFE Method in modeling steady-state potential of vertical, partially penetrating wellbores is shown. Thus it can be inferred that the error associated with the productivity obtained by using the DFE Method is negligible.

Productivities obtained by Borisov's [1964] solution is close to those obtained by the DFE Method. As, Borisov's equation is easy to calculate, it can be recommended for a fast calculation. It should be mentioned that, Borisov's equation is restricted to horizontal wells with straight configuration in an infinite slab reservoir. However, by using the DFE Method, one can take into account 1) the wellbore configuration and 2) the reservoir geometry and the no-flow barriers.

Joshi's [1991] solution underestimates the horizontal well productivity. This can be due to the type of the flow components that have been used by Joshi. He models the resistivity to flow due to a horizontal well by the linear summation of the resistivities of two 2-D flow components. These are, the resistivities of a vertical fully penetrating plane source and a fully penetrating horizontal line source in an infinite, horizontal channel. For using such flow components no justification is provided by Joshi.

CHAPTER 8

DRAINAGE AREA AND POTENTIAL DISTRIBUTION

The shape and distribution of the isopotential lines around sources with finite length provide the shape of the transient and static drainage area and the flow type. In this chapter, the transient and steady-state potential distributions inside an infinite slab and semi-infinite slab reservoir are calculated for each individual case by applying Equation 5.1.5 with uniform potential IBC. The steady-state potential equations are used for a mathematical interpretation of the geometry of the drainage area.

8.1 Graphical Study of the Drainage Area

8.1.1 Horizontal Well

The transient (at $t_D = 0.1$) and steady-state potential distributions around a horizontal well located at the mid-height of a rectilinear reservoir in three different sections are shown in Figures 8.1.1.1 and 8.1.1.2, respectively.
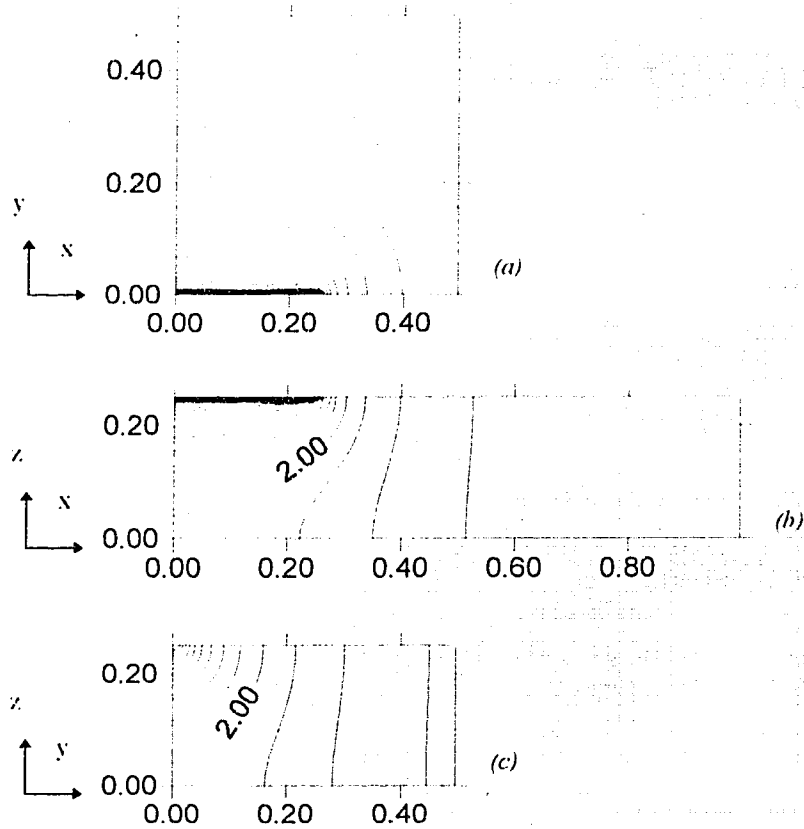
Figure 8.1.1.1: Transient potential distributions around a horizontal well with
$L_p = h_t$ at $t_D = 0.1$ for:

a) horizontal section, xy plane
b) vertical section, xz plane
c) vertical section yz plane.
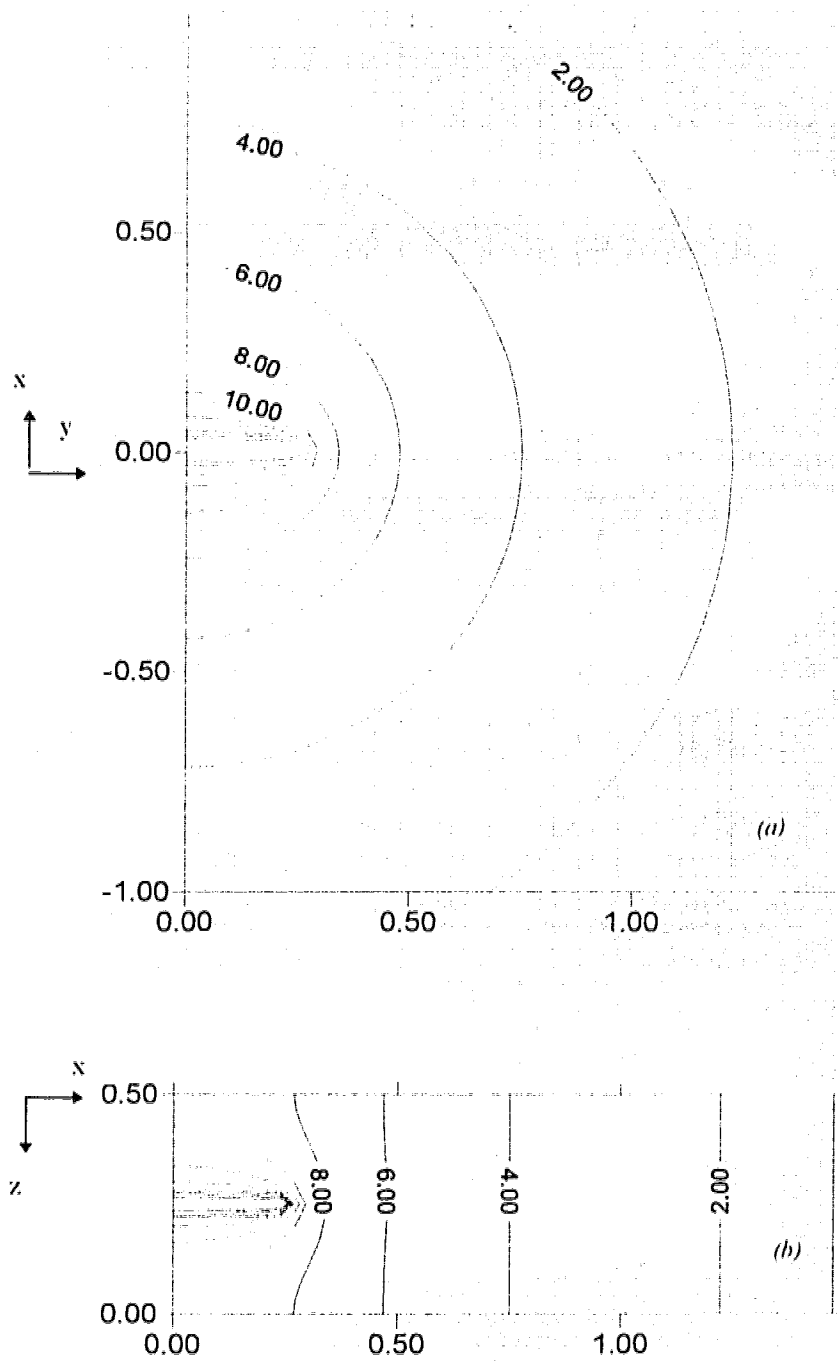
Figure 8.1.1.2: Steady state potential distributions around a horizontal well for
a) horizontal section, xy plane
b) vertical section, xz plane

In the xy-plane, the isopotentials are elliptical around the wellbore. However, they open up in the direction perpendicular to the well axis and become circular. In the xz plane, the isopotentials are again elliptical in the vicinity of the wellbore, and become vertical far from the wellbore. This indicates that the drainage area in the limit is cylindrical. Isopotential lines in the yz plane, normal to the well (x) axis, show that the streamlines are perpendicular to the wellbore surface. From these descriptions one can conclude that in an isotropic reservoir:

- the flow in the vicinity of the wellbore is always radial. However, it is spherical at both ends of the wellbore.

- the transient drainage area is ellipsoidal at the beginning of production; however, it opens up in the directions normal to the wellbore axis. If the reservoir were of infinite dimension in all directions, the drainage area would turn into a sphere in the limit. However, in the case of a rectilinear reservoir, the drainage area would be cylindrical in the limit.

The transient potential distribution around a horizontal well in two anisotropic rectilinear reservoirs is calculated and the isopotential lines are shown in Figures 8.1.1.3a and 8.1.1.3 b.

In both cases $k_y = 2$ and $k_z/k_x = 3$ for Figure 8.1.1.3.a and $k_z/k_x = 1/3$ for Figure 8.1.1.3b.

As can be expected the potential gradient in the x direction is larger for Figure 8.1.1.3a as compared to that for Figure 8.1.1.3b.
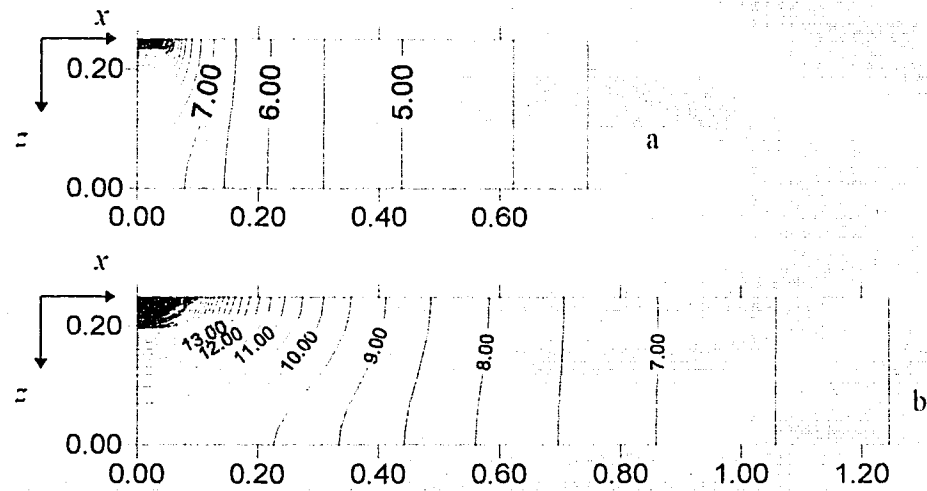
Figure 8.1.1.3: Potential distribution around a horizontal well with

$L_p = 0.2h_t$ in an anisotropic reservoir:

a) $k_x = 1$, $k_y = 2$ and $k_z = 3$ and

b) $k_x = 3$, $k_y = 2$ and $k_z = 1$.

Figure 8.1.1.4 shows the potential distribution in the lower part of a horizontal well in a semi-infinite slab reservoir. This model represents a reservoir with two parallel no-flow boundaries and a vertical no-flow barrier perpendicular to the wellbore axis.
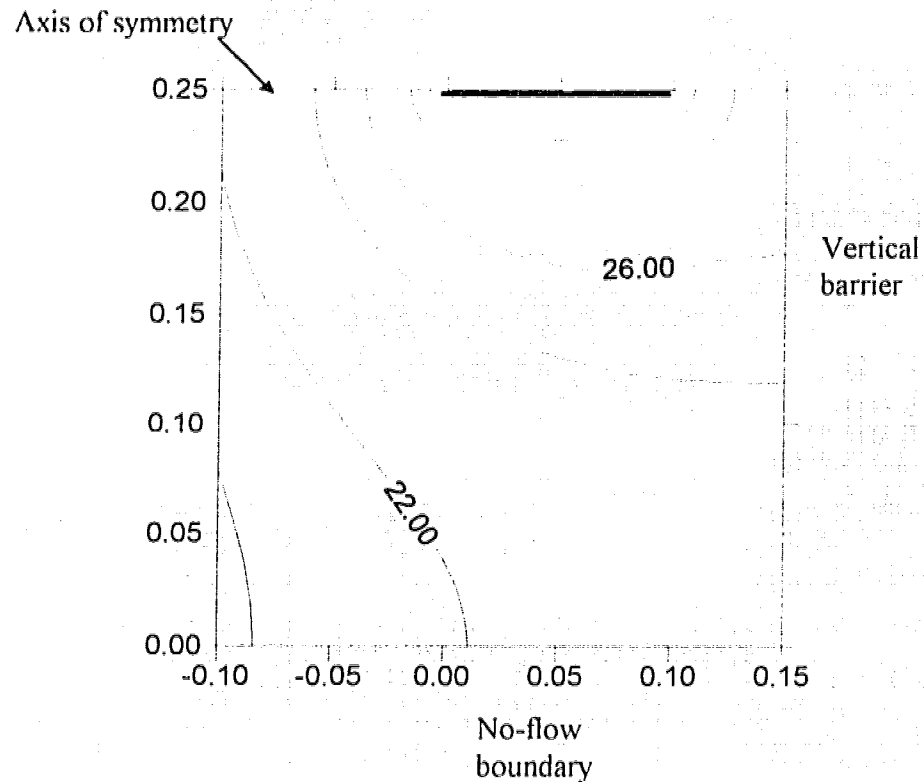
Figure 8.1.1.4: Transient potential distribution in the lower part of a horizontal well at the mid-height of a reservoir with two parallel no-flow boundaries and a vertical no-flow barrier perpendicular to the well axis.

This picture shows the application of the DFE solution to model different outer boundary conditions. Figure 8.1.1.4 indicates that the maximum vertical pressure drop is on the surface of the barrier perpendicular   the wellbore. Therefore, if this reservoir is associated with bottom water, water will :.   ne surface of this barrier and finally will break through at that end of the wellbore closer to the vertical barrier.

8.1.2 Vertical Partially Penetrating Wells

The isopotential lines around a vertical, partially penetrating well are shown in Figure 8.1.2.1. In an isotropic reservoir, the flow into the wellbore is almost radial in the plane normal to the wellbore axis and it is hemi-spherical at the wellbore ends. The near wellbore behaviour is ellipsoidal flow, with the distribution approaching cylindrical flow in the far field regions.
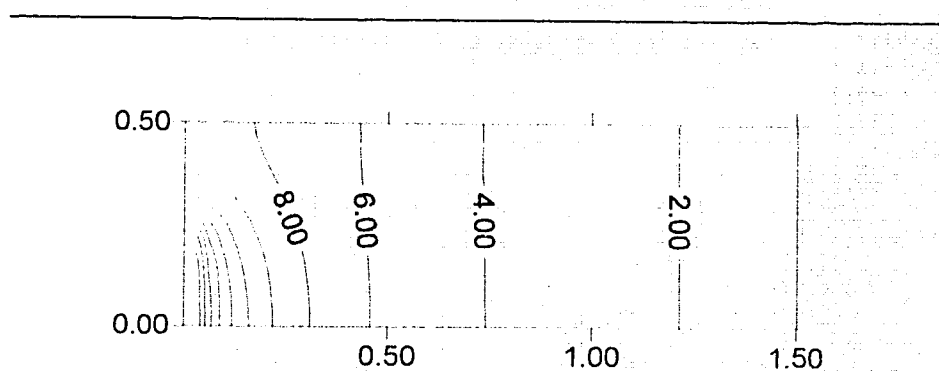
Figure 8.1.2.1: Potential distribution around a vertical, partially penetrating wellbore.

8.1.3 Curvilinear Line Sources

The potential distribution around a curvilinear wellbore is shown in Figure 8.1.3.1, representing a horizontal well with a producing heel.
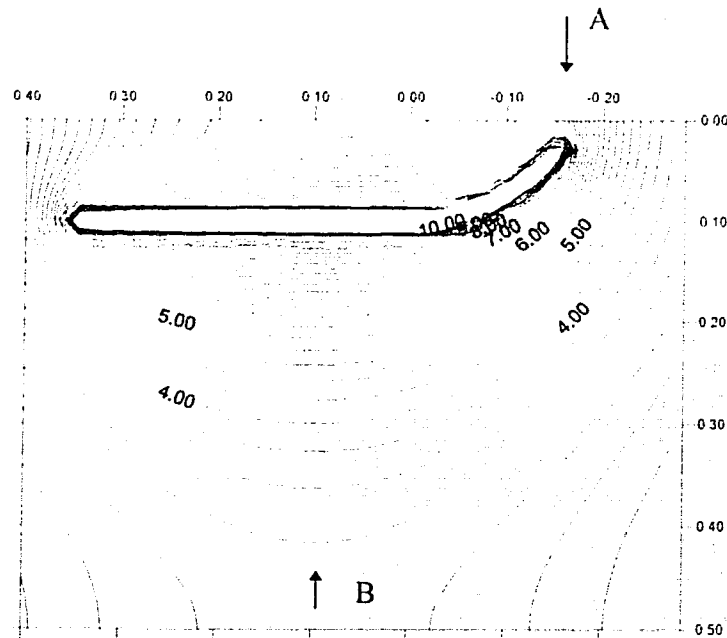
Figure 8.1.3.1: Transient potential distribution around a curvilinear line source

This is a good example to demonstrate the flexibility of the DFE method in modeling an arbitrary geometry line source. If this reservoir is associated with a gas cap, gas would breakthrough at point "A" because of the higher vertical potential drop. However, water will rise (or break through if the production rate is higher than the critical rate) at point "B" for the same reason, if there is a bottom water. The isopotential map illustrates the flow behaviour inside a reservoir that can assist with completion design.

8.1.4 Vertical Fractures

The potential distribution around a vertical fracture is shown in Figure 8.1.4.1.
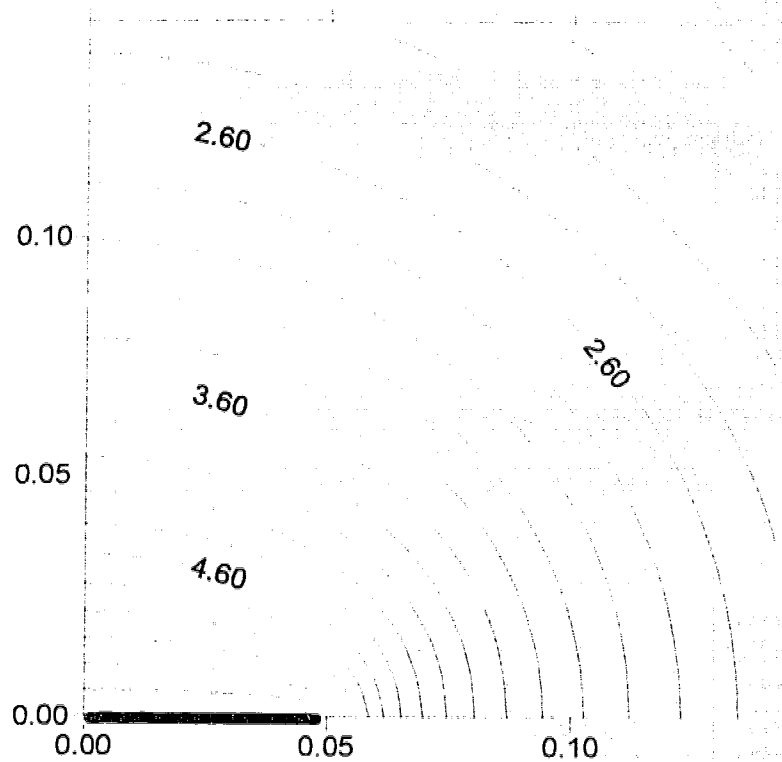
Figure 8.1.4.1: Potential distribution around a vertical, fully penetrating, fracture

The flow into the fracture is perpendicular to the fracture surface; however, at both ends it is radial. Cylindrical flow occurs far from the fracture.

8.2 Mathematical Study of the Drainage Area

8.2.1 Horizontal Well

The shape of the drainage area can be investigated by using the potential equation of a point source. Equation A.4.1 indicates that for $\rho \geq 1$ the first term will be zero [Muskat, 1932] because

$$K_0(2n\pi\rho) = 0 \qquad \text{for } \rho \geq 1 \qquad\qquad\qquad ....(8.2.1.1)$$

Thus the Equation A.4.1 reduces to:

$$\varphi = 4q\ln\frac{2}{\rho} \quad \text{for } \rho \geq 1 \qquad\qquad\qquad ....(8.2.1.2)$$

This indicates that the potential no longer depends on the vertical coordinate for $\rho \geq 1$ and the reservoir responds as if it were producing from a vertical well. In the xy plane, for the points located at distances far from the horizontal well, the difference in distance between that point and different points on the horizontal well is negligible. Therefore, as expected, the flow immediately surrounding the horizontal well is elliptical, and becomes increasingly radial away from the well. Thus the drainage area is a cylinder depending on the distance to the outer boundary.

8.2.2 Vertical Partially Penetrating Well

Because of symmetry, the potential distribution in planes xz and yz is similar in shape (in an isotropic reservoir). As it was shown in the case of a horizontal well, at $\rho \geq 1$, the potential lines are completely vertical.

8.2.3 Vertical Fracture

Since the fracture potential is obtained by superposition of a number of fully penetrating line sources, the potential lines are vertical for small and large values of ρ. In the xy-plane the isopotential lines are elliptical in areas close to the fracture surface and become circular with increasing ρ.

CHAPTER 9

AN APPROXIMATE SOLUTION FOR THE POTENTIAL OF VERTICAL

PARTIALLY PENETRATING WELLBORES

Muskat [1932] presented steady-state potential solutions for several vertical partially penetrating wellbores attached to the upper boundary. These are the wellbores with 5%, 10%, 25%, 50%, 75% and 90% penetration depths. These solutions were obtained by superposition of different uniform flux line source solutions and the solution of a point source located at the bottom of the wellbore. A schematic drawing of Muskat's model is shown in Figure 9.1.

1.2.3.4.5.6
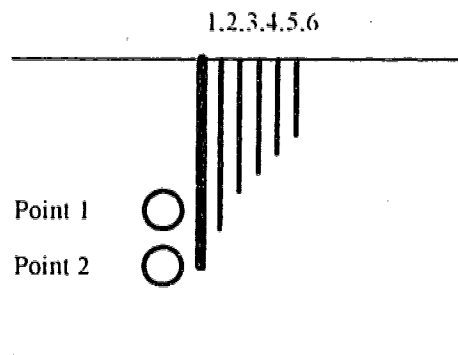
Point 1

Point 2

Figure 9.1: Schematic drawing of the superposition method used by Muskat for modeling a uniform potential, vertical, partially penetrating wellbore. The line and point elements are separated for better demonstration of the model.

Muskat's solution is not general and is restricted to only the 6 above mentioned penetration depths, each with a different solution. Table 9.1 shows the lengths of the line elements and the position of the point elements which have been used by Muskat for modeling the partially penetrating wells. Parameters are made dimensionless with respect to $2h_t$; thus, the lengths vary from 0 to 0.5 corresponding to 0 to 100% penetration depths.

Table 9.1: Length of different line sources and position of different point sources used in modeling a vertical partially penetrating wellbore.

Elements	90% [x = 0.45] Length	75% [x = 0.375] Length	50% [x = 0.25] Length	25% [x = 0.125] Length	10% [x = 0.05] Length	5% [x = 0.025] Length
line source 1	0.45	0.375	0.25	0.125	0.05	0.025
line source 2	0.44	0.36	0.24	0.115	0.04	0.02
line source 3	0.42	0.34	0.22	0.1	0.02	0.01
line source 4	0.4	0.3	0.2	0.08		
line source 5	0.375	0.2	0.15	0.05		
line source 6	0.3					
point source 1		0.37				
point source 2	0.45	0.375	0.25	0.125	0.05	0.025

Table 9.1 shows that Muskat has used different patterns for different penetration depths. For all cases he has used a point source at the bottom of the wellbore; however, for 75% penetration depth, he has used two point sources. No basis for such patterns have been

provided. It seems these patterns are obtained by trial and error. Muskat's work is first in the area of potential solutions of partially penetrating wellbores; however, his solutions have certain limitations.

i)   These solutions are for special penetration depths and cannot be generalized for other cases.

ii)   These are the solutions for wellbores attached to the upper no-flow boundary.

In other words, for a wellbore with a penetration depth other than those mentioned in the Table 9.1, none of these patterns can be applied.

In Chapter 5, the DFE Method is presented as a potential solution for an arbitrary wellbore. However, as the number of equations to be solved simultaneously is large, in this chapter an attempt is made to generalize Muskat's approach to construct an approximate solution for any type of straight vertical partially penetrating wellbore. However, the wellbore may or may not be attached to the no-flow upper boundary. Thus Muskat's solution is a special case of such a solution.

9.1   Development of the Method

The criteria for this study were

i)   the wellbore is located an an arbitrary interval inside the reservoir.

ii)   To model the uniform potential solution a minimum number of line source elements is to be used.

iii)   The potential values have to be in agreement with Muskat's solutions for wellbores

attached to the upper boundary with penetration depths 5, 10, 25, 50, 75 and 90%.

iv)   The solution must be in agreement with the DFE method solution presented in

Chapter 5.

To model a vertical wellbore not attached to the boundaries, one needs the

uniform flux potential solutions for a line source located in on an arbitrary interval inside

the reservoir. This solution is presented in Section 9.2.1. The potential along such a

wellbore is shown schematically in Figure 9.1.1.
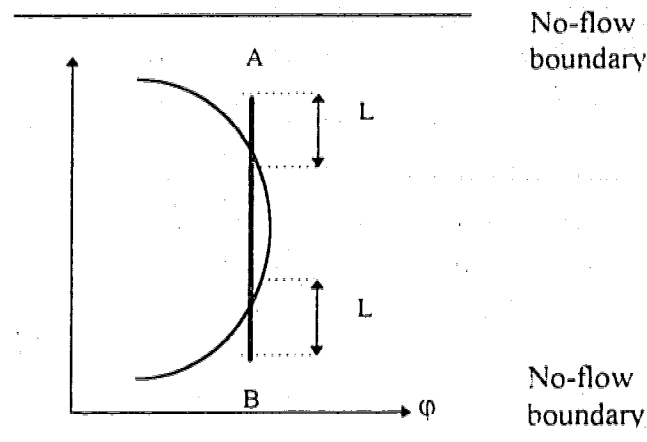
Figure 9.1.1:   Schematic drawing of the potential drop along a uniform flux,
vertical, partially penetrating line source.

Figure 9.1.1 indicates that the maximum potential drop is at the centre of the

wellbore and minimum at both ends. To modify the small potential drop at both ends of

the wellbore, additional line and point sources have to be superimposed on the main line source.

To account for the end effect, two point sources have to be introduced at the two ends of the wellbore. To modify the small pressure drop at two ends, two line sources are also added to the model. Figure 9.1.2 shows schematically the potential of each of the sources, before superposition.
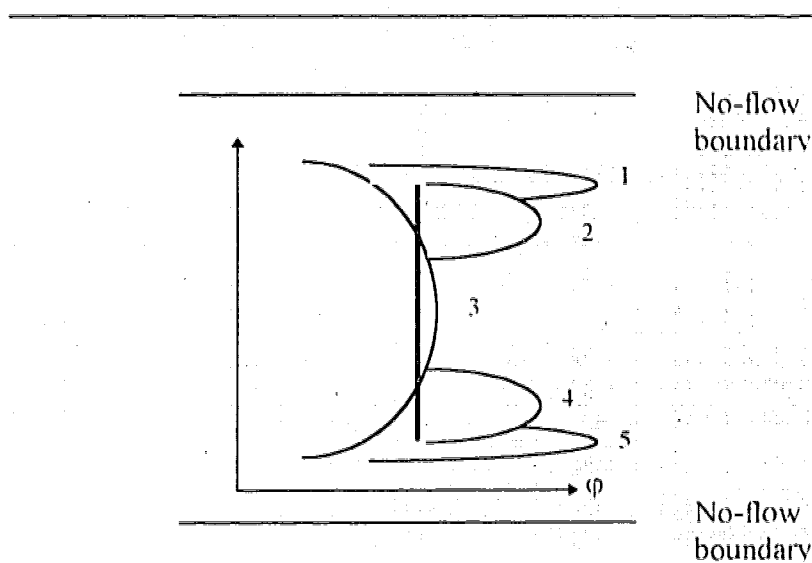
Figure 9.1.2: Schematic drawing of the potentials of line (2, 3 and 4) and point source (1 and 5) elements.

The next step is to define the strength of each element in such a way that the potential along the wellbore is almost uniform. In this model, there are 5 flux elements; thus, one needs 6 equations to solve for the strengths and the well potential. Of these, 5

equations can be found by writing the potential at five different points (observation points) along the wellbore, and 1 equation can be found from the constraint equation, which guarantee that the total flux is equal to the sum of the individual strengths.

Figure 9.1.2 indicates that the best observation points are those at which the maximum potential of the elements is located. These are shown in Figure 9.1.2 by the numbers 1, 2, 3, 4 and 5. The uniform potential solutions for different line source penetration depths are calculated. For each penetration depth, several values of h have been used where

$$h = \frac{l_T}{l} \qquad \qquad \qquad \dots\dots\dots\dots\dots\dots\dots(9.1)$$

and where l_T and l are the length of the original line source and the length of the part that has been chosen for superposition, respectively.

The results are shown in Table 9.1.1.

Table 9.1.1: The potential values obtained by superposition of 5 flux elements for different values of b compared to Muskat's and the DFE Method solutions.

Pen.%	b=3	b=4	b=5	b=6	b=8	b=10	b=20	b=100	Muskat	DFE
5	279.22	278.9	279.3	279.9	280.9	281.5	282.31	281.95	279.46	279.23
10	169.5	169.41	169.6	169.87	170.06	170.37	171.6	172.16	169.73	169.46
25	84.69	84.6	84.61	84.69	84.8	84.9	85.33	86.07	84.459	84.34
50	49.54	49.47	49.466	49.48	49.53	49.58	49.8	50.02	49.18	49.23
75	36.5	36.46	36.45	36.45	36.48	36.5	36.61	36.86	36.53	36.28
90	32.18	32.15	32.142	32.14	32.142	32.155	32.21	32.35	32.16	32.03

Table 9.1.1 indicates that the pattern of 5 flux elements is successful in modelling a uniform potential solution for small values of b (b 3 to 6). As the DFE method is the upper limit on the exact solutions, it is used as a basis for calculation of the error associated with the 5 flux elements method.

The solutions obtained using 5 flux elements and those of Muskat are in good agreement. Thus it can be concluded that the pattern for modelling a vertical well is not unique. However, other patterns might exist which provide similar results. As the aim of this study was to define a general pattern with a minimum number of elements, other patterns with a larger number of the elements have not been considered. In the following sections, the mathematical equations for modelling a wellbore with the 5 flux element method are provided.

9.2 Superposition of 5 Flux Elements

To model a uniform potential solution for a vertical partially-penetrating wellbore, the potential solutions of the five flux elements were superimposed in such a way that the potential along the wellbore is approximately uniform. The schematic drawing of this model is shown in Figure 9.2.1.

The model consists of three line source flux elements with uniform flux solution and two point sources as:

1. *Flux element no. 1. (Line source).* Its length is identical to the original perforation interval.

2. *Flux element no. 2. (Line source).* Its length is 1/3 to 1/6 of the perforation interval and is located at the top of the perforation interval.

3. *Flux element no. 3. (Line source).* Its length is identical to flux element no. 2, and is located at the lower part of the perforation interval.

4. *Flux element no. 4. (Point source).* It is located at the top of the perforation interval.

5. *Flux element no. 5. (Point source).* It is located at the lower end of the perforation interval.
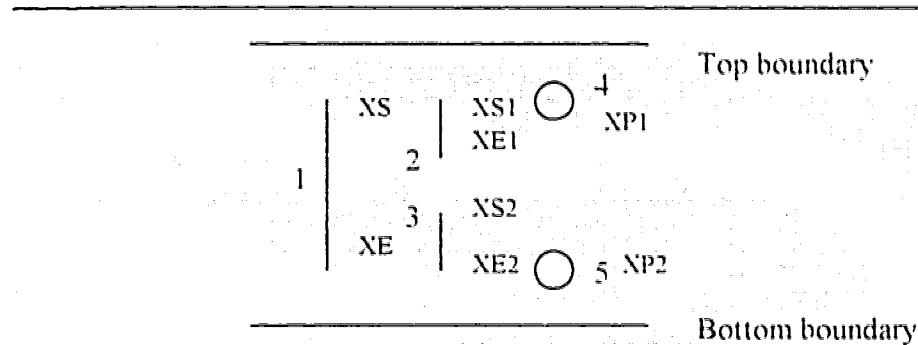
Figure 9.2.1:   Schematic drawing of a vertical partially penetrating well modeled by 5 flux elements.

Here the method is applied to the steady-state potential solution, but, it is applicable to transient flow as well.

The steady-state potential solution for a point source is given in Appendix A. Also the steady-state potential solution for a vertical, partially penetrating, uniform flux line source attached to the upper boundary is given in Appendix C. However, for the new general model the uniform flux solutions of an arbitrary perforation interval and location is needed. This is obtained by the supperposition of two flux element solutions, one for injection and one for production.

9.2.1   The Potential Solution of a Uniform Flux Vertical Partially Penetrating Wellbore with Arbitrary Perforation Location

The solution for a vertical partial penetrating wellbore at the top of the reservoir is given by [Muskat, 1932]:

$$\phi(w,\rho,x) = 4q\left[\frac{1}{\pi}\sum_{n=1}^{\infty}\left\{\frac{1}{n}K_0(2\pi n\rho)\cos(2\pi n w)\sin(2\pi n w)\sin(2\pi n x)\right\} + x\ln(2/\rho)\right].$$

..................................(C.1.1)

The function K_0 is a modified Bessel function of first kind and of order zero, x is the well penetration depth and ρ is the horizontal distance to the vertical axis

$$\rho = \left((x-x_L)^2 + (y-y_L)^2\right)^{1/2}$$ ....(C.1.2)

and flux q is:

$$q = \frac{Q\mu}{4\pi k a x}$$ ....(C.1.3)
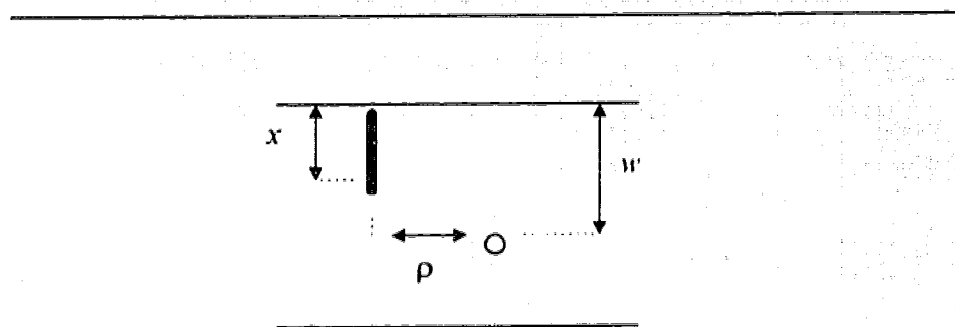
Figure 9.2.1.1: Schematic of a vertical partially penetrating

wellbore in a rectilinear reservoir

The potential solution given by Equation C.1.1 is linear. Thus by superimposing the potential solutions for two line sources given by Equation C.1.1, with positive and negative signs, representing production and injection, respectively, one can obtain a uniform flux solution for a vertical well extending from x_1 to x_2 with arbitrary perforation location and interval (Figure 9.2.1.2).

$$\phi(w,\rho,x_1,x_2) = 4q \left[\frac{1}{\pi} \sum_{n=1}^{\infty} \left\{ \frac{1}{n} K_0(2\pi n\rho) \cos(2\pi n w) \sin(2\pi n w) \left[\sin(2\pi n x_2) - \sin(2\pi n x_1) \right] \right\} + (x_2 - x_1) \ln(2/\rho) \right]$$

$$\dots\dots\dots\dots\dots\dots\dots\dots\dots(9.2.1.1)$$

where

$$q = \frac{Q\mu}{4\pi k a(x_2 - x_1)}.$$

$$\dots\dots\dots\dots\dots\dots\dots(9.2.1.2)$$

Equation 9.2.1.1 describes the potential due to a vertical, partially penetrating wellbore extending from x_1 to x_2 at a point located at vertical coordinate w and horizontal distance to the wellbore ρ.
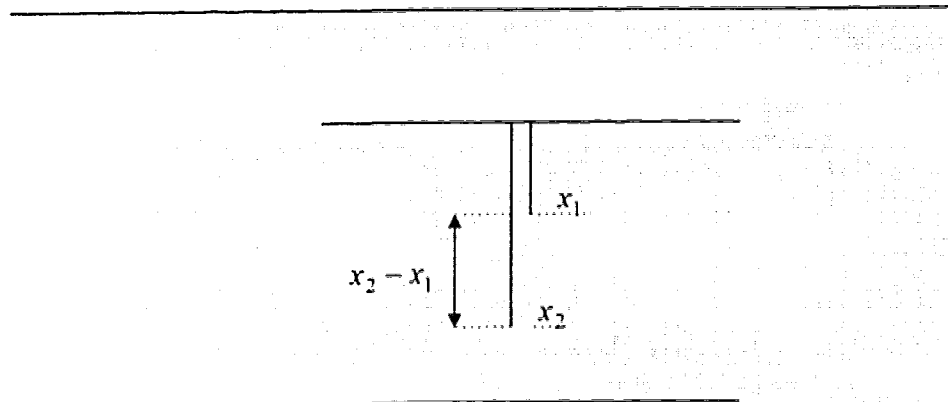
Figure 9.2.1.2: Superposition of two uniform flux vertical line sources
to obtain a solution for an arbitrary perforation location.

9.2.2 Uniform Potential Solution of a Vertical, Partially Penetrating Wellbore with an Arbitrary Perforation Location

The uniform potential solution for a vertical, partially penetrating line source is obtained through the superposition of five flux elements as shown in Figure 9.1.2.1. The elements are:

- Flux element no 1 has the same length as the original wellbore. If the top and the bottom of the well are located at X_S and X_E, respectively, then the producing length would be:

$$L_p = X_E - X_S \qquad \dots\dots\dots\dots\dots\dots\dots\dots(9.2.2.1)$$

- Flux element no. 2 is a line source with a producing length restricted between X_{S1} and X_{E1} where:

$$X_{S1} = X_S \qquad\qquad\qquad (9.2.2.2)$$

and

$$X_{E1} = X_{S1} + (X_E - X_S)/6 \qquad\qquad\qquad (9.2.2.3)$$

- Flux element 3 is a line source extending from X_{S2} to X_{E2} where:

$$X_{E2} = X_E \qquad\qquad\qquad (9.2.2.4)$$

$$X_{S2} = X_E - (X_S - X_E)/6 \qquad\qquad\qquad (9.2.2.5)$$

- Flux elements 4 and 5 are two point sources located at the top and the bottom of the first line source

$$X_{P1} = X_S \qquad\qquad\qquad (9.2.2.6)$$

$$X_{P2} = X_E \qquad\qquad\qquad (9.2.2.7)$$

By applying the superposition principle one can write the potential at any point in the reservoir as follows:

$$\varphi(w,\rho) = A_1\varphi_{L1}(X_S,X_E,w,\rho) + A_2\varphi_{L2}(X_{S1},X_{E1},w,\rho) + A_3\varphi_{L3}(X_{S2},X_{E2},w,\rho) +$$
$$A_4\varphi_{P1}(X_{P1},w,\rho) + A_5\varphi_{P2}(X_{P2},w,\rho)$$

$$\qquad\qquad\qquad (9.2.2.8)$$

where $\varphi_{l,1}$, $\varphi_{l,2}$ and $\varphi_{l,3}$ are the potentials due to the three line source flux elements, and $\varphi_{p,1}$ and $\varphi_{p,2}$ are the potentials due to the two point sources. The unknowns A_1 to A_5 are the flux strengths of the elements.

To find the flux distribution and the wellbore potential, six equations are required. Five of the equations are obtained by writing the potential equation at five different points along the wellbore (locations of these points are shown in Figure 9.1.2). The last equation is the constraint equation:

$$\sum_{i=1}^{5} A_i = 1 \qquad \qquad \text{.............................(9.2.2.9)}$$

This method provides the potential solution for any possible perforation location as follows:

$X_S = 0$, $X_L < 0.5$, well located at the top of the reservoir;

$X_S > 0$, X_L 0.5, well located at the bottom of the reservoir;

$X_S > 0$, X_L 0.5 well located between the upper and lower boundaries of the reservoir.

This general method allows one to study coning phenomena including:

1. water coning in oil and gas reservoirs with bottom water;

2. gas coning in oil reservoirs with a gas cap;

3. simultaneous gas and water coning in oil reservoirs with a gas cap and bottom water.

In Chapter 10. this new and general solution is applied to the coning problems in oil reservoirs with bottom water and/or a gas cap.

9.3   Validity of the Method

The validity of the method was checked by comparison with Muskat's solution for vertical, partially penetrating wellbores attached to the no-flow boundaries and the DFE Method. The dimensionless wellbore radii are equal to 0.001. In the 5 flux elements solution. the length of the smaller elements is chosen to be 1/6 of the original wellbore length.

Table 9.3.1 indicates a good agreement between these solutions.

Table 9.3.1:   Potential of the vertical partially penetrating wellbores with different penetration depths, obtained by the method of superposition of 5 flux elements and the DFE Method and Muskat [1932]. The error of the 5 flux element solution is obtained with respect to the DFE Method.

Penetration depth %	DFE method	Muskat	5 flux elements	% error
90	279.23	279.46	279.92	0.25%
70	169.405	169.73	169.87	0.27%
50	84.343	84.459	84.6	0.3%
25	49.23	49.18	49.48	0.5%
10	36.28	36.53	36.42	0.4%
5	32.03	32.16	32.13	0.3%

9.4   Streamlines

Streamlines are useful for studying the fluid flow mechanism in a reservoir. The streamline equations for a source under steady-state conditions in cylindrical coordinates can be derived using Equation 9.4.1 (Muskat, 1932):

$$\psi'(\rho, w) = -a\rho \int \frac{\partial \varphi}{\partial \rho} dw \qquad \qquad \text{...................................(9.4.1)}$$

Note: The stream function is represented by ψ' to prevent any confusion with ψ function which was previously used in Equation A.4.5.

Applying Equation 9.4.1 to the point source potential, Equations A.4.1 and A.4.3 for large and small values of ρ the stream function is found as:

$$\psi'_{p_i} = 4a \left[2\rho \sum_{n=1}^{\infty} \left(K_1(2n\pi\rho) \cos(2n\pi w_p) \sin(2n\pi w) + w \right) \right]$$

$$\text{...................................(9.4.2)}$$

where K_1 is the modified Bessel function of first kind of first order.

For small values of ρ (≤ 1), the streamline function is found as:

$$\psi'_{p_i} = a \left[\frac{w + w_p}{\left(\rho^2 + (w + w_p)^2 \right)^{1/2}} + \frac{w - w_p}{\left(\rho^2 + (w - w_p)^2 \right)^{1/2}} \right]$$

$$\text{...................................(9.4.3)}$$

in which ψ'_{p_i} is the streamvalue of the ith point source.

The equation of the streamlines for a line source similarly can be obtained as:

$$\psi'_{L_i} = 4\left[\frac{\rho}{\pi}\sum_{n=1}^{\infty}\frac{1}{n}K_1(2\pi n\rho)\sin(2\pi nx)\sin(2\pi nw) + xw\right] \quad\quad\quad (9.4.4)$$

Therefore the stream line value due to the vertical well can be written

$$\psi'_h = \sum_{i=1}^{5} A_i\psi'_i \quad\quad\quad (9.4.5)$$

The streamline values for a point source and a vertical partially penetrating wellbore have been calculated and plotted in Figures 9.4.1 and 9.4.2, respectively.
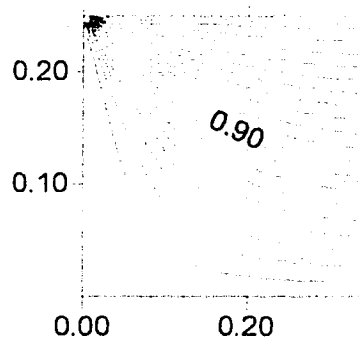
Figure 9.4.1: Streamlines around a point source
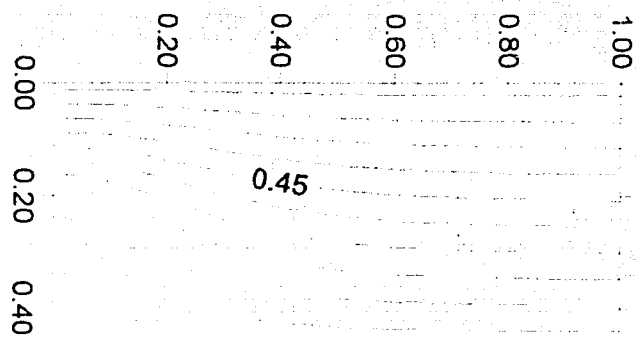
Figure 9.4.2:   Streamlines around a vertical partially penetrating wellbore using the superposition of 5 flux elements.

CHAPTER 10

CONING AND PERFORMANCE OF HORIZONTAL AND VERTICAL WELLS IN THE PRESENCE OF A GROWING CONE

In this chapter, sources with finite length in reservoirs underlain by bottom water and/or overlain by a gas cap are studied. This study is limited to coning and wellbore performance in the presence of a growing cone before breakthrough. Because of similarity, only oil reservoirs with bottom water are considered, unless otherwise specified.

The physical model is a rectilinear (infinite slab) reservoir. The assumptions for this study are those that have been made by Muskat and Wykoff [1935]:

- Small compressibility.

- Negligible viscosity contrast.

- Single phase in the oil zone.

- The cone height is controlled by static equilibrium.

- Production under steady state conditions.

  However, in this study the following assumption are used:

- The true WOC as no-flow boundary.

- Transient potential equations to calculate the breakthrough time and the performance of the wellbore.

The first assumption, that is small compressibility, limits the transient solution to oil reservoirs; however, the steady state solution can be applied to gas reservoirs as well. Høyland et al. [1989] by using a numerical simulator showed that, under steady-state conditions, the critical production rate does not depend on the mobility ratio. However, the experimental works of Sobocinski and Cornelius [1965] and Bournazel and Jeanson [1971] indicate that the breakthrough time is sensitive to mobility ratio. Thus, the second assumption, that is negligible viscosity contrast, has no effect on the results of steady-state solutions; however, it affects the time scale for transient solutions or breakthrough time. The third assumption, that is single phase fluid flow, provides an approximate solution for the oil reservoirs with a gas cap. However, this assumption has been used widely by Muskat and Wykoff [1932], Muskat [1982], Meyer and Garder [1954], Chaney and Nobel [1956], Chierici et al. [1964], Kuchuk et al. [1988] and Ozkan and Raghavan [1990].

Reservoirs with bottom water are produced with a horizontal or a vertical partially penetrating well, both of which are sources with finite length. In Chapter 5 the DFE Method was developed and introduced as a general solution for sources with finite length with any arbitrary outer boundary conditions. Knowing the boundary conditions at the water-oil contact (WOC), one can use the DFE Method to study the performance of these sources in reservoirs with bottom water. Fluid properties are left without subscript but represent the principal fluid in the reservoir unless explicitly indicated otherwise, for example oil in an oil-water system, or gas in a gas-water system.

10.1   Boundary Condition at WOC

Two types of boundary conditions have been used in the literature for the WOC in coning problrems: 1) a no-flow boundary and 2) the initial WOC as a constant potential boundary.

Muskat and Wyckoff [1935] established the fundamentals of coning for a coning problem due to a vertical well in a rectilinear reservoir under steady-state conditions. Using the concept of static equilibrium, Muskat and Wykoff found the cone height and the critical production rate. Muskat and Wykoff proposed that the proper approach is to take the WOC as a no-flow boundary. As taking an unknown and irregular geometry as the actual boundary was impractical at the time, Muskat and Wykoff used the *initial* WOC as the no-flow boundary. However, Muskat and Wykoff postulated that if the *actual* WOC were considered as a no-flow boundary, the critical production rate would have been lower. This justified their approximate approach because the critical production rate would be conservative.

Among others, Wheatly [1985] examined the same problem by assuming the WOC to be a streamline, implicitly considering the actual WOC as a no-flow boundary.

Muskat [1947] modeled an active bottom water drive for a vertical well in a fully developed reservoir by assuming the initial WOC as a constant potential boundary. In the subsequent discussion, by Elkins and in Muskat's reply [Muskat, 1947], it became clear that a constant potential at the initial WOC is not a necessary condition for an active bottom water drive. Indeed, a constant potential boundary is the necessity of steady-state solutions. That is because, the absolute. steady-state, potential at a single point inside the

reservoir does not carry a meaningful value and it is only the difference of the potential between two given points that can model the flow between them. For the same reason, the productivity of a wellbore [See Chapter 7 of this work] highly depends on the drainage radius (location of the constant potential boundary).

In the following analysis it is shown that the two models 1) the WOC as a no-flow boundary, and 2) the WOC as a constant potential boundary, are limiting cases, before breakthrough, of a single problem.

10.2   The Condition at the Initial WOC before Breakthrough

Bottom water rises in a cone to a certain height in response to production from the oil zone. The difference in the weight of the two fluids of a column with the height of the cone is identical to the vertical pressure drop [Muskat and Wyckoff, 1935]. Thus two forces with identical magnitude and opposite directions (Figure 10.2.1) are acting on the WOC:

$$\delta p = -\delta \gamma g h_w \qquad \qquad \text{............................(10.2.1)}$$

Equation 10.2.1 implies that the pressure at the initial WOC remains constant at p_i before breakthrough, and that this is a condition of static equilibrium.
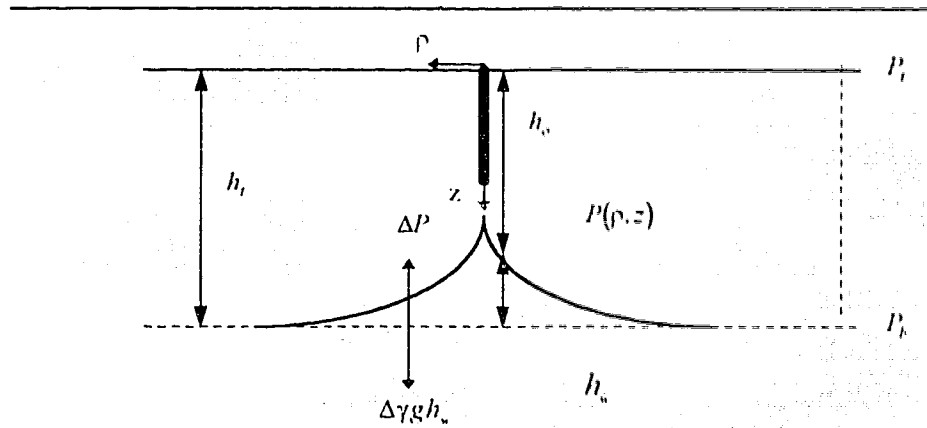
Figure 10.2.1: Schematic drawing of a cone under a vertical well

The initial potential at the original WOC can be written as:

$$\varphi_i = p_i - \gamma_o g h_i \qquad\qquad (10.2.2)$$

The potential on the surface of the interface after it has moved can be obtained as:

$$\varphi = p_i - \gamma_o g h_o - \gamma_w g h_w = p_i - \gamma_o g h_i - \Delta\gamma g h_w \qquad (10.2.3)$$

Equations 10.2.2 and 10.2.3 are identical only if the density difference is zero. Thus the solution using a constant potential at the initial interface is an approximation to the coning problem when the two fluids have identical densities.

The assumption of initial WOC as a no-flow boundary is a valid assumption if the cone height is small.

Therefore, before breakthrough, the two solutions with the original WOC position as 1) a no-flow boundary and 2) a constant potential boundary are the limiting cases of the

general coning problem. However, the exact solution is obtained by considering a no-flow moving boundary.

After breakthrough, when static equilibrium no longer exists, the original WOC position ceases to remain at a constant pressure condition. After the breakthrough period, when the wellbore is producing water directly from the aquifer, the boundary condition should be found through the knowledge of the geometry and extension of both the oil and water zones.

10.3   WOC Geometry

Coning is a general term that is used to describe the deformation of the water-oil interface. The fluid flow in a rectilinear reservoir with bottom water is illustrated in Figure 10.3.1.
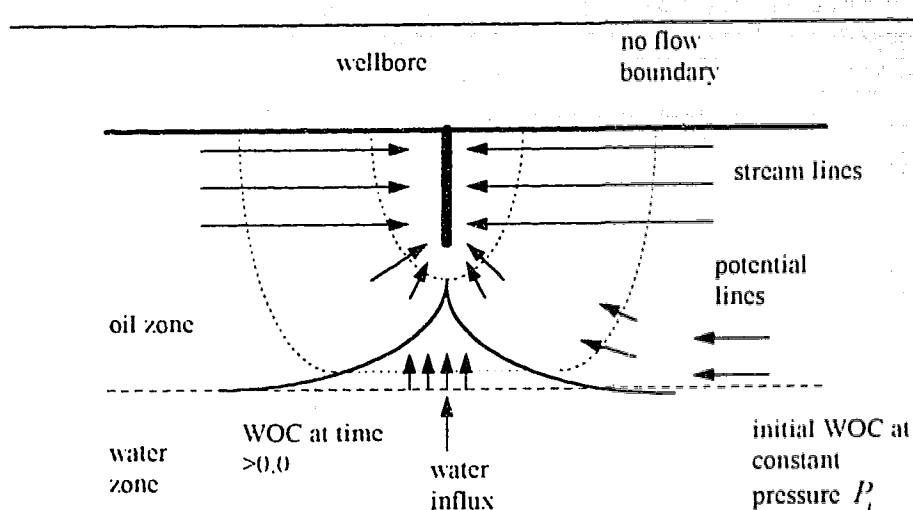
Figure 10.3.1: Schematic drawing of flow mechanism in an oil reservoir underlain by a bottom water.

In this section the cone geometry is derived using the concept of static equilibrium. For an anisotropic reservoir with vertical permeability, k_v, and horizontal permeability, k_h, the equivalent isotropic reservoir height is defined as [Muskat, 1947]:

$$t' = t\sqrt{k_h / k_v}$$ ....(10.3.1)

where t and t' are the actual reservoir height and its equivalent in an isotropic reservoir.

An equation for the cone height is developed by Muskat and Wykoff [1935] as a function of the potential and the pressure drop. The cone height for a given pressure drop has to be found graphically. Moreover, to use that method the parameters, that are reservoir thickness, oil viscosity, permeability, pressure drop and production rate must be known.

In this section a cone height equation is developed as a function of the potential drop and a dimensionless coefficient. The new cone height equation permits for a computer programing. This new equation provides the ability of predicting the wellbore performance in the presence of a growing cone.

A dimensionless potential is defined as:

$$\varphi_D = \frac{2\pi k a}{Q\mu}(p - \gamma g z)$$ ....(10.3.2)

where

$$a = 2t'$$ ....(10.3.3)

A potential drop is defined as:

$$\Delta\varphi_D = \varphi_D - \varphi_{DW}$$ ....(10.3.4)

Writing Equation 10.3.2 for a point on the WOC and applying Equation 10.3.4 one obtains

$$\Delta\varphi_{\iota\iota}(\rho,z) = \frac{2\pi k_h a}{Q\mu}\left[p(\rho,z) - \gamma_{\sigma}gz\right] - \frac{2\pi k_h a}{Q\mu}\left[p_{\iota\iota} - \gamma_{\sigma}gz_{\iota\iota}\right] \quad\text{.............................(10.3.5)}$$

where $p(\rho,z)$ is the pressure of a point at the horizontal coordinate ρ and vertical coordinate z and $p_{\iota\iota}$ is the pressure of the wellbore calculated at a vertical coordinate $z_{\iota\iota}$.
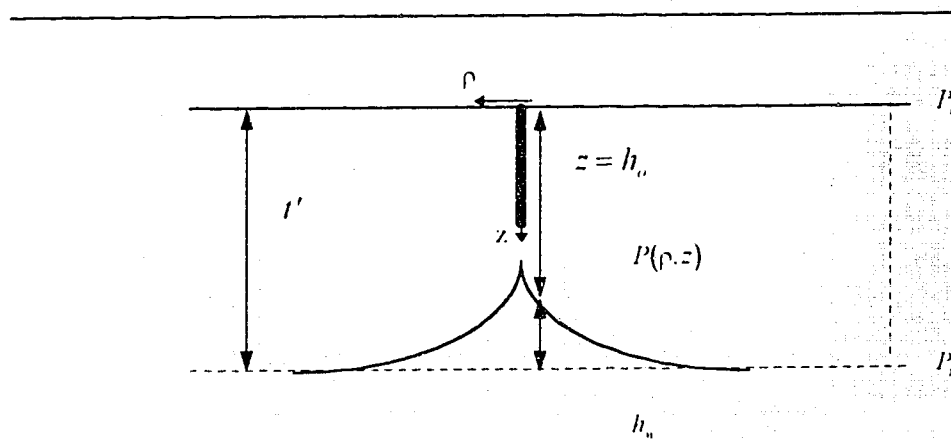
Figure 10.3.2: Schematic drawing of coning before breakthrough. Absolute pressures at different points

$$p(\rho,z) = p_b - \gamma_{w}g(t' - z) \qquad\qquad\text{...........................(10.3.6)}$$

and

$$p_b = p_t + \gamma_{\sigma}gt' \qquad\qquad\text{...........................(10.3.7)}$$

Substituting Equations 10.3.6 and 10.3.7 into Equation 10.3.5 one obtains:

$$\Delta\varphi_{D} = \frac{2\pi k_h a}{Q\mu}\left[\Delta p - \Delta\gamma g(r' - z)\right] \tag{10.3.8}$$

where

$$\Delta p = p_t - p_w + \gamma_o g z_w \tag{10.3.9}$$

At the boundary of the drainage area the height of the cone is almost zero, thus Equation 10.3.8 can be written as:

$$\Delta\varphi_{De} = \frac{2\pi k_h a}{Q\mu}\Delta P \tag{10.3.10}$$

where $\Delta\varphi_{De}$ is the potential drop between the wellbore and the outer boundary.

Dividing Equation 10.3.8 by Equation 10.3.10 and substituting Δp from Equation 10.3.10 one obtains:

$$(r' - z) = \left[\Delta\varphi_{De} - \Delta\varphi_{D}(\rho, z)\right]\frac{Q\mu}{2\pi k_h a\Delta\gamma g} \tag{10.3.11}$$

Now

$$r' - z = h_{Cone} = 2r'h_c \tag{10.3.12}$$

where h_{Cone} is the dimensional cone height and h_c is dimensionless cone height. Applying Equations 10.3.1 and 10.3.3 and 10.3.12, and assuming a formation volume factor of B_o, Equation 10.3.11 reduces to:

$$h_c = \left[\Delta\varphi_{Iw} - \Delta\varphi_{Ii}(\rho,z) \right] \frac{QB_o\mu}{8\pi \frac{k_h^2}{k_v} r^2 \Delta\gamma g} \qquad \text{...................................(10.3.13)}$$

Introducing the concept of dimensionless density

$$\Delta\gamma_D = \frac{8\pi \frac{k_h^2}{k_v} r^2 \Delta\gamma g}{QB_o\mu} \qquad \text{...................................(10.3.14)}$$

enables Equation 10.3.15 to be written as:

$$h_c = \left[\Delta\varphi_{Iw} - \Delta\varphi_{Ii}(\rho,z) \right] \left(\Delta\gamma_D \right)^{-1} \qquad \text{...................................(10.3.15)}$$

Substituting from Equation 10.3.4 one can write

$$h_c = \left[\varphi_{Iw} - \varphi_{Ii}(\rho,z) \right] \left(\Delta\gamma_D \right)^{-1} \qquad \text{...................................(10.3.16)}$$

Equation 10.3.16 indicates that the cone height, and consequently its stability, is controlled by the value of the dimensionless density. For large values of ($\Delta\gamma_D$) the cone height is very small. A sensitivity analysis shows that there is a critical dimensionless density (CDD) above which the cone is stable. As can be seen from Equation 10.3.16, the dimensionless density ($\Delta\gamma_D$) is a coefficient that accounts for: 1) reservoir geometry, 2) permeability anisotropy, 3) fluid properties, 4) production rate and 5) the density difference between the two fluids. The wellbore geometry and the drainage radius are associated with the potential solution. Therefore, every wellbore length is associated with a CDD for any given reservoir.

The parameters that affect the magnitude of dimensionless density and consequently the cone height and time of the breakthrough are:

Permeability Anisotropy Coefficient $\left(k_h^2/k_v\right)$. For very small values of vertical permeability or large values of horizontal permeability the anisotropy coefficient grows very large. Under these conditions the cone height will be small. At the limit, where k_v approaches zero, the cone height will approach zero.

Reservoir Thickness $\left(r^2\right)$. The thicker the reservoir, the smaller the cone height will be and the longer the time to water breakthrough will be if all other parameters remain constant.

Density Difference, $\Delta\gamma$. Large values of $\Delta\gamma$ result in the formation of small cones. If the density difference approaches zero, the cone height will be infinite, implying a very short time to water breakthrough. Therefore the solution for the condition of constant potential at the initial WOC, which was based on a negligible density difference, is valid only for a very short period before breakthrough.

Fluid Viscosity, μ. The greater the viscosity the higher the cone will be and the greater the risk of breakthrough. Thus it can be inferred that in viscous heavy oils a stimulation process that reduces oil viscosity reduces the risk of water or gas breakthrough.

Production Rate, Q. Production rate is the only parameter that can be changed easily and arbitrarily. By reducing the production rate one can freeze the movement of the WOC boundary.

For large values of dimensionless density the existence of bottom water or a gas cap can be neglected. Therefore, a solution to the diffusivity equation with a no-flow boundary at the initial interface of two fluids should be a valid approximation in this case for well test analysis in infinite acting reservoirs.

The solution to the diffusivity equation with constant potential at the original interface, prior to breakthrough, is valid only when the density difference is negligible.

10.4 Transformation of Domain

If one treats the WOC as a no-flow boundary, one must cope with two problems:

- The geometry of the WOC is unknown and irregular.

- Even if the geometry were known, considering an irregular geometry as the no-flow boundary in the Laplace or diffusivity equation appears to be impractical.

In this work a transformation is developed to transform the cone boundary shape into a straight line. For this transformation only the height of the cone at the point under the wellbore is required. When transforming the boundary, one must also transform the wellbore configuration accordingly. One can assume that the reservoir properties in the transformed domain are the same as in the actual domain. This is a valid assumption as the distance between the wellbore and the cone remains approximately the same as that in the actual domain.

A transformation coefficient, $\alpha(\rho)$, is defined here as:

$$\alpha(\rho) = 1 + \frac{h_{Dw}(\rho)}{0.5 - h_{Dw}(\rho)} \qquad \qquad \text{.............................(10.4.1)}$$

where $h_{Dw}(\rho)$ is the dimensionless cone height at a horizontal distance ρ from the Z axis.

Therefore any vertical coordinate can be transformed as:

$$w_T = \alpha(\rho) \times w \qquad \qquad \text{.............................(10.4.2)}$$

This transformation guarantees that any point on the upper no-flow boundary remains at

the initial coordinate value while the points on the cone surface are shifted to the initial

WOC location. The application of Equation 10.4.1 implies that:

1)   The producing length of the vertical well must be increased. The transformed well

penetration depth can be found from

$$L_{pT} = L_p \times \alpha(\rho) \qquad \qquad \text{.............................(10.4.3)}$$

where L_{pT} and L_p are the wellbore depths in the transformed and real domain,

respectively.

2)   The elevation of a horizontal well be changed while its producing length remain

constant.

The validity of this transformation is checked by comparing the results obtained using the

transformation with the results of analytical and numerical solutions of Wheatly [1985]

and Høyland et al. [1989] respectively.

For reservoirs with both bottom water and a gas cap, a combined transformation equation

has been developed:

$$z_i = z\left(1 + \frac{h_{cw}}{0.5 - h_{cw}}\right)\left(1 + \frac{h_{cg}}{0.5 - h_{cg}}\right) \quad \dots\dots\dots\dots\dots\dots(10.4.4)$$

10.4.1 Application of Transformation to Coning Analysis

Equation 10.3.16 indicates that the production rate is a function of cone height and potential. Moreover, the potential depends on the cone height or current WOC location while the cone height itself depends on the potential. Here an implicit method for steady-state and unsteady state flow to calculate the cone height and potential at the same time is presented. This method also defines the shape of the cone, which is the dynamic WOC.

10.5 Coning and Performance of Vertical Partially Penetrating Wells

In this section the steady state and transient potentials due to a vertical, partially penetrating wellbore are used to study the critical production rate and the performance of the wellbore in the presence of a growing cone. The steady state potential solution is modeled by the Five Flux Elements Method that was developed in Chapter 9. The transient potential solution is obtained through the application of the DFE method developed in Chapter 5.

10.5.1 Critical Production Rate

Steady-state flow is simpler than transient flow because of the calculation procedure, and is useful for optimizing the length and location of the perforation interval. Also it can be used to study the stability of the cone at various production rates. The uniform potential solution for a vertical well is obtained by superposition of the five flux

elements, as discussed in Chapter 9. Substituting for the values of the steady state potential (Equation 9.2.2.8) in Equation 10.2.16 the cone height can be written as:

$$h_{wcd} = \frac{1}{2\Delta\gamma_D} \frac{\left(\sum_{i=1}^{5} A_i\phi(x_i,\rho,w)\right) - 4\left(\sum_{i=1}^{5} A_i x_i\right) ln \frac{2}{\rho_e}}{\sum_{i=1}^{5} A_i x_i} \qquad \qquad (10.5.1.1)$$

or

$$h_{wcd} = \frac{QB\mu}{16\pi\left(\frac{k_h^2}{k_v}\right) r^2 g\Delta\gamma} \frac{\left(\sum_{i=1}^{5} A_i\phi(x_i,\rho,w)\right) - 4\left(\sum_{i=1}^{5} A_i x_i\right) ln \frac{2}{\rho_e}}{\sum_{i=1}^{5} A_i x_i}$$

$$\qquad \qquad (10.5.1.2)$$

The first term in the numerator is the potential on the WOC and the second term is the potential at the outer boundary.

Calculation Procedure.

1) Potential values at the cone head and at the outer boundary are first calculated for a rectilinear reservoir without considering a deformed cone shape.

2) Introducing the value of the potential at the cone head and at the outer boundary in Equation 10.5.1.2, and for a given production rate, one can calculate the cone height h_{wcd}.

3) Having a value for the cone height the transformation rule is applied and a new penetration depth is calculated for the transformed domain.

4) Calculate the values of the potential in the transformed domain.

5) Applying Equation 10.5.1.2 a new value for the cone height can be calculated

This procedure is repeated (usually 2-5 iteration) until the value of the cone height converges to a tolerance of 0.05%.

To calculate the critical production rate one should start with a small value for the production rate and calculate the cone height as explained above. The stability of the cone can be determined by comparing the cone height with the bottom of the wellbore or by checking whether static equlibrium has been violated. Figure 10.5.1.1 provides the critical production rate for different perforation depths and different drainage radii. Figure 10.5.1.2 and Table 10.5.1.1 compare the results from this method with Høyland et al. [1988] and with Wheatlty [1985].

Table 10.5.1.1:   Comparison of critical production rates (Qc) obtained by the method presented in this work and those obtained by simulation (Høyland et al., 1989) and the analytical solution of Wheatly [1985]

No	Res. height (ft)	Drainage Radius (ft)	k (md)	Penetration depth %	Simulator (Hoyland) Qc (StB/D)	Wheatly Qc (StB/D)	This Study Qc (StB/D)
1	210	1000	1500	23.8	6600	6165	6336
2	ıı	ıı	ıı	47.6	5000	4751	4809
3	ıı	ıı	ıı	71.4	2700	2642	2679
4	ıı	ıı	ıı	90.5	750	763	814
5	50	ıı	ıı	23.8	260	269	270
6	100	ıı	ıı	23.8	1200	1214	1230
7	50	ıı	ıı	71.4	115	112	116.5
8	210	5000	ıı	47.6	3400	3565	3536
9	ıı	500	ıı	ıı	6500	5500	5780
10	ıı	500	ıı	71.4	3400	3053	3165
11	ıı	1000	150	23.8	650	616	633
12	ıı	ıı	1000	ıı	4400	4110	4224
13	ıı	ıı	500	71.4	900	880	893
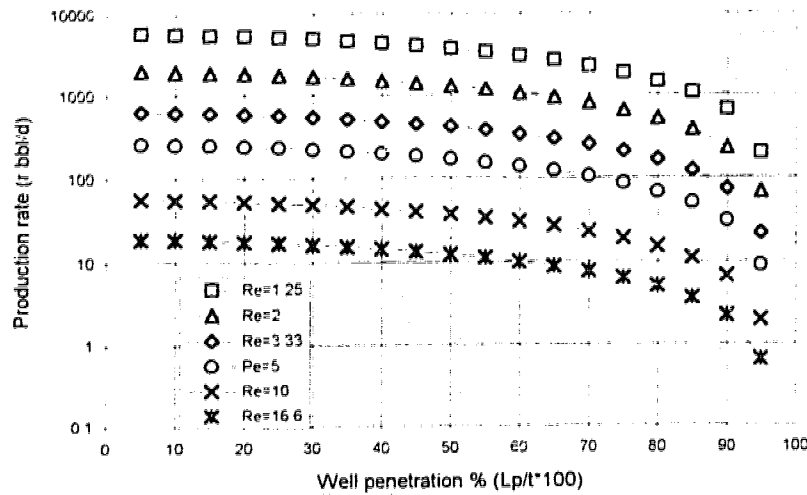
Figure 10.5.1.1: Critical production rate for different penetration depths reservoir heights and drainage radius, $\Delta\gamma = 300 \text{ kg} / \text{m}^3$, $k_h = k_v = 1$ darcy, $B=1$, and $\mu = 1$ cp.
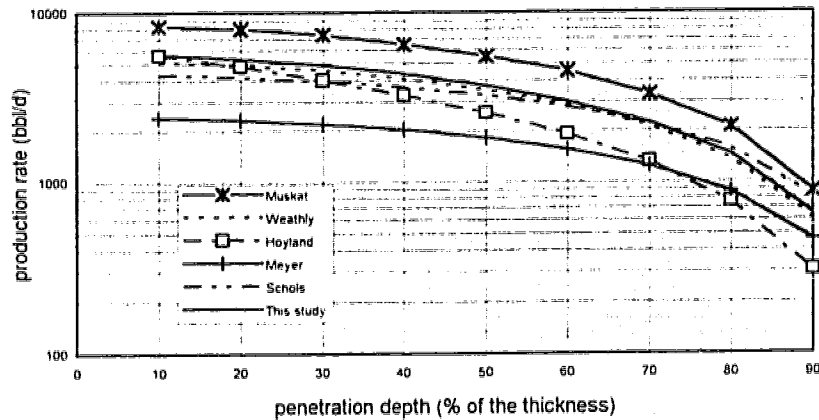
Figure 10.5.1.2: A comparison of critical production rate under steady state conditions obtained by different methods. ($h_t = 200 ft$, $R_E = 500$ ft., $\Delta\gamma = 300 \text{ kg} / \text{m}^3$, $k_h = k_v = 1$ darcy, $B=1$, and $\mu = 1$ cp

Discussion. Table 10.5.1.1 shows a good agreement between the critical production rates obtained from this study and those obtained from Wheatly's [1985] analytical solution and from the numerical simulation of Hoyland et al. [1988]. Hoyland et al. derived an empirical equation for the critical production rate by using the results of a set of simulation. The critical production rates obtained from direct simulation [Hoyland et al., 1988] are used to prepare Column 6 of the Table 10.5.1.1. However, in Figure 10.5.1.2, to plot the curve corresponding to the method of Hoyland et al., the critical production rates are obtained by using the empirical equation. Figure 10.5.1.2 indicates that the empirical equation given by Hoyland et al. [1988] are limited to short penetration depths. Critical production rates obtained by the solution presented in this study and that of the wheatly's solution are in good agreements for large penetration depths; however, they deviate by a small amount for short penetration depths. This might be due to the potential equation that has been used by Wheatly for modeling a vertical partially penetrating wellbore. Wheatly [1985], modeled a vertical, partially penetrating wellbore by superposition of different line sources with different lengths each of which are modeled by a radial flow solution. Because these line sources could only model a radial flow toward the wellbore and parallel to the no-flow boundaries, Wheatly introduced a point source at the bottom of the wellbore to consider the flow convergence at the bottom of the wellbore. Although, no justification is provided for such potential equation for a vertical partially penetrating wellbore, but it may be inferred that for large penetration depths, that the radial flow is dominant, the error of Wheatly's approximate solution is smaller. As the validity of the potential equation used in this study, Five Flux Element Method, is verified

by a comparison with the DFE and Muskat's superposition methods. thus. the general

solution presented in this study can be used for large and short penetration depths.

Shape of the Cone. Applying Equation 10.5.1.2, one can define the height of the cone at

different points on the dynamic WOC. Figure 10.5.1.3 shows the shape of the cone for a

20% penetration depth. in an gas-oil-water system.
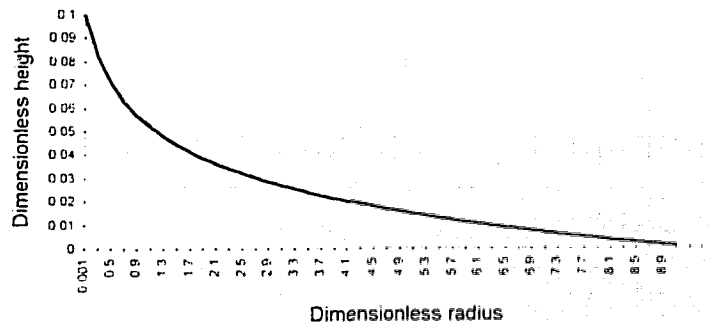
Figure 10.5.1.3: Shape of the water cone in a gas-oil-water system when the
cone head reaches 20% of the reservoir height.
($\Delta\gamma_{ow} = 300$ kg / m^3, $\Delta\gamma_{og} = 600$ kg / m^3, $h_t = 15$ ft.
$R_e = 500$ ft, $k_h = k_v = 1$ darcy. $B=1$ and $\mu = 1$ cp)

Gas Coning. Gas coning can be treated the same way as was done for water coning,

provided that the cone height is measured from the top of the reservoir and the difference

of the densities of gas and oil is considered.

Simultaneous Water and Gas Coning. For reservoirs with bottom water and a gas cap

the transformation given by Equation 10.4.4 can be used

$$z_T = z\left(1 + \frac{h_{cg}}{0.5 - h_{cg}}\right)\left(1 + \frac{h_{cw}}{0.5 - h_{cw}}\right) \qquad \text{(10.4.4)}$$

Calculation Procedure. Assume that the perforated length is l_p, and that it is located between two boundaries. The water and the gas height at the respective cone heads for a given production rate can be calculated as follows:

1. Assume a small value for the height of the water cone while the height of the gas cone is zero.

2. Using Equation 10.4.4 determine the producing length in the transformed domain.

3. Calculate the potential at the boundary and at the head of the water and gas cone.

4. Using Equation 10.5.1.1, calculate the height of the gas and water cones separately.

5. Check the stability of the gas and water cones. If water or gas has broken through, stop the calculation, and this shows that for this production rate the gas and/or water cone is not stable.

6. Compare the calculated height of the water cone with that of the previous iteration (or with the initial guess for the first iteration).

- If the values have not converged to the necessary tolerance use the new values for the water and gas cone heights and repeat the calculation from step 2. A tolerance of 0.05% is suggested.

Optimal Perforation Location and Interval. The best location of the perforated zone and optimal interval are those for which both water and gas break through into the producer at

the same time. If the perforated zone is too close to the gas cap, gas breakthrough occurs sooner, if it is too close to the bottom water, then water will break through sooner. The best location is found by trial and error, changing the location of the perforated zone and doing the calculation explained above. The length of the perforation interval also controls the critical production rate. To find the best location and length of the perforation interval for a given reservoir, one can use trial and error to change the interval length and location and do the calculation shown above. Such a calculation was performed and the results are shown in Figure 10.5.1.3.
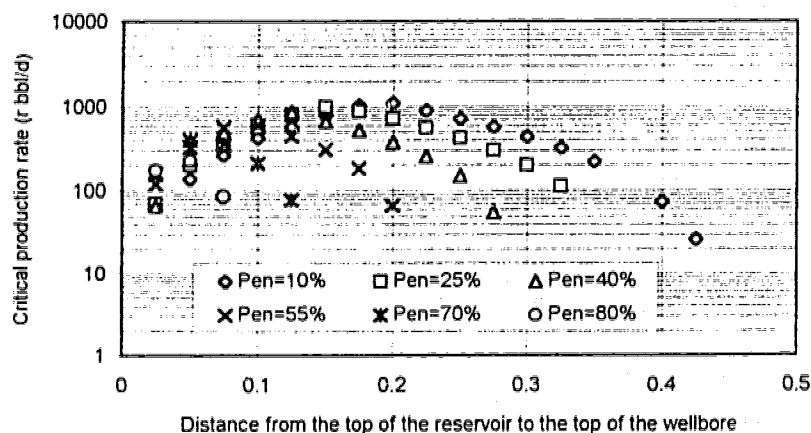
Figure 10.5.1.4: Critical production rate for a gas-oil-water system
($\Delta\gamma_{OW} = 300 \text{ kg} / \text{m}^3$, $\Delta\gamma_{OG} = 600 \text{ kg} / \text{m}^3$, $h_t = 200$ ft,
$R_E = 500$ ft, $k_h = k_v = 1$ darcy, $B=1$ and $\mu = 1$ cp)

10.5.2 Performance of the Wellbore and Breakthrough Time

In this section the transient potential equation is applied to study the performance of vertical wells in the presence of a growing cone. The wellbore is modeled by a uniform potential IBC using the DFE Method.

The WOC is a dynamic interface moving towards the wellbore. Therefore, the potential must be obtained by superposition in time of different solutions, each with a different WOC location. The movement of the boundary is controlled by the static equilibrium condition. When transforming the cone shape boundary, using Equation 10.4.4, this movement is represented in time by increases in the wellbore penetration depth in the transformed domain. Therefore, the potential is found by superposition in time of different wellbore lengths. If time is incremented by Δt, then at time $t^{(l)}$ the potential is found by the superposition of l solutions, each with a different wellbore length. At time $t^{(l)}$, the wellbore length is $L_{pf}^{(l)}$, which is normally greater than $L_{pf}^{(l-1)}$. The increase in well length is made by the addition of point sources to the base of the wellbore in the previous time step. Since the production rate is constant, then at $t^{(l)}$ one finds the new distribution of flux stength by calculating only the changes in the strength of each point. Writing the potential for the ith observation point and collecting the unknowns on the left-hand side and the known values on the right hand side, one can write the relation:

$$\delta a'_1 \varphi_{i1} + \delta a'_2 \varphi_{i2} + \ldots + \delta a'_n \varphi_{in} - \varphi_{DW} =$$

$$\left(a_1^0 \varphi_{i1}^0 + \delta a_1^1 \varphi_{i1}^1 + \ldots + \delta a_1^{l-1} \varphi_{i1}^{l-1} \right) +$$

$$\left(a_2^0 \varphi_{i2}^0 + \delta a_2^1 \varphi_{i2}^1 + \ldots + \delta a_2^{l-1} \varphi_{i2}^{l-1} \right) +$$

$$\ldots\ldots$$

$$\left(a_n^0 \varphi_{in}^0 + \delta a_n^1 \varphi_{in}^1 + \ldots + \delta a_n^{l-1} \varphi_{in}^{l-1} \right) \qquad \ldots\ldots\ldots\ldots(10.5.2.1)$$

where a_j^0 is the initial strength of the point j at time zero. The parameter δa_j^m is the

change in the strength of the jth point source at time m.

Writing the potential equations for n point sources and one constraint equation as

$$\sum_{j=1}^{n} \delta a'_j = 0 \qquad \ldots\ldots\ldots\ldots\ldots\ldots\ldots(10.5.2.2)$$

$(n+1)$ equations are obtained. Solving the new system of equations one can define the

changes in the strength of every point source as well as the wellbore potential.

Results. Water coning under unsteady state conditions was investigated for two vertical

wells with 50% and 20% penetration depths. The potential response at the wellbores for

different dimensionless densities is shown in Figures 10.5.2.1 and 10.5.2.3. Figures

10.5.2.1 and 10.5.2.3 also show the potential response of the same wells in a rectilinear

reservoir with simple solid boundaries, that is, without bottom water or a gas cap. They

show that for large values of dimensionless density, the potential response in wells subject

to water coning is almost the same as that of the wells in reservoirs with solid boundaries.

Therefore, studying reservoirs with large values of dimensionless densities, one can neglect the existence of bottom water or a gas cap. The only parameter that can be changed easily and arbitrarily in Equation 10.3.14 is the production rate. Therefore, for well test analysis, by choosing a small but practical value for production rate one can achieve a high dimensionless density value. Dimensionless cone height against dimensionless time is shown in Figures 10.5.2.2 and 10.5.2.4.
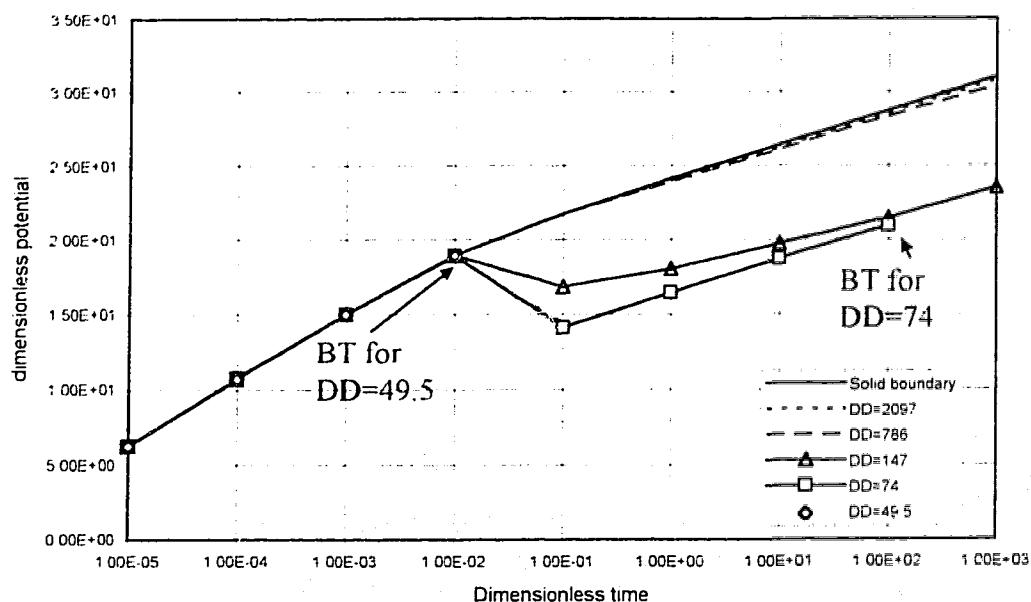
Figure 10.5.2.1: Dimensionless potential against dimensionless time of a

a 50% vertically penetrating wellbore in reservoirs with

different dimensionless densities. (Solid line indicates the

performance of the same wellbore in a reservoir without

bottom water or gas cap). (BT = Breakthrough).

Breakthrough happens when the equilibrium is violated.
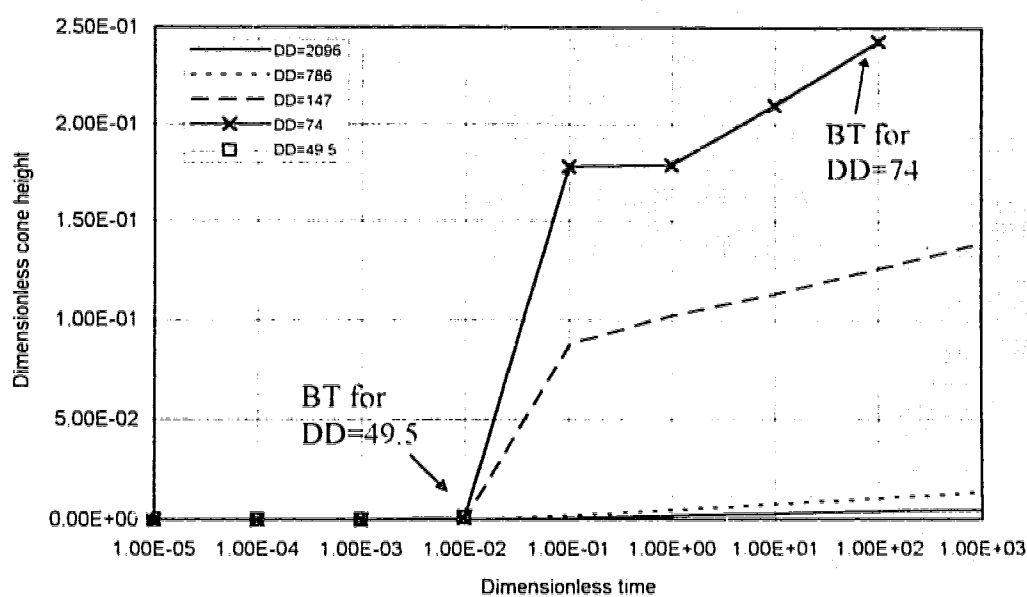
Figure 10.5.2.2 : Dimensionless cone height against dimensionless time for
a 50% vertically penetrating wellbore in reservoirs with
different dimensionless density. (BT=Breakthrough).
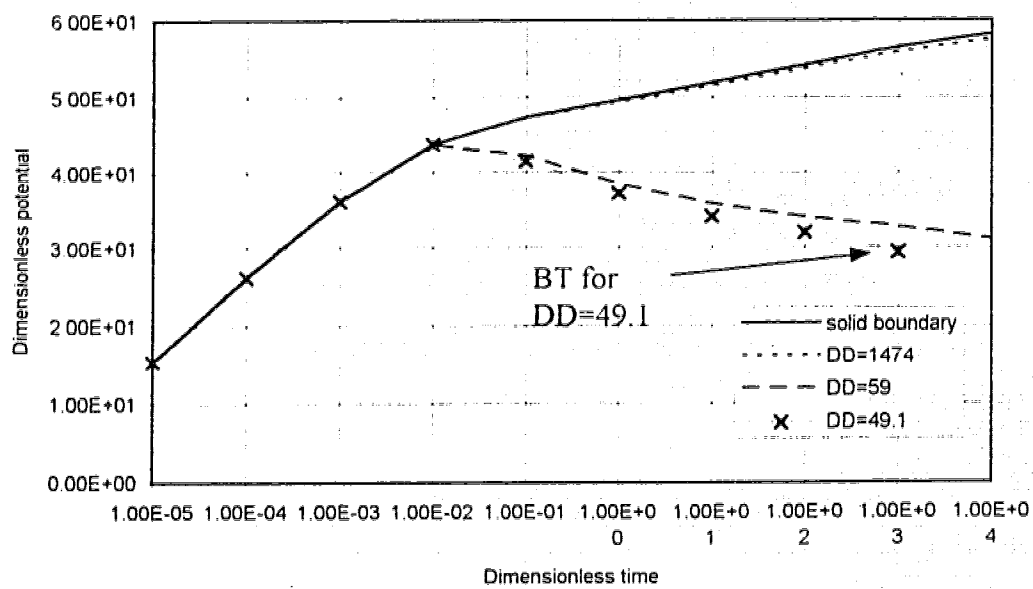
Figure 10.5.2.3: Dimensionless potential against dimensionless time of a
a *20%* vertically penetrating wellbore in reservoirs with
different dimensionless densities. (Solid line indicates the
performance of the same wellbore in a reservoir without
bottom water or gas cap). (BT = Breakthrough)
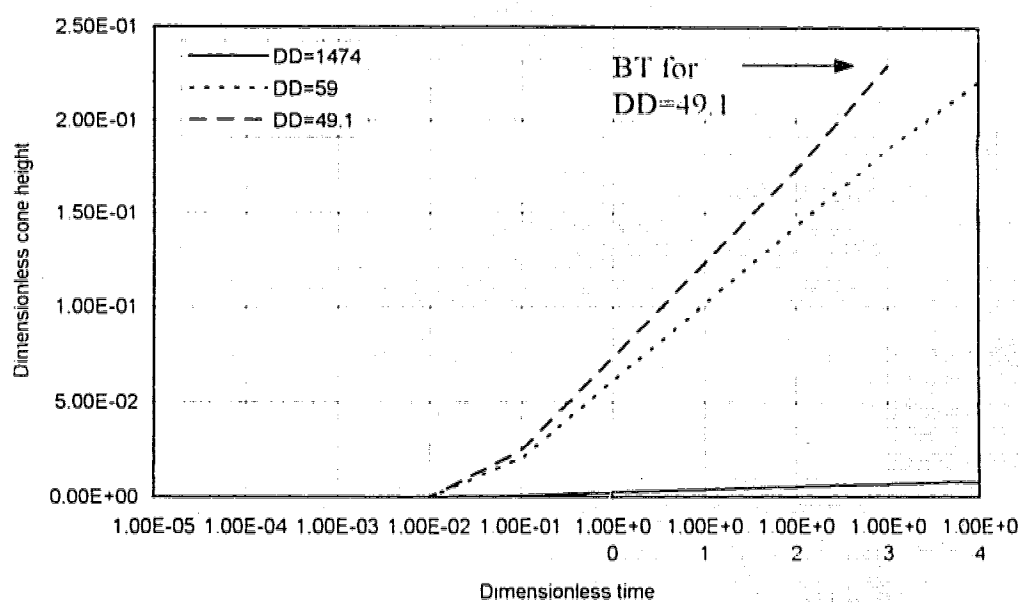
Figure 10.5.2.4: Dimensionless cone height against dimensionless time for a 20% vertically penetrating wellbore, in reservoirs with different dimensionless density. (BT = Breakthrough)

10.6 Performance of Horizontal Wells and Breakthrough Time

In this section the performance of horizontal wells in the presence of a growing cone or crest is studied. The inner boundary condition is assumed to be a uniform potential modeled by the DFE Method.

Similar to the case of a vertical well, an increase in pressure drop with time causes movement of the WOC interface toward the wellbore. Thus the wellbore potential is affected by continuous changing of the WOC boundary. The wellbore potential response can be obtained through superposition in time. As the WOC geometry is irregular the transformation given by Equation 10.4.1 is applied to shift the boundary to its original position. For a vertical well, this transformation increases the wellbore length. However, for a horizontal well, this transformation changes the vertical coordinates of the wellbore, while the producing length remains the same. The assumption of identical properties for both the transformed and the original domain is a valid approximation. as the wellbore distance to the WOC remains almost the same. The resulting irregular geometry of the wellbore is modeled by the DFE Method.

Calculation Procedure

A uniform potential IBC is used to calculate the potential distribution inside the reservoir. To apply the transformation one has to calculate the WOC height at any time step using Equation 10.3.16. The potential distribution and the WOC position directly affect each other. An implicit method through an iterative procedure is used to take into account their mutual effect. The same method has also been used for a vertical well in the

previous section. As the wellbore is modeled by a series of point sources in the DFE Method, every point source must be transformed into a new position. Based on Equation 10.4.1, transforming the vertical coordinate of any point requires only the height of the WOC beneath that point, which is a conjugate point. Thus, calculating the well configuration in the transformed domain, for a wellbore modeled by n point sources, one has to calculate the WOC height at n conjugate points beneath every flux element. For a horizontal well with a straight line configuration only one half of the wellbore need be modeled due to symmetry.

To find the potential distribution, at any time, one needs $n+1$ equations to solve for the strengths and the wellbore potential simultaneously. Writing the well potential at time step l, on the surface of ith point source and grouping the unknowns in the left hand side and the known values at the right hand side one obtains:

$$q_1^l \varphi_{DPi1}^{t_l - t_{l-1}} + q_2^l \varphi_{DPi2}^{t_l - t_{l-1}} + \ldots \cdot q_n^l \varphi_{DPin}^{t_l - t_{l-1}} - \varphi_{bill}^l = rhs_i \qquad \ldots\ldots\ldots\ldots\ldots\ldots\ldots(10.6.1)$$

where

$$rhs_i =$$

$$q_1^1 \varphi_{DPi1}^{t_l - t_0} + q_2^1 \varphi_{DPi2}^{t_l - t_0} + \cdots q_n^1 \varphi_{DPin}^{t_l - t_0} - \left(q_1^1 \varphi_{DPi1}^{t_l - t_1} + q_2^1 \varphi_{DPi2}^{t_l - t_1} + \cdots q_n^1 \varphi_{DPin}^{t_l - t_1} \right)$$

$$+ q_1^2 \varphi_{DPi1}^{t_l - t_1} + q_2^2 \varphi_{DPi2}^{t_l - t_1} + \cdots q_n^2 \varphi_{DPin}^{t_l - t_1} - \left(q_1^2 \varphi_{DPi1}^{t_l - t_2} + q_2^2 \varphi_{DPi2}^{t_l - t_2} + \cdots q_n^2 \varphi_{DPin}^{t_l - t_2} \right)$$

$$\ldots\ldots$$

$$+ q_1^{l-1} \varphi_{DPi1}^{t_l - t_{l-1}} + q_2^{l-1} \varphi_{DPi2}^{t_l - t_{l-1}} + \cdots q_n^{l-1} \varphi_{DPin}^{t_l - t_{l-1}}$$

$$\ldots\ldots\ldots\ldots\ldots\ldots\ldots\ldots(10.6.2)$$

where q_i^l is the strength of the ith flux element at time step l, and $\varphi_{PDij}^{l_l - t_1}$ is the potential due to the ith flux element at point j for the period $t_l - t_1$.

Writing similar equations for the other points along the wellbore, one can find n equations. The last equation is the constraint equation:

$$\sum_{i=1}^{n} q_i^l = 1 \qquad\qquad\qquad\qquad ....(10.6.3)$$

The system of equations in matrix notation can be written as:

$$
\begin{bmatrix}
\varphi_{PD11}^l & \varphi_{PD12}^l & \cdots \varphi_{PD1n}^l & -1 \\
\varphi_{PD21}^l & \varphi_{PD22}^l & \cdots \varphi_{PD2n}^l & -1 \\
\cdots & & & \\
\varphi_{PDn1}^l & \varphi_{PDn2}^l & \cdots \varphi_{PDnn}^l & -1 \\
1 & 1 & \cdots\cdots 1 & 0
\end{bmatrix}
\begin{Bmatrix}
q_1^l \\
q_2^l \\
. \\
q_n^l \\
\varphi_{DW}^l
\end{Bmatrix}
=
\begin{Bmatrix}
rhs_1 \\
rhs_2 \\
. \\
rhs_n \\
1
\end{Bmatrix}
$$

$$\qquad\qquad\qquad\qquad ....(10.6.4)$$

Solving the system of Equations 10.6.4 yields the wellbore pressure as well as the strength of every flux element. Knowing the strengths of the flux elements one can calculate the potential on the WOC.

The steps in the calculation can be summarized as follows:

1. For the current time step, l, and wellbore configuration, using the system of Equations 10.6.4 calculate the wellbore potential, the strengths of the flux elements and finally the potential of their conjugate points on the WOC.

2. Applying Equation 10.3.16, calculate the height of the WOC at different conjugate

   points.

   Compare the height of the WOC from step 2 against the wellbore height. If it has

   reached to the wellbore, then water has broken through at this time step; stop

   calculations.

3. Compare the WOC height with that of the previous time step, I-I;

- If the solution has not converged then, applying Equation 10.4.1, find the vertical

  coordinate of the wellbore at different points in the transformed domain, and go to

  step 2.

- If the solution has converged then increase the time and go to step 1.

Results. Figure 10.6.1 shows the pressure response of a horizontal well with $I_p = 100\%$,

for different values of dimensionless density, $\Delta\gamma_D$. For $\Delta\gamma_D$ equal to 300 and 1000, the

well responses are identical to those of a similar well in a reservoir without bottom water

(solid boundary). The corresponding interface heights, shown in Figure 10.6.2, indicate a

small displacement of the interface. Figure 10.6.2 shows that for $\Delta\gamma_D$ equal to 50, the

interface rises as high as 0.167 at $t_D = 10$, and it breaks through at $t_D > 10$. However,

Figure 10.6.1 shows that the potential response deviation from that of a reservoir with a

solid boundary is small. This indicates that the assumption of a no-flow condition at the

original interface is a good approximation for both small and large values of $\Delta\gamma_D$ before

breakthrough. Figure 10.6.3 shows the potential response of a horizontal well with

$I_p = 200\%$. Figure 10.6.4 shows the height of the cone peak for two horizontal wells

with $L_p = 100\%$ and $L_p = 200\%$, both with $\Delta\gamma_D = 50$. The shorter wellbore breaks

through at $r_D > 10$; however, the longer one is stable. As was expected, the critical

dimensionless density (CDD) was greater for the shorter horizontal well. Figure 10.6.5

shows the height of the cone peak versus dimensionless drainage radii for different

dimensionless densities, for a well with $L_p = 100\%$ under steady state conditions. Figure

10.6.5 shows one half of the cone profile, in the xz plane, under a wellbore with

$L_p = 100\%$ extended from $x = -0.25$ to $+0.25$. As can be seen from Figure 10.6.5 the

heights of the cone are not identical at different points. The difference of the height of the

center and that of the edge is larger as the cone gets closer to the wellbore. Thus one can

conclude that water breaks through into the producer at the middle of the wellbore. Figure

10.6.6 shows the shape of a stable cone in 3-D due to a horizontal well (straight

configuration with $L_p = 100\%$) in a reservoir with $\Delta\gamma_D = 200$.
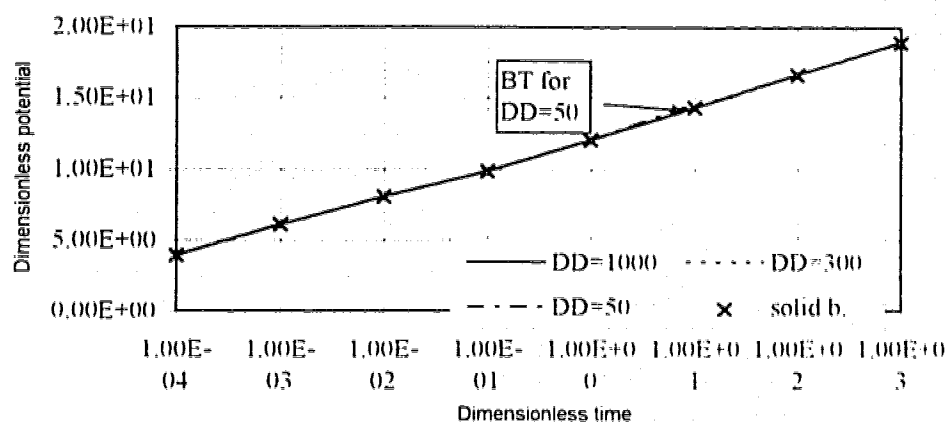
Figure 10.6.1: Dimensionless potential of a horizontal well with:
$L_p = h_t$, $r_w = 0.002$.
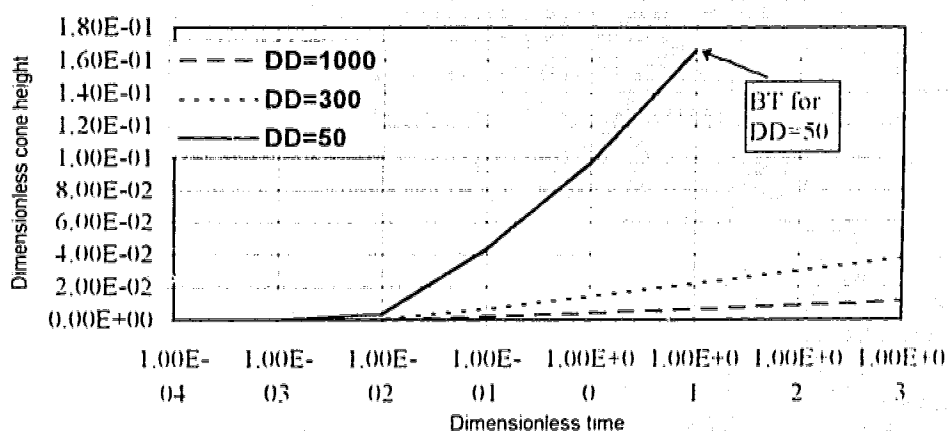
Figure 10.6.2: Dimensionless cone height of a horizontal well with:
$L_p = h_t$, $r_{pw} = 0.002$.
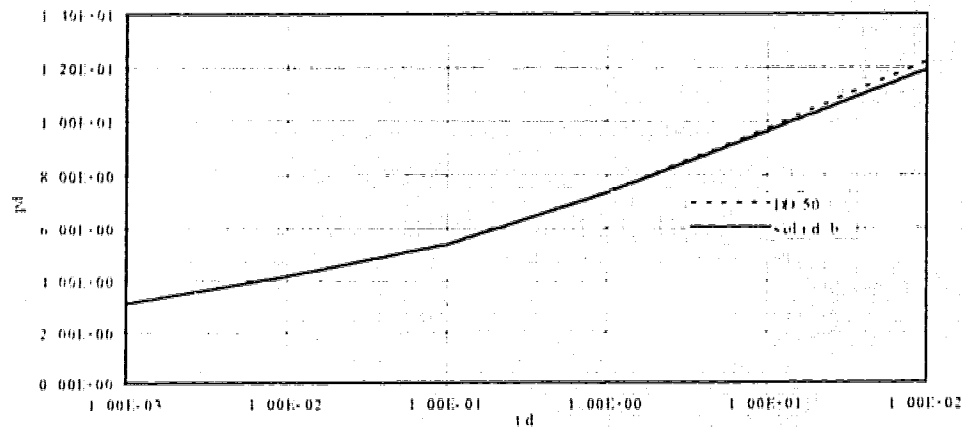
Figure 10.6.3: Comparison of the potential response of a horizontal well ($L_p = 2h_t$) in a reservoir with bottom water (DD=50) to that in a reservoir with a solid boundary.
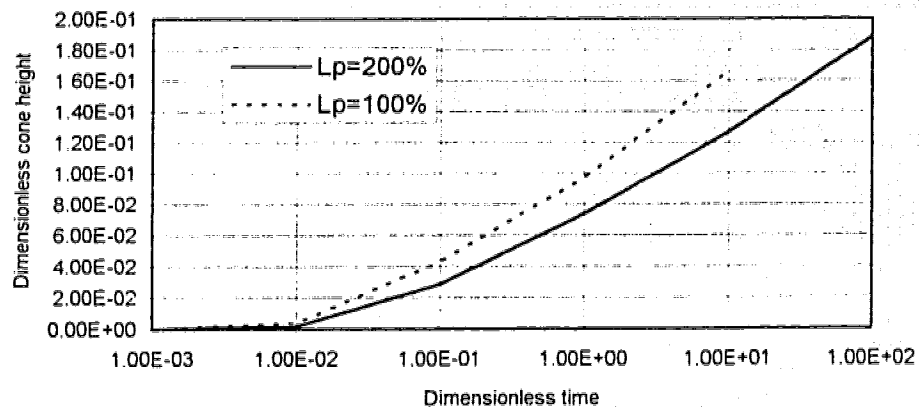
Figure 10.6.4: Dimensionless cone height of horizontal wells with: $L_p = h_t$ and $L_p = 2h_t$, both with $r_{Dw} = 0.002$.
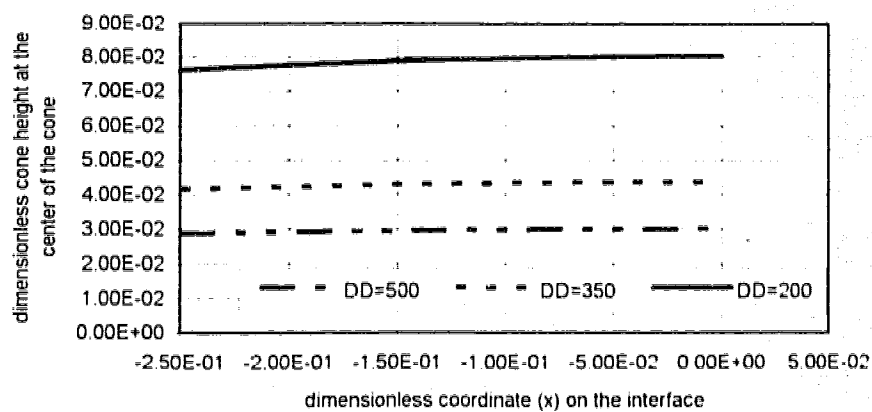
Figure 10.6.5: Profile of the cones, due to a horizontal well, in the $(x-z)$ plane for different values of DD. Well extended from $x = -0.25$ to $+0.25$ $(L_p = h_i)$.
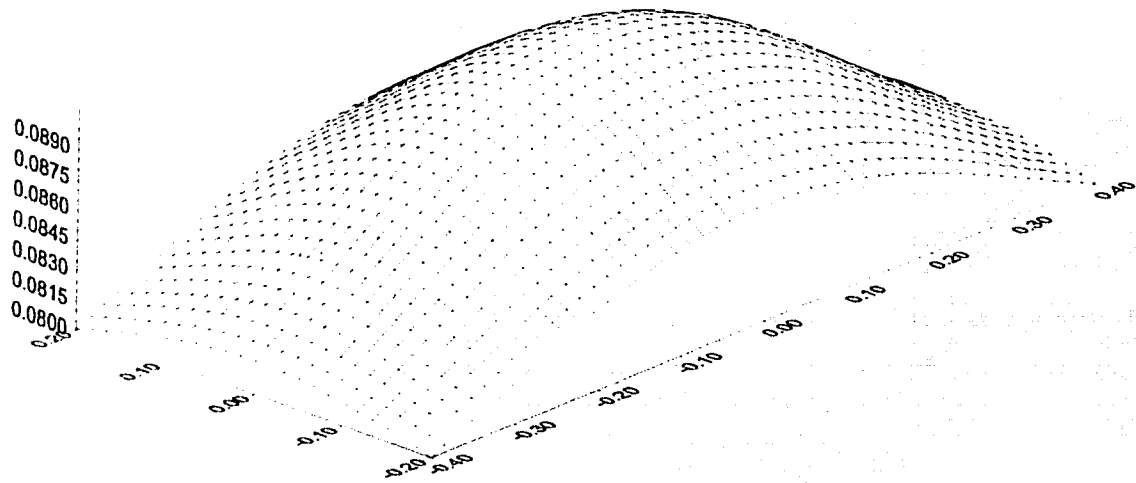
Figure 10.6.6: Shape of the cone due to a horizontal well with $L_p = h_t$ and DD=200, at $t_D = 100$ (stable cone).

10.7 Discussion of Results

This section provided a solution for the vertical and horizontal well performance in the presence of a growing cone. The interface was considered as a no-flow moving boundary. The position of the interface was obtained through the static equilibrium equation where guaranteed a constant pressure at the original WOC. Developing an equation for the cone height, this chapter presented a new parameter, the dimensionless density. It was shown that based, on static equilibrium, the solution of a constant potential

at the initial interface is an approximation to a coning problem when the density difference

is zero.

Equation 10.3.16 shows that as $\Delta\gamma$ approaches zero, the cone height approaches

infinity. In other words, once the drainage area reaches the initial WOC, water will

breakthrough. On the other hand, before the drainage area reaches WOC, the potential

responses obtained from two different solutions of sealed and constant potential

boundaries are the same. Therefore, a constant potential boundary provides no additional

information before breakthrough than a sealed boundary does. After breakthrough, the

initial interface ceases to remain at constant pressure conditions. Thus, for this period

where the aquifer is communicating directly with the producer, the real boundary of the

aquifer should be applied. Depending on the extent and geometry of the aquifer, a no-flow

boundary, at the bottom of the water zone, or a constant potential boundary inside the

water zone affects the potential response. The analysis showed that before breakthrough

the potential response obtained by the solution of a no-flow moving boundary is close to

that of a no-flow boundary at the initial position of the WOC.

10.8   Concluding Remarks

In this Chapter the cone height equation (Equation 10.3.16) was derived, based on which:

1. the stability of the interface and the time of the breakthrough are controlled by the

   dimensionless density, $\Delta\gamma_D$. The higher the $\Delta\gamma_D$ the smaller is the cone height. For a

   given reservoir, a Critical Dimensionless Density (CDD), is associated with every

   wellbore length above which the cone is stable

2. the greater the viscosity, the greater is the cone height and consequently the sooner breakthrough occurs. Thus, processes reducing viscosity such as steam stimulation can postpone breakthrough in coning.

3. the smaller the vertical permeability, the smaller the cone height and greater the time to breakthrough.

The potential response of a vertical well indicated that for large values of $\Delta\gamma_D$ movement of the interface is very small. Thus for all practical purposes, one can neglect the existence of the bottom water or gas cap in a rectilinear reservoir by choosing a large $\Delta\gamma_D$.

It was shown that before breakthrough the pressure at the initial interface is always constant based on static equilbrium. However, the potential at this level is constant only if the difference of two fluid densities is zero. Thus a solution of constant potential at the initial interface before breakthrough is a special case of a coning problem. After breakthrough, where the aquifer is directly communicating with the producer, the initial WOC ceases to remain at a constant pressure conditions. After breakthrough, the lower boundary of the aquifer or a constant potential boundary inside the aquifer should be applied, depending on the geometry and extension of the aquifer.

CHAPTER 11

CONCLUSIONS AND RECOMMENDATIONS

11.1   Conclusions

In this work a novel analytical potential solution for sources with arbitrary geometry, *Discrete Flux Element (DFE) Method*, is developed. Applying the DFE method, for the first time, the steady state potential equations for horizontal wells and fractures are obtained. The applicability of the DFE Method in reservoirs with and without bottom water operating under steady-state and unsteady state conditions is examined. The boundary conditions at the WOC, before breakthrough, in reservoirs with bottom water are defined. A new variable, *Dimensionless Density* is introduced which controls the cone height and breakthrough time. The principal conclusions of this study are:

1. The DFE Method can be used for modeling the potential of an arbitrary source with arbitrary geometry and uniform potential or uniform flux IBC.

2. Modeling a curvilinear horizontal wellbore by a straight horizontal well causes errors in the prediction of the performance of the wellbore. This error is significant for the wellbores in reservoirs with significant permeability contrast.

3. The equivalent pressure point [Clonts and Ramey, 1986, and Daviau et al., 1988] moves in time and it is not the same as that of the pressure derivative.

4 A vertical barrier perpendicular to a horizontal well causes an asymmetric flux distribution along the wellbore. The idea of using of an equivalent pressure point was based on a symmetric flux distribution; thus, it cannot be generalized.

5. The transient drainage area around line sources with finite length, in isotropic reservoirs, is elliptical and at late times it becomes cylindrical.

6. In reservoirs with bottom water, the potential at the original interface is not constant. The WOC is a no-flow moving boundary and its position before breakthrough is controlled by dimensionless density. For every wellbore geometry a critical dimensionless density exists, above which the WOC is stable.

7. A stimulation process that can reduce oil viscosity can also increase the time of water breakthrough.

8. In reservoirs with bottom water, the larger the dimensionless density the smaller the cone height and larger the breakthrough time will be. Thus, by using a large dimensionless density, it is possible to freeze the WOC. This will allow for modelling the oil reservoir by an infinite slab (rectilinear reservoir with two parallel no-flow boundaries). Thus for well testing a more realistic model will be achieved, compared to those models with a constant potential at the original WOC.

11.2 Recommendations For Further Studies

The DFE Method provides a potential solution in isotropic and anisotropic reservoirs due to a line or plane source. It can be applied in most of the single-phase flow problems. Its application should be compared with the Theis solution for a fully penetrating vertical well, particularly in well testing. For anisotropic reservoirs, further studies of modeling a wellbore with a circular cross section are recommended.

For the coning problems the following can be suggested:

- Studying the effect of the viscosity contrast of the two fluids on the performance of the wellbore and the movement of the cone.

- Coning in gas reservoirs under unsteady-state conditions.

- Coning in reservoirs with closed lateral boundaries.

- Coning in reservoirs operating under the bubble point pressure (two phase flow).

CHAPTER 12

REFERENCES

Arthur, M. G. (1944): "Fingering and Coning of Water and Gas in Homogeneous Oil Sand," Trans. AIME 45, 182-199.

Babu, D.K. and Odeh, A.S. (1989): "Productivity of Horizontal Well," *SPERE* (November), 417-421.

Borisov, Ju. P. (1964); "Oil Production Using Horizontal and Multiple-Deviation Wells," Nedra, Moscow, Translated from French into English by J. Strauss and Technical Editing by S. D. Joshi, Philips Petroleum Company.

Bournazel, C. and Jeanson B.. (1971): "Fast Water-Coning Evaluation Method," SPE 3628, presented at the 46th Annual Fall Meeting of the Society of Petroleum Engineers of AIME, New Orleans, Oct. 3-6.

Brigham W.E. (1990): "Discussion of Productivity of Horizontal Well," *SPERE* (May 1990) pp 254-255.

Carslaw, H. S. and Jaeger, J. C. (1959): *Conduction of Heat in Solids*, Second edition, Oxford at the Clarendon Press.

Chaney, P. E. and Nobel, M. D.(1956): "How to Perforate Your Well to Prevent Water and Gas Coning," *Oil and Gas Journal*, May-7, 108-114.

Chaperon, I. (1986): "Theoretical Study of Coning Toward Horizontal and Vertical Wells in An-isotropic Formations: Subcritical and Critical Rates," Paper SPE 15377, presented at SPE 61st ATCE, New Orlean, LA.

Chierici, G. L. and Ciucci, G. M. and Pizzi, G. (1964): "A Systematic Study of Gas and Water Coning by Potentiometric Models," *JPT*, August. 923-929.

Clonts, M.D. and Ramey Jr. (1986): "Pressure Transient Analysis for Wells With Horizontal Drainholes," Paper SPE 15116, presented at the 1986 California regional Meeting, Oakland, Ca April 2-4.

Collins, R.E. (1961): *Flow of Fluids Through Porous Materials*, Reinhold Publishing Corporation, New York.

Daviau, F., Mouronval G., Bourdart G. and Curutchet P. (1988): "Pressure Analysis for horizontal Wells," *SPE Formation Evaluation* (Dec. 1988) pp 716-724.

Dietrich J.K. (1995): " Discussion of Productivity of a Horizontal Well," *SPERE* (Aug, 1995), pp 229 -230.

Earlougher Robert C. JR. (1977): *Advances in Welltest Analysis*, Society of Petroleum Engineers of AIME, New York, 1977.

Giger, F. M., Reiss. L.H. and Jourdan, A.P. (1984): "The Reservoir Engineering Aspects of Horizontal Drilling," paper SPE 13024, presented at 1984 SPE Annual Technical Conference and Exhibition, Houston, Sep. 16-19.

Goode, P.A. and Thambynayagam, R.K.M., (1987): "Pressure Drawdown and Buildup Analysis of Horizontal Wells in Anisotropic Media," *SPE Formation Evaluation* (Dec 1987) pp: 683-697.

Goode P.A. and Kuchuk F.J. (1991): "Inflow Performance of Horizontal Wells," *SPERE*, (Aug. 1991) pp 319-323.

Gradshteyn, I. S. and Ryzhik, I. M. (1980): *Table of Integral, Series, and Products*, Academic Press, United Kingdom Inc.

Gringarten A. C. and Ramey, H.J. Jr., 1973: "The Use of Source and Green's Functions in Solving Unsteady-Flow Problems in Reservoirs," *SPE,* (October) pp 285-296.

Gringarten, A.C. and Ramey, H.J. Jr., and Raghavan, R.(1974): "Unsteady State Pressure Distributions Created by a Well With a Single infinite Conductivity Vertical fracture," SPEJ (Aug. 1974) 347-60; *trans., AIME,* 257.

Gringarten A. C. and Ramey, Jr., 1975: "An Approximate Infinite Conductivity Solution for a Partially Penetrating Line-Source Well," *SPEJ* (April 1975) pp 140-148.

Henley D.H. and Owens W.W. and Craig, F.F. JR (1961): "A Scale-Model Study of Bottom-Water Drives," JPT (January, 1961).

Høyland, L. A., Papatzacos, P. and Skjaeveland, S. M. (1989): "Critical Rate for Water Coning," *SPERE* (November) 495-502.

Hubbert M. King (1940): "The Theory of Ground-Water Motion," *The Journal of Geology* (November - December) pp 785-944.

Joshi, S.D. (1988): "Augmentation of Well Productivity with Slant and Horizontal Wells," *JPT,* June.

Joshi, S.D. (1991): *Horizontal well Technology,* PennWell Publishing Co., Tulsa, Oklahoma.

Kelvin (Sir William Thomson) (1884): *Mathematical and Physical Papers,* University of Cambridge, Vol. 2.

Kuchuk, F., Goode P.A., Wilkinson D.J., and Thambynayagam R.K.M. (1988): "Pressure Transient Behavior of Horizontal Wells With and Without Gas Cap or Aquifer," paper SPE 17413 presented at the 1988 SPE California Regional Meeting, Long Beach, California, March 23-25.

Kuo, M.C.T. and DesBrisay C.L. (1983): "A Simplified Method for Water Coning Predictions." SPE 12067, presented at 58th Annual Technical Conference and Exhibition, San Francisco, CA, Oct. 5-8.

Madelung, E. (1918): "Das Electrishe Feld in Systemen von Regelmassig Angeordneten Punktlaungen," *Physik*, 524.

Meyer, H. I. and Garder A. O. (1945): "Mechanics of Two Immiscible Fluids in Porous Media," *Journal of Applied Physics*. 25, 1400-1406.

Muskat, M. (1932): "Potential Distribution in Large Cylindrical Discs With Partially Penetrating Electrodes," *Physics*, **Vol. 2**, May.

Muskat, M. (1947): "The Performance of Water-Drive Reservoirs," Trans. AIME 170, 81-111

Muskat, M. (1982): *The Flow of Homogeneous Fluids Through Porous Media*, I.H.R.D.C., Boston.

Muskat, M. and Wyckoff R. D. (1935): "An Approximate Theory of Water Coning in Oil Production," Trans. AIME 114: 144-163

Odeh, A.S. and Babu, D.K. (1990): "Transient Flow Behavior of Horizontal Wells: Pressure Drawdown and Buildup Analysis," *SPE Formation Evaluation*, (March 1990) pp: 7-15.

Ozkan, E. and Raghavan, R. and Joshi, D.S. (1987): "Horizontal Pressure Analysis," SPE 16378, presented at 1987 California Regional Meeting, Ca April 8-10.

Ozkan, E. and Raghavan, R. (1990-a): "Performance of Horizontal Wells Subject to Bottomwater Drive," *SPERE*, August, 375-383.

Ozkan, E. and Raghavan, R. (1990-b): "A Breakthrough Time Correlation for Coning Toward Horizontal Wells," Paper SPE 20964, Presented at SPE Europec 90, Netherlands Oct. 22-24.

Peaceman, D.W. (1990-a): " Further Discussion of Productivity of Horizontal Well," *SPERE* (Feb. 1990) pp 149-150.

Peaceman, D.W. (1990-b): "Discussion of Productivity of Horizontal Well," *SPERE* (May 1990) pp 252-253.

Peaceman, D.W. (1990-c): " Further Discussion of Productivity of Horizontal Well," *SPERE* (August 1990) pp 437.

Rosa, A.J and Carvalho, R. de S. (1989): "A Mathematical Model for Pressure Evaluation in an Infinite Conductivity Horizontal Well," *SPEFE* (Dec. 1989) 559-66.

Schols, R. S. (1972): "An Empirical Formula for the Critical Oil Production Rate," *Erdol-Ergas*, Jan., 6-11.

Sobocinski, D.P. and Cornelius, A.J.(1965): "A Correlation for Predicting Water Coning Time," JPT, (May), 594-600.

Wheatly, M. J. (1985): "An Approximate Theory of Oil/Water Coning," Paper SPE 14210, presented at, 60th Annual Technical Conference and Exhibition, Las Vegas, NV.

APPENDIX-A

Point Sources

A-1 Instantaneous Point Source

The transient potential due to a source is a solution of the diffusivity equation in the form of:

$$\frac{\partial^2 \varphi}{\partial X^2} + \frac{\partial^2 \varphi}{\partial Y^2} + \frac{\partial^2 \varphi}{\partial Z^2} = \frac{1}{K}\frac{\partial \varphi}{\partial t} \quad\quad\quad\quad\quad\quad\quad\quad\quad ....(A.1.1)$$

Deriving the potential for a cube of zero dimensions, Kelvin [1884] developed the instantaneous solution due to a point source in an infinite domain that satisfies Equation A.1.1 as follows:

$$\varphi(X,Y,Z,t) = \frac{q}{8(\pi K t)^{3/2}} e^{-\left[(X-X')^2 + (Y-Y')^2 + (Z-Z')^2\right]/4Kt} \quad\quad ....(A.1.2)$$

Equation A.1.2 provides the potential due to an instantaneous point source, with flux q in an infinite domain, located at (X', Y', Z'). At $(t = 0)$, the potential is zero everywhere, except for the point (X', Y', Z'), where it is singular. Equation A.1.2 is a general solution for any type of flow problem such as thermal, electrical and fluid, provided that appropriate definitions for flux, q, and diffusivity coefficient, K, are used. For thermal flow, these definitions are given by Carslaw and Jaeger [1959]. Equation A.1.1 for an anisotropic domain can be written as:

$$K_X \frac{\partial^2 \varphi}{\partial X^2} + K_Y \frac{\partial^2 \varphi}{\partial Y^2} + K_Z \frac{\partial^2 \varphi}{\partial Z^2} = \frac{\partial \varphi}{\partial t} \qquad \text{.........................(A.1.3)}$$

The instantaneous point source solution in an anisotropic domain is given as [Carslaw and Jaeger [1959]]:

$$\varphi(X,Y,Z,t) = \frac{q}{8(\pi t)^{3/2}(K_X K_Y K_Z)^{1/2}} e^{-\left[(X-X')^2/K_X + (Y-Y')^2/K_Y + (Z-Z')^2/K_Z\right]/4t}$$

$$\text{.........................(A.1.4)}$$

A.2   Continuous Point Source

Integrating Equation A.1.2 with respect to time one can find the continuous solution due to a point source as follows [Kelvin, 1884, and Carslaw and Jaeger, 1959]:

$$\varphi = \frac{q}{4\pi K r} \operatorname{erfc} \frac{r}{\sqrt{4Kt}} \qquad \text{.........................(A.2.1)}$$

where

$$r^2 = (X - X')^2 + (Y - Y')^2 + (Z - Z')^2 \qquad \text{.........................(A.2.2)}$$

A-3   Steady State Point Source In An Infinite Reservoir

The steady state point source in an infinite domain was obtained from equation A.2.1 as time approaches infinity [Carslaw and Jaeger, 1959]:

$$\varphi = \frac{q}{4\pi K r} \qquad \text{.........................(A.3.1)}$$

A-4 Steady State Point Source in a Rectilinear Reservoir

The solution to a point source in a rectilinear reservoir can be found by applying the method of images to Eq A.3.1. The infinite series in the resulting equation converges slowly. A fast convergent equation is given by Madelung [Muskat, 1932] as:

$$\varphi_p\left(w, \rho, w_p\right) = 4q\left[2\sum_{n=1}^{\infty}\left(K_0(2\pi n\rho)\cos(2\pi n w)\cos\left(2\pi n w_p\right) + \ln(2/\rho)\right)\right].$$

..................................(A.4.1)

where the flux term for a fluid flow problem is given [Muskat, 1932]:

$$q = \frac{Q\mu}{4\pi k a}$$

..................................(A.4.2)

where

$$a = 2h_t$$

..................................(A.4.3)

where h_t is the reservoir thickness.

Equation A.4.1 provides the potential at a point located at vertical coordinate w and horizontal distance ρ from a point source located at vertical coordinate w_p (Figure A.4.1). The function K_0 is the modified Bessel function of the first kind and of order zero, and ρ is given by

$$\rho = \left(\left(x - x_p\right)^2 + \left(y - y_p\right)^2\right)^{1/2}$$

..................................(A.4.4)
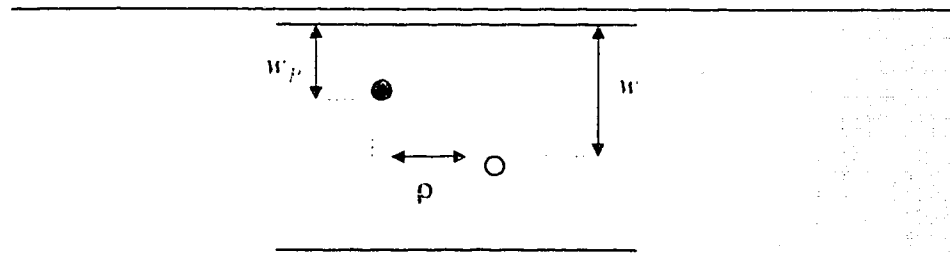
Figure A.4.1: Schematic drawing of a point source in a rectilinear reservoir

Equation A.4.1 is singular at $\rho = 0$ and it converges slowly at small values of ρ. Muskat

[1932], developed an alternative for Equation A.4.1 that provides a finite value at $\rho = 0$:

$$\varphi_P(\rho, w, w_P) =$$

$$q\left\{\frac{-2\psi(1 - w + w_P) - 2\psi(1 + w + w_P) - \pi\cot(\pi(w + w_P)) - \pi\cot(\pi(w_P - w)) +}{\dfrac{1}{w_P + w} + \dfrac{1}{w_P - w} + \dfrac{1}{\left(\rho^2 + (w_P + w)^2\right)^{1/2}} + \dfrac{1}{\left(\rho^2 + (w_P - w)^2\right)^{1/2}}}\right\}$$

...................................(A.4.5)

Inspecting Equation A.4.5 one finds that it is still singular at $w = w_P$.

APPENDIX B

Potential Equations of Sources with Infinite Length

The transient potential due to a source is a solution of the diffusivity equation in the form of:

$$\frac{\partial^2 \varphi}{\partial X^2} + \frac{\partial^2 \varphi}{\partial Y^2} + \frac{\partial^2 \varphi}{\partial Z^2} = \frac{1}{K}\frac{\partial \varphi}{\partial t} \qquad \dots\dots\dots\dots\dots\dots(B.1)$$

The inner boundary condition is to be defined by potential theory, such that the potential on the surface of the source must be uniform. For sources with arbitrary and irregular geometry, the application of such an inner boundary condition is impractical. Kelvin [1884] stated that the potential equation for any type of source can be constructed from the solution of a point source. Kelvin's statement is interpreted for line and plane sources.

The potential due to a line source is the integral of a point source solution about the path of the source:

$$\varphi_L = \int_a^b q\varphi_p dl \qquad \dots\dots\dots\dots\dots\dots(B.2)$$

The potential due to a plane source is the integral of a point source solution over the surface of the plane:

$$\varphi_f = \int_s q\varphi_p ds \qquad \dots\dots\dots\dots\dots\dots(B.3)$$

For a rectangular plane Equation B.3 can be written as:

$$\varphi_f = \int_c^d \int_a^b q\varphi_p d\mathcal{X} dZ \qquad \dots\dots\dots\dots\dots\dots\dots\dots\dots (B\text{-}4)$$

Substituting Equation B.2 into Equation B.4, the potential for a fracture reduces to:

$$\varphi_f = \int_c^d q\varphi_L d\mathcal{X} \qquad \dots\dots\dots\dots\dots\dots\dots\dots (B.5)$$

In other words, the potential solution of a plane source is the integral of a line source solution.

The function of flux, q, is unknown. Kelvin [1884], assuming a uniform flux into the source, presented the potential equations for line and plane sources with infinite length. The uniform flux assumption for such sources leads to a uniform potential distribution along the source.

The potential solution for sources with infinite length can be obtained easily by integration of the solution for a point source from $-\infty$ to $+\infty$. The solutions can also be obtained directly by solving the radial diffusivity equation for a line source or the 1-D diffusivity equation for a plane source.

Although this work is mainly concerned with potential equations for sources with finite length (SFL) a short review of the solutions for sources with infinite length will highlight the differences and similarities between them.

B.1 Instantaneous Line Source with Infinite Length

The potential due to a line source parallel to the Z-axis can be obtained by integrating the potential of an instantaneous point source solution over the length of the source [Kelvin, 1884, and Carslaw and Jaeger, 1959]:

$$\varphi_L = \frac{1}{8(\pi k t)^{3/2}} \int_{-\infty}^{+\infty} q\, e^{-[(X-X')^2 +(Y-Y')^2 +(Z-Z')^2]/4KT}\, dZ' \qquad (B.1.1)$$

This integration is possible only using uniform flux assumption. For a line source with infinite length this is a valid assumption. Therefore Equation B.1 reduces to:

$$\varphi = \frac{q}{4\pi Kt}\, e^{-[(X-X')^2 +(Y-Y')^2]/4Kt} \qquad (B.1.2)$$

or

$$\varphi = \frac{q}{4\pi Kt}\, e^{-r^2/4Kt} \qquad (B.1.3)$$

where

$$r^2 = (X-X')^2 +(Y-Y')^2 \qquad (B.1.4)$$

and q is the flux from the unit length of the line source

B.2 Continuous Line Source with Infinite Length

By integrating Equation B.1.3 with respect to time one can derive the potential equation for a continuous line source:

$$\varphi = \frac{1}{4\pi K} \int_0^t q(t') e^{-r^2/4K(t-t')} \frac{dt'}{t-t'} \qquad \text{.........................(B.2.1)}$$

By assuming a constant rate one can remove q from under the integral [Carslaw and Jaeger, 1959]. Thus Equation B.2.1 reduces to:

$$\varphi = -\frac{q}{4\pi K} E_i(-\frac{r^2}{4Kt}) \qquad \text{.........................(B.2.2)}$$

B.3.   Instantaneous Plane Source with Infinite Dimensions

The instantaneous potential due to the plane sources can be obtained by integrating Equation B.1.2 along the length of the fracture from $-\infty$ to $+\infty$.

$$\varphi_f = \frac{1}{4\pi Kt} \int_{-\infty}^{+\infty} q e^{-\left[(X-X')^2+(Y-Y')^2\right]/4Kt} dY' \qquad \text{.........................(B.3.1)}$$

where q is the flux from a unit area of the fracture. Here also the assumption of uniform flux for a fracture with infinite dimensions is made. Therefore Equation B.3.1 can be written as:

$$\varphi_f = \frac{q}{2\sqrt{\pi Kt}} e^{-(X-X')^2/4Kt} \qquad \text{.........................(B.3.2)}$$

B.4   Continuous Plane Source with Infinite Dimensions

The potential due to a continuous plane source can be derived by integrating Equation B.3.2 with respect to time [Carslaw and Jaeger, 1959]:

$$\varphi_f = \frac{1}{2(\pi K)^{1/2}} \int_0^t q(t) e^{-(X-X')^2/4K(t-t')} \frac{dt'}{(t-t')^{1/2}} \quad\quad\quad \dots\dots\dots\dots\dots\text{(B.4.1)}$$

For a constant rate problem, the flux q can be removed from under the integral. The solution to Equation B.4.1 is [Carslaw and Jaeger, 1959]:

$$\varphi_f = q\left(\frac{t}{\pi K}\right)^{1/2} e^{-(X-X')^2/4Kt} - \frac{q|X-X'|}{2K}\operatorname{erfc}\frac{|X-X'|}{2\sqrt{Kt}} \quad\quad \dots\dots\dots\dots\text{(B.4.2)}$$

Where q is the flux from a unit area of the fracture.

APPENDIX C

Sources with Finite Length

As was shown for sources with infinite length, the potential due to a line source can be obtained by integration of the solution of a point source over the length of the line source, and the potential due to a fracture can be obtained by integration of the solution of a line source over the surface of the fracture. Such integrations were possible only by virtue of the assumption of a uniform flux Inner Boundary Conditions, IBC. For sources with infinite length, a uniform flux and uniform potential IBC can be satisfied simultaneously. However, for sources with finite length, the uniform flux IBC does not provide a uniform potential IBC. Muskat [1932] suggested an approximate method for a vertical partially penetrating well under steady state conditions based on which one can simulate the uniform potential solution by using the uniform flux solution calculated at a certain point on the wellbore. That point is located at 75% of the wellbore height.

C.1 Steady State, Uniform Flux Potential Solution for Vertical Partially Penetrating Well

Integrating the steady-state point source solution in a rectilinear reservoir, Muskat [1932] derived a uniform flux potential solution for a vertical partially penetrating wellbore (Figure C.1.1) as:

$$\phi(w,\rho,x) = 4q\left[\frac{1}{\pi}\sum_{n=1}^{\infty}\left\{\frac{1}{n}K_0(2\pi n\rho)\cos(2\pi nw)\sin(2\pi nw')\sin(2\pi nx)\right\} + x\ln(2/\rho)\right]$$

...............................(C.1.1)

where

$$\rho = \left((x - x_L)^2 + (y' - y_L)^2\right)^{1/2} \qquad \dots\dots\dots\dots\dots\text{(C.1.2)}$$
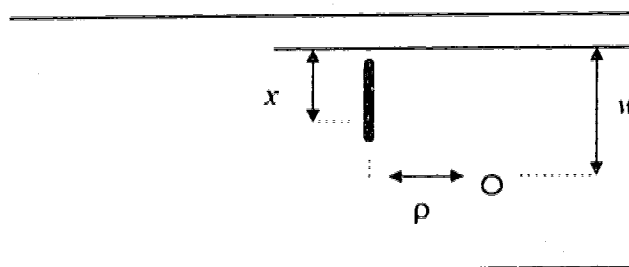

Figure C.1.1: Schematic drawing of a vertical partially penetrating wellbore in a rectilinear reservoir.

and where K_0 is a Bessel function of zero order and w, ρ are the coordinates of the point under study, and x is the length of the wellbore. Equation C.1.1 is singular on the Z axis $(\rho = 0)$. Muskat [1932] developed further equations to provide finite values at $(\rho = 0)$ as follows:

for $x - w \gg \rho_w$:

$$\phi \quad q\left[2ln\frac{2\pi}{\rho_w} - 2\ln\left(\Gamma(x + w)\Gamma(x - w)\right) - \ln\left(\sin\left(\pi(x + w)\right)\sin\left(\pi(x - w)\right)\right)\right]$$

$$\dots\dots\dots\dots\dots\text{(C.1.3)}$$

for $x - w \cong \rho_w$:

$$\phi = q \left[\begin{array}{c} \ln 2\pi^2 - 2\ln\big(\Gamma(x+w)\Gamma(x-w)\big) - \ln\big(\sin\big(\pi(x+w)\big)\sin\big(\pi(x-w)\big)\big) \\ -\ln(x-w) - \ln\left(w - x + \big(\rho^2 + (w-x)^2\big)^{1/2}\right) \end{array} \right], \quad\text{............(C.1.4)}$$

for $x = w$:

$$\phi = q\left[\ln\frac{2\pi}{\rho_w} - 2\ln\Gamma(2x) - \ln\big(\sin(2\pi x)\big) \right]$$

$$\text{............(C.1.5)}$$

and for $w > x$:

$$\phi = q\left[2\ln\frac{\Gamma(w-x)}{\Gamma(w+x)} + \ln\frac{\sin\pi(w-x)}{\sin\pi(w+x)} - \ln\left\{ \frac{1}{2} + \frac{1}{2}\left(1 + \frac{\rho^2}{(w-x)^2}\right)^{1/2} \right\} \right]$$

$$\text{............(C.1.6)}$$

where

$$q = \frac{\mu Q}{4\pi k a x} \qquad\qquad\qquad \text{............(C.1.7)}$$

C.2 Steady State Uniform Potential Solution for Vertical Partially Penetrating Wellbore

Equation C.1.1 and its variations do not provide a uniform potential along the wellbore. Muskat [1932] and [1982] applied superposition to model the wellbore by different line sources with various lengths, each with uniform flux. To consider spherical flow at the end of the wellbore (end effect), Muskat introduced a point source at the bottom of the wellbore. Equating the wellbore potential at different locations along the

wellbore, Muskat calculated the flux distribution along the wellbore to maintain a uniform

potential.

C.3   Steady State Potential Solution for Fully Penetrating Wellbore

Putting $x = 0.5$ in Equation C.1.1, one can find the potential due to a vertical fully

penetrating wellbore as:

$$\varphi = 2q\ln(2/\rho).\qquad\qquad\qquad\text{.................................(C.3.1)}$$

where ρ is the horizontal distance to the wellbore and q is the flux of the wellbore given

by Equation C.1.7.